



**Critical Analysis of Determining Induction Motor
Operating Power Factor Using Measurement and
Estimation Techniques**

**By
Mohammadali Khodapanah**

**A thesis submitted in partial fulfilment for the degree of
Doctor of Philosophy**

**Department of Electronic and Computer Engineering
Brunel University London**

January 2018

Abstract

Induction motors are the most used in commercial and industrial areas that consume the majority of generated electrical energy. The induction motors always create a low power factor. The low power factor not only create a penalty charge for industrial customers, but also produces energy losses in electrical systems. To prevent such issues, the users responsible to maintain the power factor to unity. Many researchers expressed that reactive power compensation by capacitors bank can be a substantial solution to maintain the power factor in the desired level at any loads, but providing the optimal reactive power still is a controversial topic. In the last decade, the power factor correction formula leads to obtain the optimal reactive power using measurement of input power and the operating power factor. However, measurement of these values synchronously create difficulties at any loading points.

This research will examine a solution to determine the operating power factor of induction motors against input power from no-load to full/over-load conditions using measurement and estimation techniques. In this thesis, estimation techniques including Kriging, regression, neural network and support vector regression are implemented in three different induction motors with the size of 250 W, 10 HP and 100 HP in order to identify the best estimation technique. In these cases, the support vector regression technique with some inputs data determined the power factor and input power at every desired loading points with high accuracy. These estimated values contributed to obtain the optimal reactive power and so prevent under or over correction at any loading points.

Acknowledgment

I would like to express my appreciation to my supervisor Dr. Ahmed Zobaa for his continuous helps and encouragement, my second supervisor Dr. Maysam Abbod, also for his valuable advises during my research. It is also my regards to academic members in the Department of Electronic and Computer Engineering for their support during my research. I would like to thank my dear colleagues, relatives and friends, Dr. Mohsen Mohammadi Alamuti, Dr. Ronak Rabani, Dr. Mohammad Shahrazad, Dr. Hassan Vafamehr, Dr. Mohsen Moslemin Koohpai, Dr. Mansour Salehi Moghadam, Dr. Masoud Asad Zoka, Dr. Keyvan Dayani. Dr. Mohammad Reza Behjati. Finally, my deepest gratitude goes to my parents, Mr. Nader Khodapanah and Mrs. Narges Esteghamat for their prayers and infinite support in every single aspect of my life. Also greatest pleasure to thank my lovely sisters Miss Mahboubeh Khodapanah and Miss Mina Khodapanah.

Declaration

The work described in this thesis has not been previously submitted for a degree in this or any other university and unless otherwise referenced it is the author's own work.

Dedication

Dedicated to my Mother, Father and Fiancée.

Statement of Copyright

The copyright of this thesis rests with the author. No parts from it should be published without his prior written consent, and information derived from it should be acknowledged.

©COPYRIGHT Mohammadali Khodapanah

All Rights Reserved Jan 2018

Table of Contents

Abstract	ii
Acknowledgment	iii
Declaration	iv
Dedication	v
Statement of Copyright	vi
Table of Contents	vii
List of Figures	x
List of Abbreviations	xiv
List of Symbols	xvi
Chapter 1: Introduction	1
1.1. Background Information	2
1.2. Problem Statement	3
1.3. Research Aim and Objective	4
1.4. Research Methodology	5
1.5. Principal Contributions to Knowledge	6
1.6. List of Publications Arising from the PhD	6
1.7. Organisation of the Thesis	7
Chapter 2: Literature Review	9
2.1. Introduction	10
2.2. Impact of Electrical Loads on Power Factor	10
2.3. Effect of Variation of Induction Motor Load on Power Factor	12
2.4. Importance of Power Factor Determination	13
2.5. Issue of Power Factor Determination	15
2.6. Power Factor Estimation Against Load	16
2.7. Past Research on Estimation Techniques	19
2.8. Past Research on Power Factor Correction	37
2.9. Summary	47
Chapter 3: Determination of Load and Power Factor	50
3.1. Introduction	51
3.2. Theory of the Induction Motor	51

3.3. Load Determination of Induction Motor.....	53
3.4. Effect of Load on Induction Motor Characteristics	55
3.4.1. The Speed.....	55
3.4.2. The Efficiency.....	56
3.4.3. The Power Factor	57
3.5. Power Factor Description of Induction Motor.....	63
3.6. Impact of Low Power Factor in Electrical Systems.....	66
3.7. Power Factor Correction of Induction Motor	67
3.8. Power Factor Determination of Induction Motor	70
3.8.1. Zero Crossing Method	70
3.8.2. Instantaneous Power Method.....	71
3.8.3. Direct Measurement Method	72
3.9. Experimental Work.....	72
3.10. Summary	78
Chapter 4: Estimation Techniques	79
4.1. Introduction.....	80
4.2. Method Using Measured Current.....	80
4.3. Kriging Method.....	83
4.4. Regression Method	91
4.4.1. Goodness of Fit	92
4.4.2. Linear and Non-linear Regression Models.....	93
4.4.2.1. Exponential Model	94
4.4.2.2. Gaussian Model.....	95
4.4.2.3. Power Series Model	95
4.4.2.4. Polynomial Model.....	96
4.5. Artificial Neural Network	98
4.6. Support Vector Regression Method.....	108
4.6.1. Linear Support Vector Regression	110
4.6.2. Non-linear Support Vector Regression	114
4.7. Summary	120
Chapter 5: Results and Discussion.....	121
5.1. Introduction.....	122
5.2. Results of Measured Power Factor	122

5.3. Results of Measured Current Method	125
5.4. Result of Kriging Method	131
5.5. Results of Regression Method	135
5.6. Results of Artificial Neural Network.....	143
5.7. Results of Support Vector Regression	152
5.8. Obtaining Reactive Power Required to Improve Power Factor.....	161
5.9. Discussion	164
5.10. Summary	180
Chapter 6: Conclusions and Future Work.....	181
6.1. Conclusions.....	182
6.2. Future Research	185
References.....	186

List of Figures

Title	Page
Figure 3-1: Output power versus motor load.....	55
Figure 3-2: Speed versus motor load	56
Figure 3-3: Efficiency versus motor load	57
Figure 3-4: Power factor versus motor load	58
Figure 3-5: Equivalent circuit diagram of induction motor	58
Figure 3-6: Current versus motor load.....	60
Figure 3-7: Power factor versus motor efficiency	62
Figure 3-8: Voltage and current phase angle	64
Figure 3-9: Power triangle diagram	65
Figure 3-10: Methods of correcting power factor of induction motors	68
Figure 3-11: Power factor correction diagram.....	70
Figure 3-12: Phase angle measurement between voltage and current waveforms	71
Figure 3-13: Experimental set-up of induction motor	73
Figure 3-14: Simulation of induction motor by MATLAB/Simulink	75
Figure 3-15: The main flowchart of estimating power factor of induction motor.....	77
Figure 4-1: Illustration of an unknown point surrounded by known points [105].....	85
Figure 4-2: Example of empirical semivariogram graph [105]	85
Figure 4-3: Semivariogram models [106].....	86
Figure 4-4: Characteristics of semivariogram model [107].....	87
Figure 4-5: Linear and non-linear regression models [114]	94
Figure 4-6: Simplified mathematical model of real nerve [116]	100
Figure 4-7: Structure of Multi-layer Feedforward with 2 hidden layers [118].....	101
Figure 4-8: Support vector regression structure.....	109
Figure 4-9: Hyperplane with upper and lower bounds [122].....	110
Figure 4-10: Hyperplane with a point out of margin target [122]	111
Figure 4-11: Mapping non-linear model into the feature space [122].....	114
Figure 5-1: Measured PF of IM 250 W	123
Figure 5-2: Measured PF of IM 10 HP	123
Figure 5-3: Measured PF of IM 100 HP	123
Figure 5-4: Measured THD of IM 250 W.....	123

Figure 5-5: Measured THD of IM 10 HP	123
Figure 5-6: Measured THD of IM 100 HP	123
Figure 5-7: PF measurement by simulation and power analyser.....	124
Figure 5-8: Measured reactive current in IM 250 W	126
Figure 5-9: Measured reactive current in IM 10 HP.....	126
Figure 5-10: Measured reactive current in IM 100 HP.....	127
Figure 5-11: Estimated PF of IM 250 W using MCMD.....	128
Figure 5-12: Estimated PF of IM 10 HP using MCMD	128
Figure 5-13: Estimated PF of IM 100 HP using MCMD	129
Figure 5-14: Estimated PF of IM 250W using Kriging.....	132
Figure 5-15: Estimated PF of IM 10HP using Kriging.....	133
Figure 5-16: Estimated PF of IM 100HP using Kriging.....	133
Figure 5-17: The residual models of the polynomial degrees in IM 250 W.....	137
Figure 5-18: The residual models of the polynomial degrees in IM 10 HP	137
Figure 5-19: The residual models of the polynomial degrees in IM100 HP	138
Figure 5-20: Estimated PF of IM 250W using regression	139
Figure 5-21: Estimated PF of IM10HP using regression.....	139
Figure 5-22: Estimated PF of IM100 HP using regression.....	140
Figure 5-23: Error results of ANN considering IMs within 10 running times	144
Figure 5-24: Fitness of ANN in IM 250 W.....	145
Figure 5-25: Fitness of ANN in IM 10 HP	146
Figure 5-26: Fitness of ANN in IM 100 HP	147
Figure 5-27: Estimated PF of IM 250 W using ANN.....	148
Figure 5-28: Estimated PF of IM 10 HP at using ANN.....	149
Figure 5-29: Estimated PF of IM 100 HP using ANN.....	149
Figure 5-30: Observing the optimum value of sigma in the considered IMs	154
Figure 5-31: Residual model of SVR in IM 250 W	155
Figure 5-32: Residual models of SVR in IM 10 HP.....	155
Figure 5-33: Residual model SVR in IM 100 HP.....	156
Figure 5-34: Estimated PF of IM 250W using SVR.....	157
Figure 5-35: Estimated PF of IM 10 HP using SVR	158
Figure 5-36: Estimated PF of IM 100 HP using SVR	158

Figure 5-37: Comparison of results of recent methods with SVR..... 179

Figure 5-38: Comparison of results of MATLAB/Simulink and MCMD with SVR
..... 179

List of Tables

<u>Title</u>	<u>Page</u>
Table 3-1 Specifications of considered induction motors.....	74
Table 4-1 The main features and issues of proposed methods	119
Table 5-1 Measured PF of IM 100HP using MATLAB/Simulink	124
Table 5-2 Estimated PF of IMs using MCMD from no-load to over-load	130
Table 5-3 Validity and accuracy of MCMD	130
Table 5-4 Estimated PF of IMs using Kriging from no-load to over-load	134
Table 5-5 Validity and accuracy of Kriging method	135
Table 5-6 Obtained coefficients of polynomial degrees in considered IMs	136
Table 5-7 Fitness of polynomial degrees in considered IMs	136
Table 5-8 Estimated PF of IMs using regression from no-load to over-load	141
Table 5-9 Validity and accuracy of regression results.....	142
Table 5-10 Validity and accuracy of all the proposed methods.....	142
Table 5-11 Selected input data and progress results (IM 250W).....	145
Table 5-12 Selected input data and progress results (IM 10 HP)	146
Table 5-13 Selected input data and progress results (IM 100 HP)	147
Table 5-14 Estimated PF of IMs using ANN from no-load to over-load	151
Table 5-15 Validity and accuracy of the ANN	151
Table 5-16 Selection of SVR parameters for predicting model of PF in the IMs ...	153
Table 5-17 Designed SVR parameters in the IMs	154
Table 5-18 Fitness of the models in IMs	157
Table 5-19 Estimated PF of IMs using SVR from no-load to over-load	159
Table 5-20 Validity and accuracy of the ANN and SVR.....	160
Table 5-21 Estimated kVAR in IM 250 W	162
Table 5-22 Estimated kVAR in IM 10 HP.....	163
Table 5-23 Estimated kVAR in IM 100 HP.....	164

List of Abbreviations

ANN	Artificial Neural Network
ANFIS	Adaptive Neuro Fuzzy Interface System
CPFC	Central Power Factor Correction
DPSO	Dynamic Particle Swarm Optimization
EPF	Estimated Power Factor
FGRNN	Fuzzy Based General Neural Network
GPFC	Group Power Factor Correction
HNN	Hybrid Neural Network
HPFC	Hybrid Power Factor Correction
IEC	International Electro Technical Commission
IM	Induction Motor
IPFC	Individual Power Factor Correction
IPM	Instantaneous Power Method
HV	High Voltage
VA	Volt Ampere
VAR	Volt Ampere Reactive
W	watt
Wh	watt Hour
LMA	Levenberg-Marquardt Algorithm
LS	Least Square
LWR	Locally Weighted Regression
MAPE	Mean Absolut Percentage Error

MCMD	Measured Current and Manufacturer Data
MLF	Multi-layer Feed-Forward
MSE	Mean Square Error
MRAS	Model Reference Adoptive System
NEMA	National electrical Manufacturer Association
NR	Newton Raphson
NNBP	Neural Network Back Propagation
PF	Power Factor
PFD	Power Factor Displacement
PI	Proportional Integral
PLC	Programmable Logic Controller
PR	Polynomial Regression
RBF	Radial Basis Function
RMS	Root Mean Square Error
RSW	Resistance Spot Welding
SCIM	Squirrel Cage Induction Motor
SVC	Static Var Compensator
SVM	Support Vector Machine
SVR	Support Vector Regression
STATCOM	Static Synchronous Compensator
THD	Total Harmonic Distortion
ZCM	Zero Crossing Method

List of Symbols

ϕ	Power Factor Angle
μf	Miro Farad
B	Magnetic Flux
v	Velocity of the bar
C	Capacity
E	Voltage Induced
f	Frequency
I_a	Active Current
I_M	Magnetizing Current
I_r	Reactive Current
I_S	Stator Current
L	Reactance
l	Length of Conductor
n_r	Rotor Speed
n_s	Synchronous Speed
P_{in}	Input Power
Q	Reactive Power
Q_c	Capacitor Capacity
R	Resistance
R_c	Core Loss
R_S	Stator Resistance
R_R	Rotor Resistance

S	Slip
T	Torque
V	Voltage
V_T	Voltage Terminal
w	Weight
W	Watt
X_M	Magnetization reactance
X_S	Stator reactance
X_R	Rotor reactance

Chapter 1: Introduction

1.1. Background Information

An induction motor is classified by single and three phases. The three-phase induction motor is the main work-horse of industrial factories. Also, it is known as an inductive load that consumes the majority of generated electrical power. The induction motor is composed of a stator and rotor. A single or three-phase voltage to the stator creates a rotation in the rotor shaft. This rotation requires active and reactive power to create a magnetic field and support the mechanical load in the rotor shaft. Variation of the mechanical load in the rotor shaft produces a change in the induction motor characteristics, including the equivalent circuit parameters, speed, efficiency and power factor. This change affects the induction motor's performance.

Among these parameters, the power factor is an important element as not only does its variation affect the performance of the grid efficiency, but it also increases the cost for the user and utility companies. In the induction motor, the load variation causes the power factor to be low in particular at no-load and light load. A lower power factor than the desired value produces energy losses and also induces a penalty charge for the user. Therefore, to prevent this issue, a technique is required to maintain the power factor at unity. A capacitor is able to generate the reactive power and make a unity power factor. However, determining the amount of required reactive power in each induction motor is necessary because it contributes to the selection of the capacitors before installation.

The power factor correction method is one of the significant techniques to calculate the exact amount of required reactive power at any loading point in individual or group induction motors, or even at the point of common coupling. In this method, three components, including the input power, initial power factor and target power factor, have major roles in determining the reactive power at any loading point.

The target power factor is normally between 0.9 and 1. However, the input power and initial power factor are unknown. Finding these two values requires a measurement at any loading point, from no-load to full-load and over-load conditions.

Several techniques are available to determine these two values. The first technique is to measure the voltage and current waveforms and then use zero crossing sensors to determine their angle. Hence, by having the voltage, current and cosine angle, the input power and power factor can be computed. An installed wattmeter and current meter in the induction motor can be used for measurement. The second method uses a power analyser to measure and save the voltage, current, power and power factor at any loading point. A power analyser is very helpful and is able to store the data at every point from no-load to full-load. The next technique uses MATLAB/Simulink to model any size of induction motor and then measure the power factor from no-load to full-load conditions. Consequently, once those values are obtained, the method of power factor correction determines the amount of reactive power at any loading point. Then, the proper size of capacitors can be selected based on the obtained kVAR.

1.2. Problem Statement

It is understood that determination of the input power and initial power factor versus load is important in order to find the optimum value of reactive power for making a unity power factor. Determining the initial power factor of an induction motor against load is not easy, since there is no equation between the load and power factor. In spite of the fact that the installed devices in the induction motor can be used to measure the power factor and input power, a load controller is required to avoid numerical fluctuation at reading time.

A power analyser is a suitable instrument that is able to measure and record data. However, in this approach, the induction motor must be shut down for cable connection, which may create a cost for the user. Although by simulating the induction motor in MATLAB/Simulink the power factor against load can be determined, the parameters of the induction motor are required for this simulation. Finding such parameters is difficult.

1.3. Research Aim and Objective

The main aim of this research is to implement a mathematical technique in order to create a model and determine the power factor against motor load from no-load to full-load and over-load conditions. This research is also aimed to implement the proposed technique in three different induction motors, small, medium and large, and then to provide a comparison with all the conventional methods to identify the best method for estimating the power factor of any size of induction motor at different loading points. The aim of this project will be achieved through the following objectives:

- Analysing the importance of the power factor against load and the effect of under- or over-compensation in the induction motor
- Considering a practical work in the laboratory to measure the power factor of the induction motor from no-load to full-load and over-load
- Investigating a method to determine the induction motor load
- Investigating a proper estimation technique to determine the power factor of different sizes of induction motor
- Implementing the proposed technique and conventional methods in three different induction motors using MATLAB programming

- Comparing the estimated power factor with the measured power factor to validate the accuracy of the proposed method
- Presenting a comparison between the conventional techniques and the proposed technique in order to substantiate the accuracy of the proposed method

1.4. Research Methodology

This thesis expresses a methodology to identify the difficulties and presents a new idea in order to determine the operating power factor of various induction motors including 250 W, 10 HP and 100 HP from no-load to full/over-load condition. To determine the power factor of induction motor at different loads both torque and power factor measurement are required at the same time. As previously mentioned, the practical work discovers the difficulties of this determination. In this research, a new idea using mathematical equations and estimation techniques will be used to solve the recent difficulties.

The study found that implementing input power and power factor equations can obtain the load and power factor at the same time. Then, implementing the SVR method to the obtained values of load and power factor, it is able to determine and store the power factor at any single load from no-load to full load and over load condition. To identify the accuracy of SVR method, recent techniques including measured current and manufacturing data, Kriging, regression and ANN will be implemented in the considered induction motors. Furthermore, A simulation and practical measurement are used to validate the outcome of SVR and input power equation.

1.5. Principal Contributions to Knowledge

The principal contributions to knowledge presented in this thesis can be summarised as follows:

- A comprehensive review is conducted on past research surrounding the issue of power factor determination against motor load from no-load to full-load and over-load conditions.
- Extensive study is presented on an input power measurement method to obtain the load and power factor against each other. Also, it contributes to finding the support vector regression method for estimation of the power factor against load at missing points between the no-load and over-load conditions.
- The combination of the input power measurement method and support vector regression method provides a great means to determine the active power and initial power factor at any loading point. Therefore, this combination provides a principal contribution to knowledge in order to obtain the required amount of volt ampere reactive and make the power factor unity.

1.6. List of Publications Arising from the PhD

The work detailed in this thesis has resulted in a number of refereed publications as follows:

- M. Khodapanah, A. F. Zobaa and M. Abbod, "Monitoring of power factor for induction machine using estimation technique," in *2015 50th International Universities Power Engineering Conference, UPEC 2015*, Stoke On Trent, United Kingdom, September 1-4, 2015, pp. 1-5.
- M. Khodapanah, A. F. Zobaa and M. Abbod, "Estimating power factor of induction motors using regression techniques," in *17th International Conference on Harmonics and Quality of Power (ICHQP)*, Belo horizonte, Brazil, Oct 16-19, 2016 , pp. 502-507

- M. Khodapanah, A. F. Zobaa and M. Abbod, "Estimating power factor of induction motors at any loading conditions using support vector regression," in *Journal of Electrical Engineering*" Submitted on October 2017.

1.7. Organisation of the Thesis

Chapter 1 – Introduction

The sections in this chapter will outline the motivations of the research presented in this thesis. This research has been conducted to gain a greater understanding of power factor determination against load in order to obtain the optimal reactive power for making a unity power factor at any loading point with a view to saving energy. A description of the relevant background information is provided. The overall objectives of this research project are presented within three different sizes of induction motors.

Chapter 2 – Literature Review

This chapter details the concept of power factor measurement and correction in induction motor and electrical systems. The chapter discusses various methods of estimating induction motor characteristics and electrical systems indices. The proposed solutions for estimating the power factor versus load will be presented.

Chapter 3 – Determination of Load and Power Factor

This chapter gives an overview of the induction motor characteristics and analyses the load and power factor against each other. The theory of power factor determination and power factor correction are described in detail. In addition, the experiment and simulation for measurement of the power factor of different induction motors against load are presented.

Chapter 4 – Estimation Techniques

This chapter describes the theory of five mathematical techniques for power factor estimation versus load. The first technique is a method using measured current and manufacturer's data. The second and third methods are the statistical methods of Kriging and regression respectively. The fourth and fifth methods are an artificial neural network and support vector regression as intelligent techniques.

Chapter 5 – Results and Discussion

This chapter presents the results of the proposed methods, including measured current and manufacturer data, Kriging, regression, and the artificial neural network and support vector regression methods that are implemented in 250 W, 10 HP, and 100 HP induction motors in sequence. The discussion section describes the features of and issues with the considered methods. A comparison of the results is presented to identify the best methods.

Chapter 6 – Conclusions and Future Work

In the final chapter, a summary is provided of the work presented in this thesis and the main contributions of the research are discussed. In addition, outlines of proposed future work are presented.

Chapter 2: Literature Review

2.1. Introduction

This chapter details the papers reviewed about the importance of the power factor in induction motor and electrical systems. Several reviewed articles are analysed for measuring and correcting the power factor. In addition, the chapter discusses various methods for measuring and estimating the induction motor characteristics and electrical systems indices. The capabilities and requirements of the various estimation approaches with a proposed solution will be examined through a critical review.

2.2. Impact of Electrical Loads on Power Factor

The power factor in electrical systems is defined as the cosine angle between the voltage and current. Electrical and mechanical loads have significant roles in the behaviour of the power factor. Electrical loads are divided into passive and active loads. These loads provide a change in the angle between the waveforms of the voltage and current. For example, if the load is purely resistive, the angle becomes zero and as a result the power factor will be unity [1, 2]. However, if the load is inductive or capacitive, the angle will be 90 degrees (lagging or leading) so that the cosine angle obtains a power factor of zero. In the inductive load, the current waveform always lags behind the voltage, while in the capacitive load, the current leads the voltage. In electrical systems, a lagging power factor means consuming reactive power. A leading power factor means generating reactive power [3].

The power factor is also described as a ratio between the active and apparent power. It can be calculated by active power over apparent power. In electrical and power systems, most electrical loads are resistive and inductive, both active and reactive power are required in the loads. Therefore, the power factor will not be zero or unity. It will be higher than zero or less than one [4].

Utility companies are always concerned with reactive power because increase of reactive power causes the current increases and also a voltage drop occurs. This results in equipment failure. To avoid this problem, the power factor must be maintained between 0.8 and 1 [5]. Commercial and industrial users are always concerned with a lower power factor than the standard level (due to penalty charges). Hence, this indicates the importance of the power factor in the electrical system.

Electrical loads can be described as linear and non-linear loads. Non-linear loads create harmonics, which distort the voltage and current waveforms. This distortion also has an effect on the power factor, such that power factor distortion must be taken into account. The power factor distortion can be obtained by considering the total harmonic distortion of the voltage and current [6].

The effects and consideration of the power factor and harmonic distortion is presented. A harmonic is defined as a sinusoidal component of a periodic wave in a frequency. An AC periodic voltage and current are represented by a Fourier series of pure sinusoidal waves which contain the basic or fundamental frequency other than 50Hz and its multiples, called harmonics. However, harmonic distortion is distortion factor of voltage and current waveforms. Voltage and current distortion are commonly caused by non-linear loads in the system. In addition, the voltage distortion corresponds to the current distortion in case of source impedance, whereas the current distortion results in voltage distortion. The root mean square of voltage or current harmonics over the fundamental voltage or current computes the total harmonic distortion. The fundamental component of the voltage and current to the total voltage and total current obtains the power factor distortion [6, 7].

Harmonic distortion is usually produced by non-linear load such as from arc furnaces, fluorescent lighting and rectifiers. Non-linear load reduces the power factor

not only due to the phase shift of the fundamental of the voltage and current, but also because of higher harmonics in the voltage and current caused by noise and heat. In addition, in induction motors, the majority of motor loads are linear, but there are non-linear characteristics. Electrical motors can be influenced by large harmonic currents, resulting in higher noise, oscillating torque and increasing copper and iron losses. Voltage harmonics cause a growth in iron loss, while current harmonics cause an increase in stray flux losses and copper losses. Both components have an effect on the power factor in electrical systems.

It is described power factor distortion and power factor displacement based on IEEE Std. 18-2002, observing that the power factor displacement can be described as the cosine angle of the voltage and current in a sinusoidal wave. However, with increase of the non-linear load, harmonic distortion will be produced, where the total power factor will be presented by power factor distortion times power factor displacement. A large phase shift and harmonics create low power factor displacement and distortion. A capacitor is useful to correct the power factor displacement in linear loads. However, it is not recommended in the case of non-linear loads, since power resonances produce higher harmonics. A harmonic filter is recommended to eliminate harmonic distortions [8].

2.3. Effect of Variation of Induction Motor Load on Power Factor

Among electrical loads, the induction motor is important due to its extensive industrial use. They consume more than 50% of generated electricity. [9].

The induction motor is associated with slip speed, which depends on the motor frequency and number of poles. The difference between synchronous speed and actual speed provides slip. The slip increases when the actual speed decreases by adding mechanical load. Since the induction motor is recognized as an asynchronous

motor, the slip cannot be zero at the no-load condition because if the slip speed and actual motor speed were equal, there would be no rotation due to no voltage being induced on the rotor side [10, 11].

The induction motor needs both active and reactive power, where the active power is used for providing mechanical power and the reactive power is used for the existing magnetic field. The power factor and efficiency are two important elements in terms of energy-saving in industrial applications. Efficiency is a ratio to indicate the losses existing between the input and output power. However, the power factor is a ratio between active and reactive power. It indicates how much active and reactive power is being consumed from no-load to full-load and over-load conditions. In induction motors, the mechanical load affects the power factor because the active and reactive power are proportional to the mechanical resistance and magnetization reactance. Variation of these two parameters creates different demands for active and reactive power and therefore results in the power factor changing exponentially [12].

2.4. Importance of Power Factor Determination

An induction motor with linear load at the steady state condition provides sinusoidal waveforms. In this condition, using the conventional power factor equation is enough to determine the power factor of the induction motor. As previously mentioned, induction motors are inductive loads. Inductive loads always cause a low power factor due to consuming more reactive power. The low power factor of induction motors not only creates a penalty charge for industrial customers, but also produces energy losses in electrical systems. It is understood that decreasing and increasing the mechanical load in the induction motor produces a change in the power factor. In industry, since many induction motor loads change due to different applications, the power factor also changes and becomes lower, which needs to be taken care of. To

solve this problem, reactive power compensation is required by the user. A capacitors bank is a substantial solution to generate reactive power [13, 14, 15].

In the last decade, a technique using no-load test has been used to obtain the required reactive power in the induction motor. For instance, if the motor set to the no-load, the reactive current can be estimated as 90% of the no-load current. However, if full-load current is available, the no-load current can be predicted as 30% of the full-load current. Then, 90% of the full-load current provides the required reactive power in VAR [16]. However, this method is not sufficient to determine the proper size of capacitor because it only provides an approximation, in particular at fixed load. Therefore, this empirical technique may create under- or over-correction at operating time, where under-correction causes a penalty charge for the user while over-correction produces self-excitation, which is harmful for the induction motor winding [17].

The study found that the power factor correction equation is a suitable technique to calculate the exact amount of reactive power required at any loading point in individual or group induction motors, or even at a point of common coupling. In this method, three components including input power, initial power factor and target power factor have the main roles in determining the reactive power at any loading point. The target power factor is normally between 0.9 and unity. However, the input power and initial power factor need to be measured from no-load to full-load and over-load conditions. Once these two values are obtained, the power factor correction equation determines the amount of volt ampere reactive for improving the power factor [18, 19].

Several techniques are available to determine these two values. The first technique is to measure the voltage and current waveforms and then use zero crossing sensors to

determine their angle. Hence, by having the voltage, current and cosine angle, the input power and power factor can be computed. The installed wattmeter and current meter in the induction motor can be used for measurement. The second method uses a power analyser to measure and save the voltage, current, power and power factor at any loading point. The power analyser is very helpful and is able to store the data at different point from no-load to full-load [20, 21, 14].

The next technique uses MATLAB/Simulink, which is able to model any size of induction motor and then measure the power factor from no-load to full-load conditions. Consequently, once those values are obtained, the method of power factor correction determines the amount of reactive power at any loading point. Then, the proper size of capacitors can be selected based on the obtained kVAR [13].

2.5. Issue of Power Factor Determination

Determining the initial power factor of the induction motor against load is not easy since there is no equation between the load and the power factor. In spite of the fact that the installed devices in the induction motors can be used to measure the power factor and input power, a load controller is required to avoid numerical fluctuation at reading time. A power analyser is a suitable instrument for the measurement, being able to measure and record data. However, in this approach, induction motors must be shut down for cable connection, which may create a cost for the user. Although by simulating the induction motor using MATLAB/Simulink the power factor against load can be determined, the parameters of the some induction motors are required for this simulation. In this chapter, various reviewed papers will be presented with regard to how the power factor against load can be determined. Since the power factor will be obtained from the impedance of the equivalent circuit, determination of the equivalent circuit parameters is reviewed as well.

Although many past papers are reviewed to indicate the problems, much research are still needed to find a proper technique for determining the power factor against load. The next section will discuss several past papers on estimation of the power factor [22, 23].

2.6. Power Factor Estimation Against Load

It is presented a method using the measured current and manufacturer's data (MCMD) to estimate the power factor of the induction motor (2.2 kW) at any desired loading point. In this method, a simple numerical equation is used to provide a good solution [14]. In this technique, some measured value of current from no-load to full-load are required. Also nominal reactive power of induction motor requires in this method. The motor current is measured by current meter. The nominal ractive power obtained by nominal power factor from motor name plate. Conducting values of measured current and and the nominal reactive current into the equation, power factor obtained at value of measured current. In this approach, the measured current method is used to obtin the load. The results of the proposed method are compared with the instantaneous power method and zero crossing method, and show errors of +0.04 at the full-load condition and -0.18 at the no-load condition [14].

In this method, two weaknesses have been found. One is in the measurement of the current. In the measurement process, the meter provided a numerical fluctuation at reading time because increasing and decreasing the motor load must be controlled during the measurement, which is difficult. Another weakness relates to the nominal reactive current. In induction motors, the reactive current from no-load to full-load is not constant, while in this equation the reactive current is considered to be constant. This consideration creates high error at many loading points.

Consequently, this method is not suitable for induction motors that have not been installed and coupled to the load.

Rajesh presented two techniques including Kriging and regression to estimate the power factor in residential houses. It is observed that due to the increase of load, determining the power factor is necessary for improving energy efficiency. In this paper, statistical methods provided a solution to determine the power factor. In the regression method, a locally weighted regression technique with an exponential function is used. The Kriging method with a semivariogram model is considered. Both methods require some observed points in order to establish a model. Then, based on the created model, the power factor is predicted at the desired points. In this case, a number of houses with some random measurement of the power factor were considered as input data. The output results indicated that the Kriging and regression methods estimated the power factor with the average error of 1.824% and 1.944% [24, 25].

A zero crossing method and instantaneous power method are presented to determine the power factor of a small induction motor (250 W) from no-load to full-load conditions. The Kriging method is also applied in this induction motor to estimate the power factor. The results showed that the zero crossing and instantaneous method produced errors of 22% and 35%. However, the Kriging method created an average error of 14% [22].

It is presented a regression method with a polynomial technique to estimate the power factor from no-load to full-load condition. In this technique, the voltage, current and input power at a few points are randomly measured. Then, the power factor with the conventional method and the motor load with the input measurement methods are computed.

The obtained values are considered as dependent and independent values in this method. Polynomial degrees of the 1st, 2nd, and 3rd orders are applied in this technique. The results showed that the 3rd order provided the best model, very close to the sample points, and then the unknown points are estimated accurately. In this induction motor, MCMD and Kriging are also applied to estimate the power factor from no-load to full-load conditions [26].

Both methods produced average errors of 3% and 0.6% respectively. The compared results showed that regression with the 3rd order provided the highest performance with the lowest average error of 0.3% compared with the other methods from no-load to full-load conditions. However, the Kriging and regression methods were not able to estimate the power factor from full-load to over-load conditions because both methods are interpolation techniques and cannot extrapolate unseen points.

It is introduced an intelligent technique to estimate the power factor in distribution systems by analysing the real parameters of the power system. In this research, an ANN trained by a feed-forward back propagation is used. The hourly average values of different power quality parameters over 92 days were taken from a power distribution company in Victoria, Australia. The structure of the network was considered as two layers, where tan sigmoid and log sigmoid functions are used in the first layer and hidden layer respectively. The output layer observed the estimated values of the power factor. The results showed that the ANN is able to estimate the power factor at unseen points with an accuracy of 93% [27].

It is mentioned that using equivalent circuit parameters in the induction motor can be a great way to determine the power factor because the total resistances over impedance obtain the power factor.

The next section will discuss past research on induction motor parameters. Also, evaluating estimation techniques through the reviewed papers presents a solution for power factor estimation [11].

2.7. Past Research on Estimation Techniques

It is stated that an equivalent circuit is a diagram to represent the rotor, stator, losses and magnetization of the induction motor. The rotor and stator are indicated in resistance and reactance. Losses and magnetization are modelled by a resistance and reactance respectively. The mechanical load or output power is indicated by rotor resistance over slip. Using all these parameters would be effective for obtaining the power factor from no-load to full-load at steady state conditions because they affect the motor current and the motor current also affects the power factor at any loading point. It is reported that a no-load test and locked-rotor test are used to determine the magnetization reactance and total impedance [10].

A DC test can be applied to determine the stator resistance at no-load. However, these procedures had the limitation that estimation techniques had to be applied to determine the parameters of the induction motor individually. Once all the parameters were found, the motor impedance could be easily computed with its angle. Then, the cosine angle provided the power factor of the induction motor at steady state conditions. The study found many articles on the subject of how to find the parameters of the induction motor. For example, Phuc estimated the parameters of an induction motor using test measurement data. It is mentioned that a DC test, a locked-rotor test, and a no-load test were used to obtain the equivalent circuit parameters.

However, the results of the parameters would not be as accurate as measurement because the core loss resistance with slip is not constant from no-load to full-load.

This paper developed an algorithm to determine the core loss resistance by using a Newton–Raphson (NR) algorithm, and then adding the obtained value into a direct parameter calculation method [28].

Therefore, this paper presented a new methodology to match the parameters of the equivalent circuit into the measurement under various test conditions. The results indicated that by adding the core loss resistance, the estimated parameters are fitted into the both the active and reactive power at various slips compared with direct calculation. For example, at a slip of 0.0083 the active power, direct calculation and Newton–Raphson (N–R) algorithm were 202.75, 124.5 and 164.30 in watt respectively. It can be observed that the N–R algorithm provides closer results than direct calculation.

It is discussed parameter estimation of a squirrel-cage induction motor without torque measurements. In this paper, some problems in the determination of the parameters using methods in IEEE standard 112 are clarified. The parameters are determined by a no-load test, locked-rotor test and over-load test. An iterative algorithm that needs no torque measurement is used. The proposed method is tested with 16 different rating powers. It is noted that IEEE standard 112 provides four methods for determination of the equivalent circuit parameters. Methods 1 and 2 estimate the rotor resistance using a locked-rotor test with a supply frequency where the rotor resistance is considered as a maximum 25% of the rated frequency. Methods 3 and 4 are used to estimate the rotor resistance in a full-load slip test. The results of these methods indicated significant errors. Therefore, the proposed method is used to minimise the problems in these methods and the results indicate a very good convergence [29].

It is presented a methodology to obtain the parameters of asynchronous machines by using the nameplate and manufacturer's data sheet. The motor nameplate often provides the mechanical shaft power, voltage, current, efficiency, speed and power factor at full-load condition. However, it is mentioned that a data sheet provides the efficiency and power factor at different loads including quarter, half and full-load. The stator resistance can be obtained by considering efficiency, output power, slip and current. Rotor resistance is estimated by providing the output power, slip and current. Rotor and stator reactance are obtained using the voltage current, rotor and stator resistance. The resistance losses are computed from the output power, efficiency and slip. However, magnetization reactance is calculated by considering no-load current and voltage drops in the stator impedance. The methodology was implemented in hundreds of motors and the results indicated a very good agreement between the calculated value and supplied information [30].

It is presented a methodology to estimate the parameters of an induction motor using motor nameplate data. It is mentioned that several previous papers have discussed estimating the parameters using the motor nameplate and data sheet from the manufacturer. For example, a recent method required the nameplate information, the ratio of the starting torque, full-load torque, power factor and efficiency at four loading points (25%, 50%, and 75% and 100%). The proposed method only required the motor nameplate information since this provides easy access compared with the data sheet from the manufacturer [31].

A motor that is already installed may not have a data sheet or it may be difficult to find the data from the manufacturer. It is indicated that the proposed method is suitable for such cases. In this paper, the algorithm considered the full-load rated, starting power, and a set of non-linear equations that refer to the motor power and

losses in circuit parameters. Finally, an iterative Gauss–Seidel method solves the non-linear equations. The proposed method had several limitations. The rotor resistance and reactance were assumed equal under the locked-rotor test. The parameters are fitted into the full-load condition. All motor losses are assumed constant at full-load. Therefore, the results show that the proposed method provided satisfactory values close to the actual values. For instance, the proposed method obtained a stator resistance of 0.657 while the actual value was 0.641 Ohm.

Phumiphak proposed a technique to estimate the parameters of the induction motor. The proposed technique used a few sets of data such as voltage, current, speed and power factor from the field test of the motor instead of a locked and no-load test rotor. The proposed method is suitable for motors connected to the load permanently and cannot operate at no-load. There are two difficulties in determining the parameters of equivalent circuits at operation time. Firstly, it is too difficult to lock the rotor while the motor is in service. Secondly, in the no-load test, the motor cannot cut from the motor load since it is coupled [32].

The equivalent circuit parameters are estimated by a genetic algorithm, in which the measured voltage, current, power factor and speed (while the motor is in service from light-load to full-load) are considered as the input of the genetic algorithm. Two sizes of induction motor, 3 HP and 5 HP, are used to substantiate the feasibility of the proposed method. The results showed that the estimated performance of the six-impedance equivalent circuit provided an average error of 5% compared with the measured power factor, efficiency and current.

It is presented an artificial neural network (ANN) for estimating the parameters of the equivalent circuit of the induction motor. It is mentioned that the rotor resistance is not constant and changes with time, temperature and speed.

The ANN aimed to identify the rotor resistance and mutual inductance. The delta method for the output layer and back propagation for the hidden layer are used in ANN training. A simulation and experimental tests with an induction motor with a power rating of 1.1 kW are implemented. The performance of the ANN in estimating the rotor resistance and inductance of the induction motor is high. It is seen that the estimation process was significantly improved and the whole control system operates better [33].

It is presented a method using regression based on a 3rd order for estimating the parameters of the induction motor. The proposed method used least squares (LS) to estimate the non-linear model parameters and then transformed the 3rd order non-linear model to a linear regression equation. In this case, the voltage and current are considered as inputs and the active and reactive power and motor speed as the output of the induction motors. Consequently, the proposed method could identify the parameters through an experiment. The simulation results indicated that the proposed method performed well with high accuracy in the estimation of induction motor parameters [34].

It is presented a new method to estimate the single-cage induction motor parameters from the manufacturer's data. In this case, the algorithm minimizes the error through a non-linear optimization problem. In addition, by defining the variable slip, the proposed method predicts the induction motor characteristics at low and high slip with satisfactory accuracy. When the proposed method was tested on eight induction motors with different sizes, the results showed that the proposed method is capable of estimating the different motor characteristics at low and high slip [35].

It is described a set of algorithms based on a linear regression model to estimate the stator resistance, stator inductance and leakage inductance of an induction motor

without using rotor speed and rotor resistance data. The proposed method estimated these parameters based on the stator current and voltage measurement. The algorithm was tested on a 15 kW induction motor. The output results indicated that the stator inductance can estimate properly at any rotor speed and the accuracy will be improved when the torque is low. In addition, when the speed is very low and the torque is high, the stator resistance can be estimated, and also when the speed and torque are high, the leakage inductance can be predicted accurately [36].

A hybrid genetic algorithm presented for estimating the equivalent circuit parameters of an induction motor, where the genetic algorithm method is combined with a conventional method. The genetic algorithm is only used for the initial search and the conventional method is used for the final stage of optimization. The output results showed that the main advantage of the hybrid genetic algorithm is in providing a good solution to the conventional method. In addition, the hybrid genetic algorithm reduced the optimization time of genetic algorithm schemes [37].

Advanced particle swarm optimization algorithms are used for equivalent parameter estimation of induction motors. The proposed method combines two significant algorithms, namely dynamic particle swarm optimization (dynamic PSO) and chaos PSO algorithms, in order to improve the performance of the standard PSO algorithm and modify the parameters with better results. The proposed method required the measurement of three-phase stator currents, voltages and the speed of the induction motors as inputs. The experimental results compared with the estimated results indicated that the dynamic PSO and chaos PSO algorithms performed better than the standard PSO and genetic algorithm in terms of parameter estimation of induction motors [38, 39, 40].

A numerical method is implemented to estimate the parameters of double-cage induction motors using the manufacturer's data including the full-load power factor, full-load mechanical power, starting current, maximum torque and full-load efficiency. Since the model parameters are non-linear, a modified Newton is selected. The most critical parameters are the starting current and maximum torque. In this situation, the proposed algorithm makes it possible to find the critical parameters in order to solve the non-linear equation. The significant advantage of the proposed algorithm was the high convergence and the classified solvable and unsolvable data [41].

A simple method is presented for the estimation of the equivalent circuit parameters from the National Electrical Manufacturers Association (NEMA) using manufacturer's data such as the starting torque, breakdown torque, efficiency and power factor at rated output power. A non-linear least squares algorithm is applied to solve the non-linear equation in order to determine the parameters. The non-linear least squares employed the Levenberg–Marquardt algorithm to train the data and the least squares converged well. The results showed that the proposed method, which was tested on 300 large induction motors, performed very well [42].

A curve-fitting technique using the least squares method is used in order to estimate the off-line equivalent circuit parameters of an induction motor. In this case, the proposed technique solves the non-linear relationships between the magnetizing current and inductances. The Levenberg–Marquardt algorithm (LMA) minimised the cost function based on the error between the measured and estimated points. The output results demonstrated that the inductances in the presented case are estimated with a 3rd order fitting, the rotor flux is estimated by a 4th order fitting and the total leakages are estimated by a 5th order fitting with satisfactory errors [43].

A method presented for the estimation of induction motor parameters, stating that the parameters of the induction motor such as the stator resistance create a high temperature in the operating condition. For instance, in a heavily loaded induction motor, magnetic saturation might take place in the rotor and stator. This saturation creates a non-linear model of the motor's behaviour. Because of this issue, estimation of the parameters is important in terms of evaluating the condition of the motor. In this case, the stator currents and the angular speed of the rotor under motor start-up are added into the algorithm. The proposed method converges very fast and provides satisfactory results [44].

A statistical method is used to estimate the parameters of the equivalent circuit for an induction motor. Indeed, obtaining the equivalent circuit parameters of the induction motor is an efficient way to evaluate the electrical, mechanical and energy behaviour before purchasing or installing the systems. The proposed method used the data from the motor nameplate and manufacturer's catalogue for parameter estimation. The output results demonstrated that the proposed method was able to estimate the parameters of the equivalent circuit in the absence of further data. Moreover, the estimated values compared with real values showed the high performance of the proposed method in terms of high accuracy [45, 46].

It is proposed a hybrid method combining N-R and a genetic algorithm for estimating the parameters of the induction motor by using the manufacturer's data available. Both algorithms are tested on the National Electrical Manufacturers Association (NEMA) and International Electro-technical Commission (IEC) motors. The results indicated that the N-R algorithm provided poor convergence and high average squared errors of 0.5411 and 0.2514 for the NEMA and IEC motors. However, by implementing the hybrid algorithm, a significant improvement took

place, with very low average squared errors of about 0.0625 and 0.0282 in the IEC and NEMA motors respectively [47].

It is presented a technique to estimate the parameters of a linear induction motor and focused on a suitable cost function to optimise the algorithm. Estimating the variation of the magnetic parameter versus the magnetizing current is proposed. The proposed method is verified by a test set-up. The results illustrate the robustness of the proposed approach when estimating the parameters under different magnetic conditions. The significant advantage of this method is that it does not require any control technique in no-load and locked tests [48].

It is used a hybrid artificial neural network (HANN) in a three-phase induction motor with a size of $\frac{1}{4}$ HP in order to estimate the rotor speed and resistance. Parameter estimation was done using a large number of methods in order to obtain the magnetic flux, motor speed, rotor resistance and rotor time constant. These methods consist of observers, adaptive systems, spectral analysis and artificial intelligence such as neural networks and fuzzy logic. The HANN estimator uses two hidden layers to estimate the resistance and rotor speed of the induction motor. The output results showed that the HANN has a good performance with minimum error [49].

It is presented a hybrid method in order to estimate the rotor parameters of an induction motor. The rotor parameter is quite important for the control system since it fluctuates during the operating condition. In this paper, a combination of the least squares (LS) method and a genetic algorithm is applied to identify the rotor parameters at operating times. The genetic algorithm is applied for initial estimation and LS is used for iterative steps. The hybrid method is able to take advantage of both algorithms. The results demonstrated that the new approach converges faster than LS and performs better than the genetic algorithm in accuracy after longer

iteration. The simulation results show that the control system can achieve a good performance of dynamic and steady-state responses [50].

A support vector machine (SVM) is used to estimate the rotor resistance of a squirrel-cage induction motor (SCIM). In this case, flux and variable rotor resistance are considered as inputs of the SVM, which uses SVR to estimate a non-linear model using a set of linear functions including the kernel function among a Gaussian function, which is known as a radial basis function (RBF). The result showed that SVR is able to estimate the rotor resistance value with a small amount of data compared with the original training values. In addition, SVR is a robust computation algorithm with an excellent performance in regression applications, where the rotor resistance can be estimated in different operation conditions [51, 52].

It is presented a comparison between the performance of a classical model reference adaptive system (MRAS) and SVM for rotor resistance estimation of a SCIM. The results showed that the performance of the SVM-based estimator was better than that of the classical MRAS-based estimator for the same operation conditions of the drive system. This work showed that the SVM, which uses SVR, is more powerful to estimate an unknown and inaccessible rotor resistance parameter of the SCIM [53].

It is used a radial basis function neural network (RBFNN) for rotor speed estimation. Measured stator voltages and current are selected as inputs to the network and the output of the network is the estimated rotor speed. In this case, two hidden layers are used. Then, a gradient descent training algorithm is used to obtain the weights and biases of the NN. The results show that the RBF performs very well with satisfactory results. It is observed that the number of neurons and layers can have a significant role in the performance of the neural network. Both neurons and layers will be selected based on different cases in order to get a suitable result compared with the

input data. The artificial neural network allows a reduction of the cost of the industrial drive and also avoids measurement of the induction motor variables involved in this process. The ANN has significant advantages consisting of reducing the weight matrix, lower cost in the probability of the solution, and being able to approximate non-linear functional relationships [54].

An artificial neural network is also used to estimate motor speed. The input of the network considers the RMS current and rotor speed at a voltage range of 214–226 V. In this study, the neural network used a back propagation algorithm with a different structure to adjust the weights. In this case, five neurons in the first hidden layer, ten neurons in the second layer and one layer of neurons in the output layer are applied. However, at different voltages, five neurons in the first and second hidden layers and one neuron in the output layer are used. The neural network is also used to estimate the speed of the induction motor at different loads within 800 rad/s. RMS voltage and current are selected as the input of the network. Then, the speed of the motor is estimated at different loads of 2 Nm, 4 Nm and 6 Nm at a voltage of 220 V. The results showed that by selecting the number of neurons and layers at a loading of 4 Nm, the output results provided high error compared with the actual value. In the same case study, a neural network was used to estimate the speed by increasing the voltage from 216 to 224 V and the load torque from 25% to 150% at each voltage. In this work, the neural network considered only five neurons in the first layer and one neuron in the output layer with a linear activation function. There was an average relative error of 0.54% and standard deviation of 0.41% [55, 56].

It is used a fuzzy neural network for speed control in an induction motor with a range of 15 kW. The ANN is used to estimate the motor speed and provide a sensor speed estimator in the systems.

The proposed method is evaluated at any operating conditions of the induction motor consisting of unknown load torque and parameter variations. The network is based on a multi-layer back propagation neural network that consists of two phases, namely a training phase and recall phase. In the training phase, the weight of the network is randomly initialized. Next, the output of the network is calculated and compared with the desired value. The error of the network is calculated by adjusting the weight of the output layer. In such cases, the voltage and current are considered as the input of the network. Then, one hidden layer is used for generalization. The results obtained show that the NN provides reasonable speed estimation under such operation conditions [57].

It is presented an adaptive network-based fuzzy interface system (ANFIS). This method replaces the model reference adoptive system (MRAS) method. It is reported that in the induction motor, the conventional MRAS creates some difficulties in meeting the requirement for a fast dynamic response under dynamic operating conditions. Therefore, a back propagation algorithm is used in the proposed method, with two input layers, five hidden layers and one output layer to generalize the non-linear model. The gradient descent method is used to reduce the error which is propagated from the output layer to the input layer by the back propagation algorithm. The experimental results demonstrated that the ANFIS method is powerful and performs better than the conventional method under unknown conditions. In addition, it produced better results compared with real data during speed and load variation. Thus, the speed estimation by the ANFIS provided very good accuracy in both transient and steady-state conditions for all ranges of speed control [58].

It is used a fuzzy-based general regression neural network (FGRNN) for the speed control of an induction motor. The general regression neural network would be good at estimating the motor speed, and also control the speed at operating time. The output result indicated that the proposed method provided satisfactory speed estimation under operation conditions. The response time was also very fast. Therefore, the method could be used for achieving the desired performance level [59].

It is presented a HNN in order to estimate the rotor speed and resistance of an induction motor. The NN and fuzzy logic are combined in this proposed algorithm with a two-neuron structure. The HNN is implemented in real-time with a three-phase induction motor and obtains the rotor resistance and speed with minimum error. It is observed that the results are satisfactory compared with real data. Another significant parameter of induction motors is torque, which has a substantial role in the performance of the motor. Although speed information assists in monitoring torque, there are still many other methods to determine the motor torque [60].

It is presented an artificial neural network for online rotor and stator resistance estimation of an induction motor. Rotor flux and voltage are used for training. The back propagation algorithm trains the network and estimates the resistance. Both the rotor and stator resistances are obtained successfully and accurately. In order to verify the stator and rotor resistance, an experimental set-up with measurement is considered. It is observed that the neural network produces results very close to the measurement results [61].

It is presented a method to estimate the torque of a three-phase induction motor without any mechanical sensor. In this case, the slip method is used, where only the measured stator current is required.

The results of the estimated torque were very similar to the measured torque value. The proposed method showed that it could be helpfully applied in many induction motors due to its robustness and simplicity [62]. A technique is presented to estimate the shaft torque of an induction motor under different loading conditions in terms of efficiency monitoring and mentioned that the induction motor consumes total energy. It is shown that 40% of the induction motor loads is oversized or under-loaded at operating time. Oversizing reduces the efficiency and performance of the motor and needs to be taken care of. In this paper, a shaft torque estimation method is considered with a no-load test and measurement of the stator resistance. By obtaining the shaft torque and available indices like the voltage, current, and power factor, the operating efficiency and motor load can be determined at any speed. The results showed that the ratio of estimated shaft torque can be helpful to compute the percentage loading. It is shown that the accuracy of the proposed method is comparable with the power measurement method which is normally used for calculating the percentage loading in induction motors [63].

It is presented a practical method to estimate the motor efficiency. The efficiency could be estimated by the slip method at any operating condition, but the motor speed must be determined very accurately. Since measurement of speed creates a difficulty, the proposed method was applied to estimate the efficiency of an in-service motor using the recorded voltage, current, watt and var by a digital analyser. The output results from the proposed method indicated satisfactory values compared with the measured efficiency [64].

It is presented a method to estimate the full-load efficiency of refurbished induction motors. In fact, full-load efficiency estimation after repair creates a simple way to evaluate the quality of the work.

Also it enables a better decision on whether to replace or repair machines in a very low efficiency condition. In this case, to estimate the full-load efficiency, the proposed method requires only uncoupled no-load testing under refurbishment. The proposed method is tested on several types of induction motor, at 7.5, 15, 25, 50, 100 and 125 HP and estimated the efficiency at loadings of 50, 75 and 100 percentage load. The actual efficiency value is compared with the estimated value and the estimated result shows that the proposed method estimated the efficiency with an acceptable range of error [65].

It is estimated the induction motor field efficiency using a genetic algorithm. In this paper, the proposed method estimated the efficiency using field test data and nameplate information to evaluate the equivalent circuit parameters instead of no-load and blocked-rotor tests. The field test data considered is the measured input voltage, current, power, stator resistance and output speed of the motor. Then, the efficiency is determined by the impedance of the equivalent circuit. The equivalent circuit method is effective because the impedance of the equivalent circuit indicates the performance of the motor, particularly from no-load to full-load condition. The genetic algorithm with such procedure estimated the efficiency with high performance, especially in the short term, when the motor is in service [66].

It is presented a method to estimate the voltage profile in electrical distribution systems. It is stated that the utility company must monitor the voltage at each feeder due to power quality improvement. Since measuring the voltage creates a limit at every node, estimation techniques become important. Using such techniques reduces the number of meters. In this paper, locally weighted regression with three techniques, linear, non-linear and quadratic, is used in a radial bus system. The results showed that non-linear regression performed very well compared with the

other techniques. Non-linear regression can be the best choice for estimating the voltage profile given its high performance in the results [67].

It is presented a method to estimate the voltage in distribution systems using independent component analysis (ICA). The proposed method was applied in an example of an IEEE 69 bus system. It is observed that the voltage source is one of the significant key points in the distribution system that needs to be monitored. The ICA algorithm is implemented to predict the voltage at unknown points. This method helps to minimise the cost of the installation and maintenance of equipment. The proposed method gave results very close to the real values. The satisfactory results confirmed the performance of this method [68].

It is presented a method for estimation of the voltage drop in radial distribution networks. The method is called ‘global parameters’, in which the equivalent line is considered. The proposed method is applied in 16 distribution sectors in Montenegro where the parameters of the network and load in 1995 and 1996 are used. In this case, the parameters are taken from existing measurements. Two case studies including urban and rural consumption are analysed. The results obtained confirm that the proposed method can be satisfactory for voltage drop estimation in distribution systems [69].

It is presented a method to estimate the voltage sag in distribution systems, given the impossibility of voltage sag measurement at every node. The estimation technique becomes important in order to determine the voltage sag at unmonitored nodes. An IEEE 123 radial bus system is considered as a case study. A least squares method is used to estimate the sag profile at a distribution line. The main objective of this paper was to estimate the voltage profiles of feeders based on a limited number of metering

points. The results showed that the proposed method provided high performance in voltage sag estimation at unmonitored nodes [70].

It is presented a method to estimate the voltage in a smart distribution network and reported that the integration of distributed generations (DGs) at lower voltage levels created a voltage rise problem in distribution systems. Voltage estimation in a distribution network is important due to online voltage control. In this paper, a technique is used to estimate the voltage profile of radial distribution systems with multiple DG systems. The technique is tested in two rural radial distribution systems. The results showed that the estimated values match and the proposed method is able to estimate the voltage profile along the smart distribution systems for online voltage control [71].

It is presented a new technique for voltage sag estimation in distribution systems. The objective is to estimate the number of voltage sags at unmonitored buses. Linear programming techniques are used to solve the estimation problem. The proposed method is tested in IEEE 24 and 118 radial bus test systems, in which two monitors are placed at the 24 bus systems and eight monitors are placed at the 118 bus systems. Comparison of the results for the estimated voltage and actual voltage showed that the proposed method provided a very good agreement, indicating that it can be very useful to estimate the average sag in the network [72].

It is presented a method to estimate the voltage profile for control of a distribution feeder. It is stated that monitoring of the voltage profile in the distribution feeder can improve the reliability and quality of the distribution power system. The article presented a method to estimate the voltage profile of a radial distribution feeder where there is a limited number of monitoring points. A radial bus system with 343 buses and 83 load conditions is considered. An ANN is used for load forecasting and a

least squares method for voltage profile estimation. The proposed method provided results very close to the actual points, confirming the satisfactory performance of the proposed method. This paper also obtained the optimal capacitor-bank with the estimated voltage profile along the feeder for a 24-hour period [73].

It is applied a genetic algorithm for voltage sag estimation of distribution systems, observing that monitoring of voltage sag at non-monitored buses is important for the security and reliability of power systems. The proposed method was implemented in an IEEE 57-bus test system. The output results are compared with linear programming methods in order to indicate the high performance of the proposed method. The results showed that the genetic algorithm and linear programming produced average errors of about 2.79% and 3.27% in 24 buses respectively. In addition, in the case of the 57-bus system, the genetic algorithm provided a better result than the linear program, with average errors of 5.54% in the genetic algorithm and 7.48% in the linear program. Comparison of the results indicated that the genetic algorithm not only acted faster, but also provided satisfactory results at different nodes [74].

Estimation techniques and their related application in distribution networks are applied. It is reported that estimation techniques are useful to monitor and control the voltage in transmission distribution systems because they are not only economical, but can also be a good solution to determine the voltage profile at unmonitored points. The proposed technique can be used also for online monitoring to improve the voltage drop [75].

It is used a neural network method to estimate the voltage profile caused by the presence of small-scale generation in a distribution network and notes that the presence of distributed generation in distribution network affects the voltage of the

feeder. Monitoring of the voltage profile is necessary in order to prevent a voltage rise or drop. It is observed that this economical technique is able to obtain the voltage at any desired point. Then a tap changer transformer can regulate the voltage along the feeder. The results showed that the artificial neural network can be very good at properly estimating the voltage profile of distribution systems [76].

2.8. Past Research on Power Factor Correction

There are several procedures to correct the power factor of induction motors using the capacitors bank. One is individual power factor correction (IPFC), where the power factor is corrected by adding capacitors into the motor terminal individually. This kind of power factor correction is suitable in the case of constant motor load and power. However, the IPFC method has the problem that, when the motor disconnects, the motor shaft is still rotating (due to residual kinetic energy) and the reactive energy that is extracted from the capacitor creates a risk of dangerous over-voltages in the motor terminal.

The second is group power factor correction (GPFC) that is used to correct the power factor of groups of induction motors. This technique is more applicable for induction motors of the same size that are operating together. GPFC also provides a compromise between an inexpensive solution and the proper management of the installation. The advantages of this method are similar to the individual correction method. This method can only be used in the condition where all the induction motors are always operating at the same loads.

The third method is central power factor correction (CPFC), which automatically switches the capacitors in and out of service by an automatic reactive power control (ARPC) relay and contactors. The central power factor correction method has several advantages.

It is easy to monitor and provide power factor correction at various motor loads, unlike IPFC and, in addition, it is more reliable in coincidence conditions. The main disadvantage is the cost of the automatic control system.

The fourth method is hybrid power factor correction (HPFC). In this method, all the abovementioned techniques are combined, providing a significant power factor correction in any size of induction motor with constant and inconstant motor loads. HPFC provides multiple advantages since all the power factor correction methods are considered. The main disadvantage of this method is the high cost of installation.

Ghosh presented the theory of power factor measurement and the correction technique. In electrical systems, there are several methods to correct the power factor, including the static VAR compensator (SVC), fixed capacitors, switch capacitors and synchronous generator or motor, static synchronous compensator (STATCOM) and modulated power filter capacitor compensator. The SVC is a shunt device in the flexible AC transmission systems (FACTS) and uses power electronics to regulate the voltage at its terminal by controlling the amount of injected reactive power. For instance, when the voltage is low, it generates reactive power and when the voltage is high, it absorbs reactive power.

The variation of reactive power is controlled by switching the capacitors bank and inductor bank. Each capacitors bank is switched on and off by thyristor-switched capacitors (TSC) and a thyristor-switched reactor. Fixed and switched capacitors are significant techniques used particularly in industrial factories to correct the power factor. Fixed capacitors are suitable for power factor correction in the application of induction motors with fixed loads. Switched capacitors are suitable for centralized power factor correction in the application of load variation, and need the amount of

reactive power at any loading point. A synchronous generator is more economical than capacitors to correct the power factor [15, 77].

It is described a new approach to improve the power factor and reduce the total harmonic distortion (THD) of induction motors. In this technique, an active filter is considered in order to eliminate the harmonic current and improve the power factor. The measured results of the induction motor showed that with increase of the voltage step by step from 180 V to 240 V, the speed and the THD % increase because both are proportional to the increment of the input voltage. However, increase of the input voltage indicated a decrease of the power factor by about 18%. Adding an active filter not only causes the THD to decrease from 172.76% to 48.71%, but also improved the power factor from 0.72 to 0.89 at a voltage of 180 V. As a result, using such techniques reduces the effect of loss and heating and improves the efficiency and the power factor of the induction motors [78].

It is used an algorithm in order to find the optimum number of fixed capacitors and reduce the harmonic distortion to maintain the power factor displacement at the desired level. The test results in two cases indicated that the performance of the proposed method is satisfactory and the transmission losses, distortion level and the power factor are improved. It is understood that a high angle between the voltage and current, even with harmonic distortion in the induction motor or in electrical systems, provides a low power factor, which creates power quality problems. In this chapter, several articles have been reviewed and discussed about power factor measurement and correction techniques as follows [8].

It is presented a finite element method to calculate the power factor of a single induction motor. It is stated that the power factor and manufacturer's data sheet are vital because they indicate how much reactive power is consumed by the induction

motor. It is observed that obtaining the value of the power factor is not an easy task and requires a significant technique for estimation. In this work, finite element analysis is used to estimate the power factor of a single-phase induction motor. The components of the input power and the RMS value of the first harmonic of the input current are considered for the power factor estimation. Simulation results and tests indicated that the proposed method provided a good solution to obtain the power factor of the induction motor [20].

It is presented a significant algorithm for measuring the power factor of resistance spot welding (RSW). It is stated that the power factor is quite important for safe operation and analysing the welding operation, since RSW is non-linear and time-varying. The power factor of RSW cannot be determined online because direct measurement of the power factor angle is difficult in real time. Therefore, a new algorithm is developed to determine the power factor angle in real time. The results indicated that the proposed algorithm is able to obtain an accurate value of the power factor angle better than other methods. The value of the power factor angle obtained from the proposed algorithm is very close to the result of numerical simulation [21].

It is implemented a novel method to measure the instantaneous power factor of non-sinusoidal single-phase systems based on wavelet transform. An algorithm is implemented with a digital signal processor along with a data acquisition system card. The results confirmed that the proposed method can be successfully used for online measurement of the instantaneous true power factor for both sinusoidal and non-sinusoidal waveforms. In addition, the proposed algorithm is able to indicate lagging and leading measured power factors. The unique advantages of the proposed algorithm for measuring the power factor are its fast response and frequency independency.

It is stated that the real-time monitoring of the power factor is more applicable for tariff assessment in a deregulated environment [79].

It is examined how the power factor changed due to the loading effect. In this paper, the power factor is obtained from recorded voltage and current waveforms using a digital signal processing algorithm. The load is a combination of resistance, reactance and capacitance (RLC). The values of resistance and capacitance are fixed, but the value of reactance is considered to be varying. The results showed that variation of the load affects the change of power factor. For instance, keeping the capacitance constant and varying the value of inductance from 269.1 mH to 1.232 H and with resistance of 36 ohm and 124 ohm, resulted in different values of the power factor. The minimum and maximum value of the power factor for the resistance of 36 ohm is 0.02 and 0.03, and for the resistance of 124 ohm is 0.104 and 0.148 respectively [80].

It is described the effect of the compensating power factor on harmonic distortion. In this article, two case studies with linear and non-linear loads are analysed in which client-1 is switchable loads containing R load and RL loads with a capacitor. Client-2 is a rectifier load. The test results indicated that with the presence of client-1 as a linear load with connected capacitors, the power factor and power factor displacement become unity since the load is linear and the THD of the voltage and current are near zero. However, by adding client-2 (which is non-linear) with the presence of the capacitor, the total harmonic distortion has values of 11.34% and 83.5% in the voltage and current respectively. The power factor was reduced to 0.707, but the power factor displacement did not change due to the presence of the capacitor. It can be observed that disconnecting the capacitor decreases the THD of the voltage and current by 5.5% and 1.3% respectively.

The power factor displacement was reduced to 0.707. To optimize the power factor and power factor displacement, an inductive reactance connecting in series with the capacitor is required [81].

It is presented a new method to obtain the LC compensators for optimal power factor correction in non-sinusoidal systems. Such compensators serve two purposes. The first is to improve the power factor at non-linear loads. The second is to eliminate the harmonic current in the network. Determination of the optimal LC compensator with conventional methods is difficult because it needs multi-objective optimization. In this paper, a new solution algorithm with a penalty function has been developed to find the desired value for the LC. The results indicated that the proposed method improved the conventional approach compared with existing publications [82].

A method is used to design a passive LC compensator for power factor correction in non-linear loads. The penalty function method as an optimization tool is considered for selection of an appropriate inductor and capacitor. The results of the proposed method showed lower losses and a higher efficiency, and a higher power factor displacement than the uncompensated case. The presented method implemented two important tasks. One is the level of reactive power and the other is harmonic currents. The significant advantage of the proposed method was to reduce the harmonics in the lines, cables and switchgear. It is noted that the power factor curve is required for selecting the capacitor for the best average performance [83, 84].

A reason for maintaining the desired power factor in electrical systems is presented. It is explained that utilities often encourage consumers to provide a power factor toward unity because a high power factor reduces system losses and increases the internal electrical distribution capacity and therefore improves the voltage stability.

In addition, holding the power factor at the desired value prevents a monthly penalty

charge from the utility company. For consumers, using a capacitors bank can be a good solution to compensate a low power factor. This approach not only saves money, but also increases the capacity of the cable in order to take the maximum useful power in kW [5, 85].

It is presented a technique to reduce the harmonics and improve the power factor of a three-phase 1 HP induction motor using a passive LC component. The result showed that by adding the passive LC filter, the harmonics reduced from 93.5% to 57% at a load of 200 W, and at a load of 600 W they reduced from 102% to 65.8%. In addition, by adding the filter, the power factor improved from 0.6 to 0.724. Therefore, passive LC is a simple technique to design and helps to eliminate the THD. The presence of passive LC also improves the quality of power and maintains the power factor in a high range at different loading conditions [86].

Shunt capacitors have been used for many years to improve the power factor of induction motors. However, connecting the capacitors directly to the motor terminal has created over-voltage due to self-excitation. Self-excitation occurs when the capacitive reactance becomes greater than the magnetic reactance. Since the power factor is proportional to the motor load from no-load to full-load, fixed capacitors may create self-excitation. Ensuring the proper value of the capacitors and using switching capacitors can be a good solution to prevent self-excitation problems. As a result, it is stated that selecting the proper size of shunt capacitors can not only prevent over-voltage due to self-excitation but also maintain the power factor at the desired point from no-load to full-load and over-load conditions [87, 88].

An optimization technique is designed for a linear induction motor in order to improve the power factor and efficiency. It is observed that induction motors are mostly used in industry. Induction motors produce a low power factor and low

efficiency, which increase the input current and create more losses in the systems. A genetic algorithm with an appropriate objective function is used to improve both the power factor and the efficiency. The parameters of a three-phase induction motor are selected as the basis of design optimization. The minimum value of the power factor and the minimum value of efficiency are chosen as the initial values in the algorithm. The results indicated that the power factor improved by up to 7% and the efficiency increased by about 2% [89].

A method is presented to correct the power factor using a microcontroller automatically. It is reported that the initial power factor is corrected by adjusting the capacitor manually. However, many industrial factories have trouble using this technique since under- and over-correction occur due to variation of loads. In this paper, an automated power factor corrector using a capacitors bank is proposed to solve this problem. The proposed method involves a power factor meter and microcontroller, which are connected together. The power factor meter is used to measure the value of the power factor at different loads and the microcontroller is used to detect the low power factor and then connect the required capacitors automatically to take the power factor close to unity. Selecting the size of each capacitor is estimated based on the active power and initial power factor from no-load to full- and over-load condition. The results show that this technique not only helps to reduce the time, but also increases the efficiency through the entire electrical systems [90, 91, 92].

It is presented a programmable logic controller (PLC) to switch the capacitors bank so as to correct the power factor of induction motors at any loading condition. It is noted that the power factor of induction motors is always low, particularly at no-load and light-load conditions. These conditions draw a large magnetization current and also deliver low active power into the motor. Based on the determined value of the

power factor from no-load to full-load/over-load conditions, the PLC switches the appropriate capacitors into the circuit to correct the power factor. The results from the 3 HP induction motor indicated that the capacitors switched by the PLC in five different load conditions reduced the current and improved the power factor to the desired value, which consequently provided an energy-saving and power quality improvement [93].

It is researched the power factor regulating tariff standard. The study reported on the actuality and the problem of the existing power factor regulating tariff. The study indicated that the regulating tariff power factor can be determined based on different types of client, and could be classified as 0.8, 0.85 and 0.9. The standard power factor level is fixed by the voltage quality and line loss. It is concluded that the power factor adjustment tariff creates the simplest and most convenient way to enhance the performance of the electrical grid. In addition, it motivates users to improve the power factor by using generating reactive power [94].

It is presented the effect of power quality indices containing voltage distortion, voltage unbalance and voltage dips on a 4 kW induction motor. The power factor and efficiency are analysed based on the motor load, rated frequency and standard level of power quality. The experimental results showed that the characteristics of the induction motor are significantly impacted by voltage dips. The efficiency decreased linearly with the level of voltage distortion in a specific range of motor load. The decrease of efficiency was about 3% at the rated motor load in both voltage unbalance and voltage distortion and in a voltage dip it was higher than 1%. Unbalanced voltage mainly affected the power factor, which decreased by about 2% [95].

It is presented a power factor controller for a three-phase induction motor using a

programmable logic controller (PLC). The PLC switches the capacitors on and off in order to improve the power factor. Variation of motor load affects the power factor and particularly when the motor load is low the power factor also is low. Therefore, capacitors must be added to improve the power factor. However, when the motor load increases, the power factor becomes high so the capacitor must be disconnected. This process is implemented by the PLC. The algorithm is divided into four sections. Firstly, read the phase angle between the voltage and current. Secondly, calculate the power factor. Thirdly, switch the capacitor to correct the power factor. This controller cannot consider the harmonics in the systems, and is only responsible for switching capacitors at different loadings at the steady-state condition [96].

It is presented a power factor improvement of an induction motor using a capacitors bank. It is found that improving the power factor of the induction motor saves more energy. However, a low power factor needs more current, which creates losses in the system. In the induction motor, no-load and light load produce a low power factor. In this paper, a capacitors bank is applied to the stator side with parallel connection to improve the power factor in such conditions. The simulation obtained the power factor from no-load to over-load with six loading points. The measured result showed that the power factor at no-load is very low, at about 0.17. By increasing the mechanical load, the power factor is improved in the rated power. The results of adding capacitors indicated that the power factor at no-load improved, reaching 0.977. Therefore, a capacitors bank is one significant device to improve the low power factor at any loading point. It is observed that the proper size of capacitors can be selected by having the old value of the power factor from no-load to full-load, which is obtained by measuring devices [13].

It is presented a static switched capacitor for improving the power factor of a three-

phase induction motor when starting and operating. It is stated that improving the power factor of the induction motor requires reactive power compensation that can be generated by a synchronous machine, fixed and switched capacitors. Such techniques create some problems, such as voltage rising and very high inrush current during starting. Also, a large harmonic current in machines and lines take place. The proposed method prevents harmonics and inrush current when starting and eliminates the over-or under-voltage problems [97].

It is presented a technique using an artificial neural network to improve the line power factor with variable loads. A synchronous motor is controlled by a neural network to handle the generated reactive power. A back propagation algorithm is used for training. The results indicated that the proposed method developed the work and eliminated the problems occurring in conventional compensators, such as over-or under-compensation, time delay and step change of the reactive power. Also, it creates a low-cost solution with fast compensation compared with other techniques [98].

2.9. Summary

It is understood that the power factor is an important element in electrical motors and power systems because it affects the energy efficiency, voltage drop, line capacity, self-excitation and so on. The reviewed papers indicate that there is a non-linear relation between the power factor and load whereby the power factor will always take different values with variation of the load. A lower power factor than the desired level produces a disturbance. Many researchers stated that power factor compensation is an important technique to maintain the power factor at the desired level. However, determination of the required reactive power for power factor compensation is needed. Whereas many papers presented various techniques to

compensate the power factor, the VAR needs to be predicted before compensation. Predicting the proper size of capacitors in VAR is not only cost-effective, but also helps to prevent under- or over-correction at operating time. Therefore, this important subject represents a research gap, still needing an accurate solution for power factor determination against load.

This chapter presented several techniques to determine the power factor from no-load to full-load conditions. Many papers have discussed how the presence of equivalent circuit parameters can evaluate the performance of the induction motor and determine the power factor. However, these parameters are unknown. Many papers examined ways to determine the equivalent circuit parameters using the available manufacturer data and proposed estimation techniques. [14] reported that determining the power factor from no-load to full-load conditions by using equivalent circuit parameters created difficulties and made the work more complicated because several estimation techniques are required to determine all the parameters, including resistance and reactance in the rotor and stator side, magnetization reactance, and core loss resistance. Also, leakage reactance on both sides is needed because all these parameters require computation of the impedance, as the cosine angle of impedance provides the power factor. In other words, to find the power factor at different loads, the mechanical resistance must be estimated. All these processes make the solution complicated. It is found that MCMD is able to estimate the power factor without using equivalent circuit parameters.

[26] notes that although this method is sufficient to determine the power factor of the induction motor, it requires the induction motor to be installed and the current needs to be measured from no-load to full-load conditions. In addition, using this method is not suitable for medium and large induction motors. Since the reactive current is not

constant, high errors will be produced. However, [26] provided a solution by implementing a Kriging and regression method in the induction motor, as introduced by [24, 25]. It is observed that both methods are able to create models of the observed data, and then estimate the power factor from no-load to full-load conditions. However, both methods produce high error from full-load to over-load conditions because they are interpolation techniques and are not able to extrapolate the unseen points.

Since the motor load is variable in some cases, this variation will be reflected in the power factor. Therefore, determination of the power factor at any loading point with high accuracy remains a research gap. In this project, statistical and intelligent techniques drawn from the reviewed papers will be implemented in different size induction motors in order to identify the best method.

This chapter described the impact of power factor determination and correction in electrical systems. It also reviewed the various methods to determine the power factor in electrical loads in particular induction motors. In addition, estimation of the equivalent circuit parameters for the purpose of determining the power factor and analysing the performance of the induction motor is reviewed. The reviewed papers assert that determining the power factor of the induction motor at any loading point with high accuracy is very important due to power factor compensation. This subject is still open for further research. Therefore, through the reviewed estimation technique, in this project, implementation of statistical and intelligent techniques in different ranges of induction motors will be considered in order to determine the power factor of induction motors at any loading conditions.

Chapter 3: Determination of Load and Power Factor

3.1. Introduction

The following sections will outline the theory of the induction motor, and the effect of load variation on the induction motor characteristics, and then describe the power factor and its behaviour versus motor load. The procedures for calculating the power factor and motor load and also correcting the power factor are detailed. The experiment and simulation have been considered to determine the power factor of various induction motor loads, from no-load to full-load and over-load conditions.

3.2. Theory of the Induction Motor

Induction motors are constructed with a stator and rotor. The stator includes a series of wire windings. The rotor consists of a number of thin aluminium bars which are mounted in a laminated cylinder horizontally and parallel to the motor shaft. At both ends of the rotor, the bars are connected together with a short ring. The rotor and stator are separated by an air gap to allow free rotation of the rotor. A three-phase voltage connected to the induction motor creates a three-phase stator current [11]. These currents generate a magnetic field named B_s that rotates in a counter-clockwise direction. The rotating magnetic field B_s moves through the rotor bars and induces a voltage. The voltage induced in the rotor bars is expressed by Equation (3-1).

$$e_{ind} = (v \times B) \cdot l \quad (3-1)$$

where v is the velocity of the bar, B is the magnetic flux density, and l is the length of the conductor in the magnetic field. Then, the voltage of the rotor creates a rotor current flow, which lags behind the voltage due to the rotor's inductance.

The rotor current generates a rotor magnetic field B_R lagging 90° behind itself and B_R interacts with B_{net} to generate a counter-clockwise torque in the motor. The speed of the magnetic field's rotation expresses the speed of the rotor, which is called synchronous speed (n_s), which is a function of the frequency of the power source and the number of poles in the motor. Calculation of the synchronous speed for the induction motors is given in Equation (3-2).

$$n_s = \frac{2}{P} f_e 60 \quad (3-2)$$

where f_e is the frequency in Hz and $\frac{2}{P}$ is the resultant of one complete cycle, where P is the number of poles in the motor. n_{sync} is the synchronous speed in rpm. In the induction motor, rotor speed n_r and the stator speed or synchronous speed n_s have different values during operating time from no-load to full-load. This difference is expressed as a ratio of the synchronous speed in percentage, which is also referred to as slip, indicated with s as follows:

$$s = \frac{n_s - n_r}{n_s} \quad (3-3)$$

The slip (s) is between 0 and 1 where the motor speed falls between those limits. For instance, if the rotor reaches the synchronous speed, the slip becomes zero, while if the rotor is at a standstill, the slip is one. The reason why these speeds cannot be equal to each other is that if the rotor speed of the induction motor reaches the synchronous speed n_s , no voltage will be induced.

If the voltage induced is equal to zero, the rotor current will be zero and, as a result, the rotor magnetic field becomes zero. Then, with no magnetic field, the induced torque becomes zero and there is consequently no rotation. Therefore, in the induction motor, the presence of slip is required, in which n_r is always smaller than n_s . Due to these phenomena, the induction motor can be termed an asynchronous motor [9]. Slip can also be expressed as in Equation (3-4), where n_{slip} is the slip speed of the induction motor, n_s is the speed of the magnetic field, and n_r is the mechanical rotor speed of the motor.

$$n_{slip} = n_{sync} - n_r \quad (3-4)$$

3.3. Load Determination of Induction Motor

The mechanical or resistance load, which is coupled to the induction motor, indicates the output power, also known as the induction motor load. The equation (3-5) computes the output power.

$$P_{out} = \frac{2\pi NT}{60} \quad (3-5)$$

where T is the motor torque and N is the rotor speed. Since the torque and speed sensors may not be available in many induction motors, the motor load can be estimated by an empirical method known as input power measurement.

- **Input Power Measurement**

Input power measurement is one of the significant methods used to estimate the motor load due to the torque and speed limits of the induction motors [99]. In this method, it is required to obtain the input power at any loading point, from no-load to full-load and over-load. This value can be determined either by directly measuring the input power or by measuring the voltage, current and power factor, and then applying these in Equation (3-6).

$$P_i = \frac{\sqrt{3} \times V \times I \times PF}{1000} \quad (3-6)$$

where P_i is the three-phase input power in kW, V is the RMS volt, mean line-to-line of 3 phases and I is the RMS current in amp. In addition, the full rated input power is necessary in calculating the motor load. Equation (3-7) computes the full rated input power, then Equation (3-8) determines the load of the induction motor.

$$P_{ir} = \frac{HP \times 0.7475}{\eta_n} \quad (3-7)$$

$$Load = \frac{P_i}{P_{ir}} \times 100\% \quad (3-8)$$

where P_{ir} is the input power at full rated load in kW, HP is the nameplate rated horsepower, and η_n is the efficiency at full rated load. Consequently, the motor load will be calculated by the measured three-phase power (kW) over the full rated input power (kW) in Equation (3-8). To substantiate the accuracy of the input power measurement, Figure 3-1 indicates that the motor load obtained from the input power

measurement method has an approximate linear relationship with the output power. These linear relationships verify that the input power measurement method can determine the acceptable motor load.

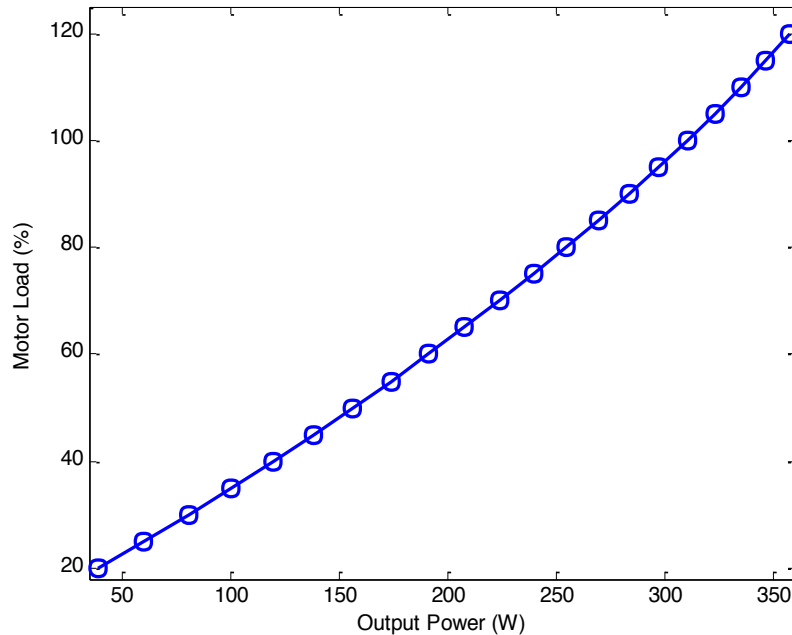


Figure 3-1: Output power versus motor load (IM 250 W)

3.4. Effect of Load on Induction Motor Characteristics

In the induction motor, the load is an important element and has a significant role in the performance of the induction motor because variation of the motor load will change many elements, including the speed, efficiency, the parameters of the equivalent circuit and the power factor. The effects of load variation on the induction motor elements are described in detail below.

3.4.1. The Speed

In the induction motor, the rotor speed is the rotation of the motor shaft indicated in revolutions per minute (rpm). It can be observed that variation of the load affects the rotor speed of the induction motor where increase of the load decreases the rotor speed. The reason is change of motor slip because the difference between the

synchronous speed and rotor speed, is slip. With increase of the motor load, the slip increases and therefore, according to the rotor speed equation $n_r = n_s(1 - s)$, the speed decreases. Figure 3-2 indicates the motor load versus speed, where increase of the motor load decreases the speed slightly.

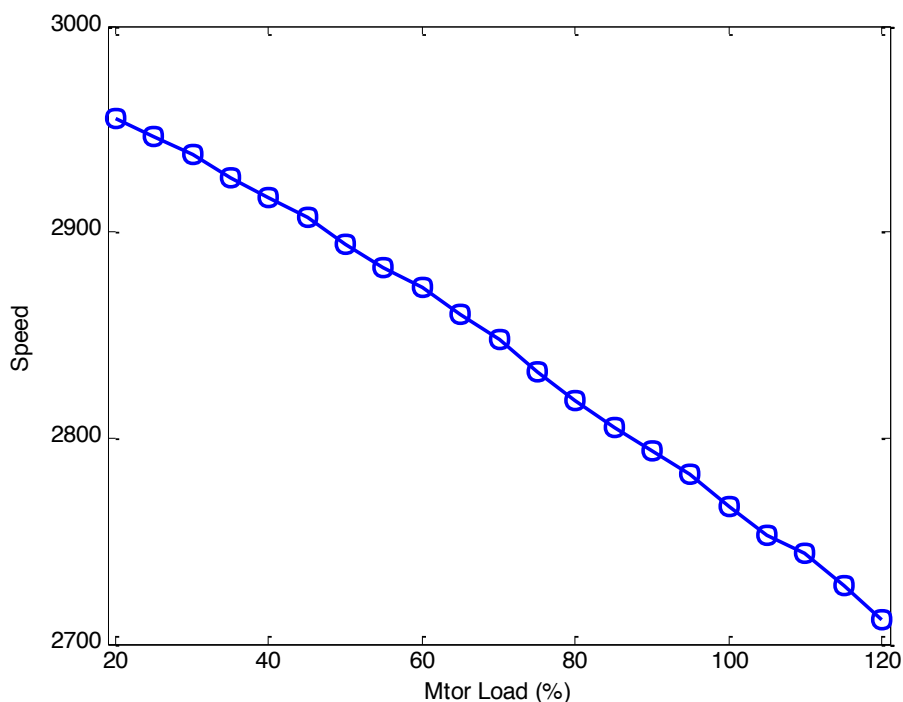


Figure 3-2: Speed versus motor load (IM 250 W)

3.4.2. The Efficiency

In the induction motor, the efficiency is a ratio of mechanical output power over electrical input power, indicated in percentage. Figure 3-3 shows that the motor load affects the efficiency, such that the efficiency is very low at the no-load condition when there is no mechanical power. However, by increasing the motor load, the input power increases and so the efficiency increases as well. In the induction motor, the losses comprise core losses, windage, friction losses and copper losses and create a low efficiency.

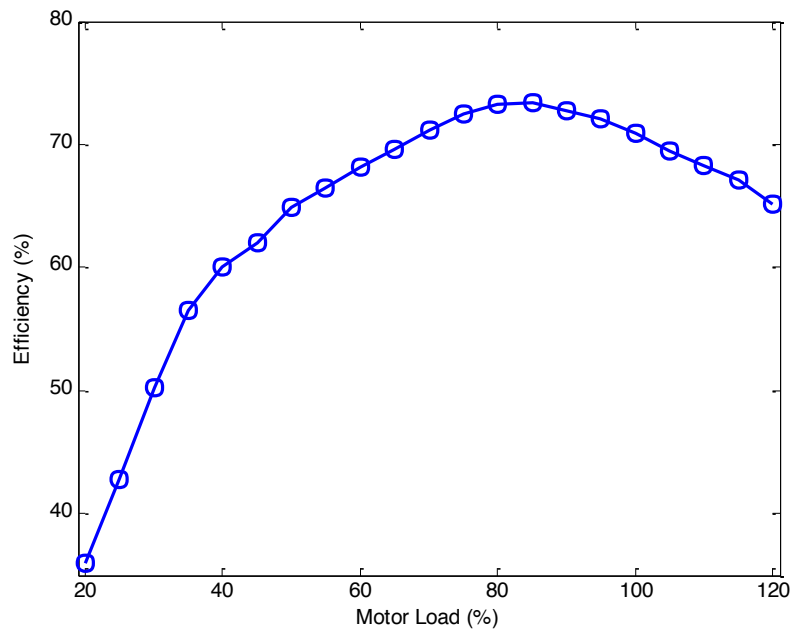


Figure 3-3: Efficiency versus motor load

3.4.3. The Power Factor

In addition, in the induction motor, the load affects the power factor because when the motor load changes from no-load to full-load and over-load, the power factor also changes. Figure 3-4 indicates that variation of the motor load has a non-linear relationship with the power factor. This variation causes the motor impedance to change and the motor impedance provides a change in the stator current that results in power factor variation. The equivalent circuit of an induction motor can be used to describe the reason for the variation in detail.

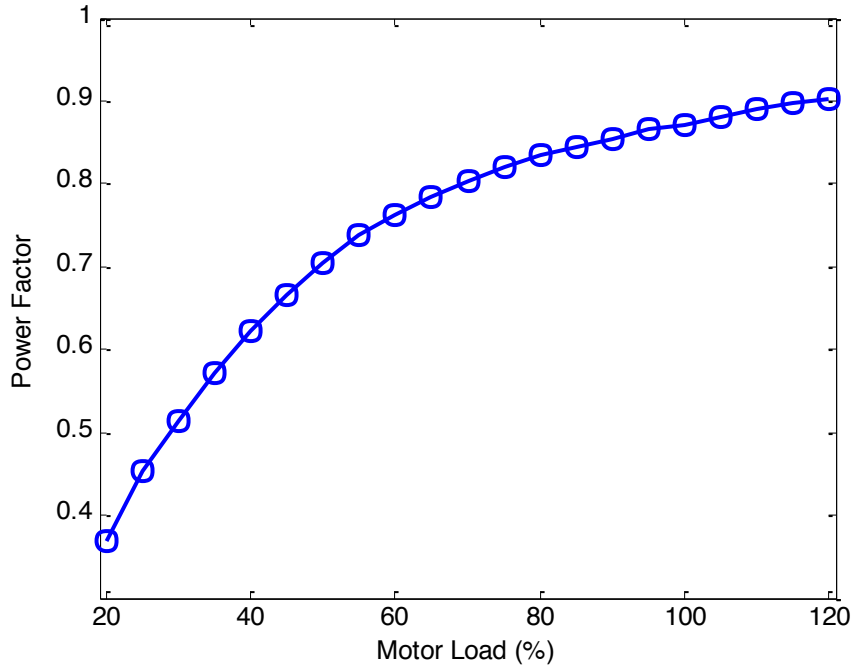


Figure 3-4: Power factor versus motor load (250 W)

The equivalent circuit of the induction motor is a diagram to describe the behaviour of the power factor versus the motor load. Figure 3-5 indicates that the diagram contains resistance and reactance, where V and I_s are the voltage terminal and stator current [9].

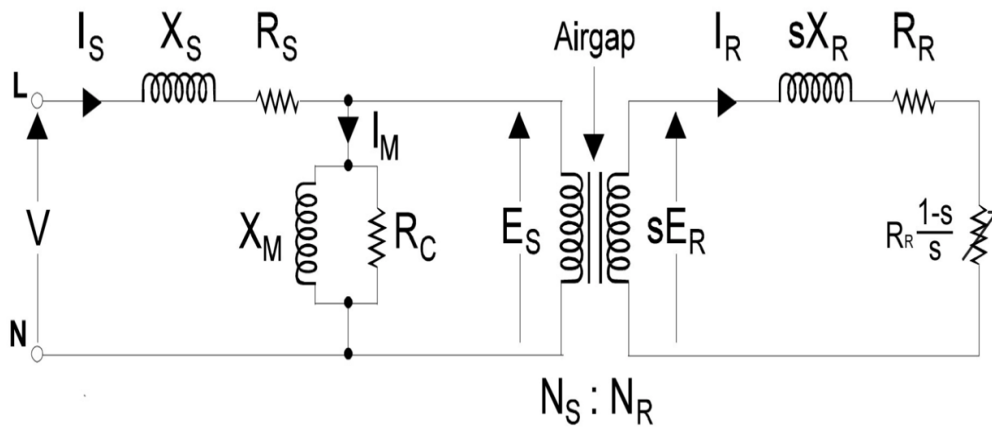


Figure 3-5: Equivalent circuit diagram of induction motor

E_S and E_R are the stator and rotor induced voltage, R_S and X_S are the stator resistance and stator leakage reactance, R_R and X_R are the rotor resistance and rotor leakage reactance respectively, I_R is the rotor current, X_M and I_M are the magnetizing inductance and magnetizing current, R_C is the losses (core losses, bearing friction, windage losses, etc.), $R_R \frac{1-s}{s}$ is the mechanical load where the s is motor slip, and N_S and N_R are the stator and rotor turns.

In this diagram, the stator current has a significant role in the behaviour of the power factor because the stator current can be decomposed into the active current and reactive current, which are consumed in the resistance and reactance components respectively [10]. Since the impedance of the equivalent circuit changes with variation of the load, the active and reactive current change, which causes the power factor to change. The reason for impedance variation is that when the induction motor is working at the no-load condition, the slip and mechanical resistance are approximately zero, which causes the rotor current to become zero, so all the input current flows through the stator side. In the stator side, the majority of the current is pass through the magnetizing reactance to create magnetic field. Only a small amount of the current is required in stator resistance and core losses. Therefore, at this condition, the stator current lags the stator voltage by the angle of θ_0 in the range of $75 - 85^\circ$, and therefore the power factor in the stator side will be approximately between 0.1 and 0.3.

However, when the motor load increases gradually, the mechanical resistance increases, and consequently the demand for active current will be high, for supporting the rotor resistance and mechanical resistance. Since the rotor resistance is constant, the mechanical resistance consumes the majority of the active current.

The high consumption of active current will be greater than the reactive current and so provides a high increase of the power factor.

Although rotor and mechanical resistance demand more active current from light-load to full-load, rotor leakage reactance requires reactive current as it will appear from light-load to full-load conditions. This can be a significant reason why the reactive current from light-load to full-load is not constant. Consequently, from Figure 3-6 it can be understood that from no-load to full-load condition, variation of the active current is higher than variation of the reactive current, so the active current has a major role in the power factor changing versus load.

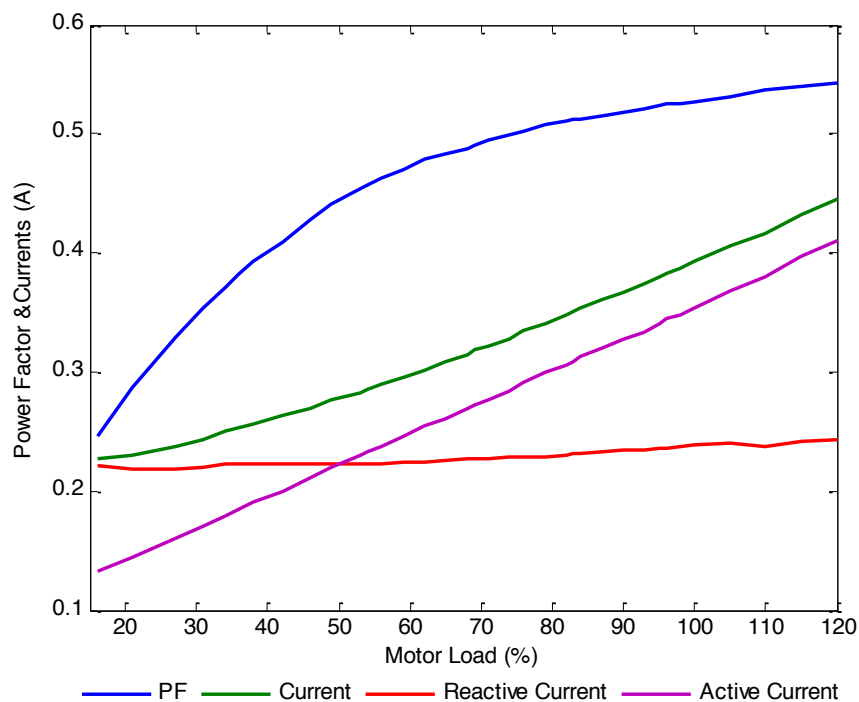


Figure 3-6: Current versus motor load (IM 250 W)

To find the value of the power factor against motor load, it is necessary to determine the parameters of the equivalent circuit by performing significant tests on the induction motor. The no-load test method is used to determine the losses of the induction motor and indicates the reaction of the magnetization reactance.

In the no-load test, the balance voltages are connected to the stator terminals at a rated frequency. The current, voltage and power at the input to the motor are measured when there is no mechanical load. The measured input power shows only the losses consisting of core losses, winding and friction losses.

In the no-load test, the rotor side acts as an open circuit, which means that the rotor current is zero (as there is no mechanical resistance). Hence, R_R and X_S are neglected. As a result, the magnetization current will be approximately equal to the input current. However, a DC test can be applied to determine the stator resistance at no load. By connecting a DC voltage to the stator windings of the induction motor, it produces a current. As the current is DC, there will not be any induced voltage in the rotor circuit, which results in no rotor current flow and no magnetization reactance. Hence, only limited current is drawn in the stator resistance R_S .

At the rotor side, the rotor resistance is neglected because the mechanical resistance is too large and acts as an open circuit, which means there is no current ($I_R = 0$) through the rotor side, and so the DC test obtains the stator resistance R_S . The locked rotor test is applied to provide the impedance of the equivalent circuit. The locked rotor test requires the motor shaft to be locked while the AC voltage is applied. The voltage, current and power are measured when the current is at a maximum (at full-load current, before heating up the motor). In this situation, since the rotor shaft is not moved, the slip is equal to one.

Therefore, the rotor resistance $\frac{R_R}{s}$ corresponds to R_R . Since R_R and X_R are considerably smaller than the magnetizing reactance, most of the input current will flow through the R_R and X_R . Consequently, under this condition, the circuit will be a series combination of R_S , X_S , R_R and X_R . In such method, the total impedance is obtained, where the angle of the motor impedance can provide the power factor.

It is understood that the efficiency and the power factor have significant roles in the performance of the induction motor, in which low efficiency means consuming more active power in losses and a low power factor means consuming more reactive power in the magnetizing reactance and reactance leakage losses. In spite of the fact that by reducing the losses, the power factor can be improved, reducing the air gap between the rotor and stator causes the power factor and the efficiency to improve. However, a higher load with a smaller air gap increases the stray load losses in the motor, which tends to decrease the efficiency. Consequently, from Figure 3-7 it can be understood that the power factor has a relationship with the efficiency from no-load to full-load, in which, as the motor load increases from no-load to full rated, the power factor and motor efficiency increase. However, the efficiency tends to decrease at higher/over-load due to induction motor losses.

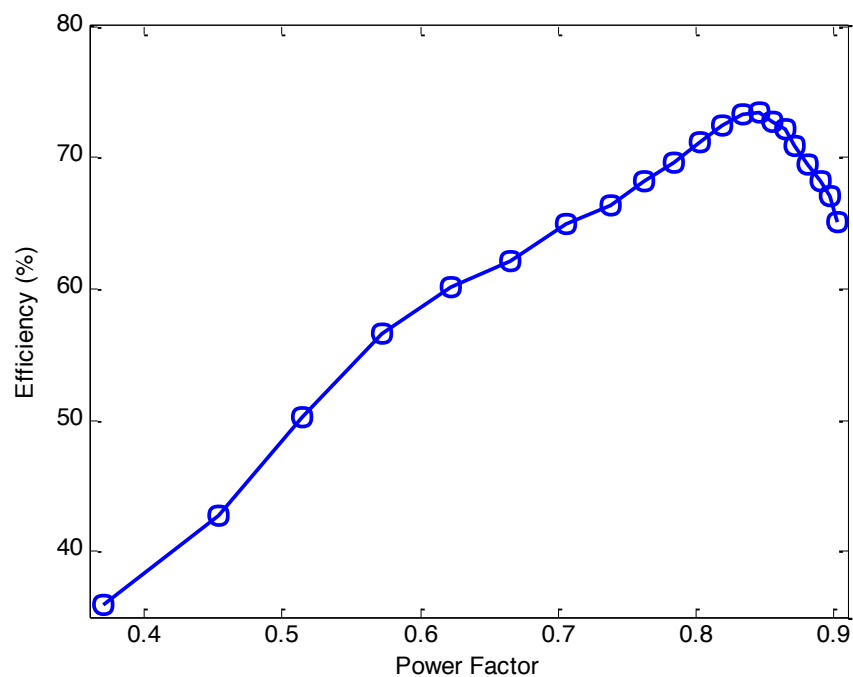


Figure 3-7: Power factor versus motor efficiency (IM 250 W)

3.5. Power Factor Description of Induction Motor

In electrical motors and systems, the presence of a power ratio is quite important in indicating how much useful power is being consumed [12, 4]. This ratio can be called the power factor. Indeed, the power factor has been described in two aspects.

The first is power factor displacement (PFD), which is recognised as the cosine angle ($\cos \phi$) between the fundamental voltage terminal and stator current, as shown in Equation (3-9), where the stator current can be expressed by Equation (3-10). The second is power factor distortion, which appears when the voltage terminal and stator current waveforms are distorted.

$$\cos \phi = \frac{P_{in}}{V_T I_S} \quad (3-9)$$

$$I_S = \frac{V_T}{\sqrt{R_S^2 + X_S^2} + \frac{1}{\sqrt{\left(\frac{1}{X_M}\right)^2 + \left(\frac{1}{\frac{R_R}{S}}\right)^2 + \left(\frac{1}{X_R}\right)^2}}} \quad (3-10)$$

where P_{in} is the input motor power, V_T and I_S are the voltage terminal and stator current that provide $\cos \phi$. I_S is the voltage terminal over motor impedance, where the motor impedance contains the stator resistance R_1 , leakage stator reactance jX_M , magnetizing reactance jX_M , rotor resistance over slip $\frac{R_R}{S}$ and rotor leakage reactance jX_M . This equation can only be used when the terminal voltage and motor current waveforms are sinusoidal. Indeed, the power factor displacement is suitable as an indication of lagging and leading load. For instance, from Figure 3-8, if the current lags the voltage, the cosine angle will be positive, which means that the load is

inductive and consuming reactive power or current. However, if the current leads the voltage, the power factor will be negative, which means that the load is capacitive and reactive power or current are being generated.

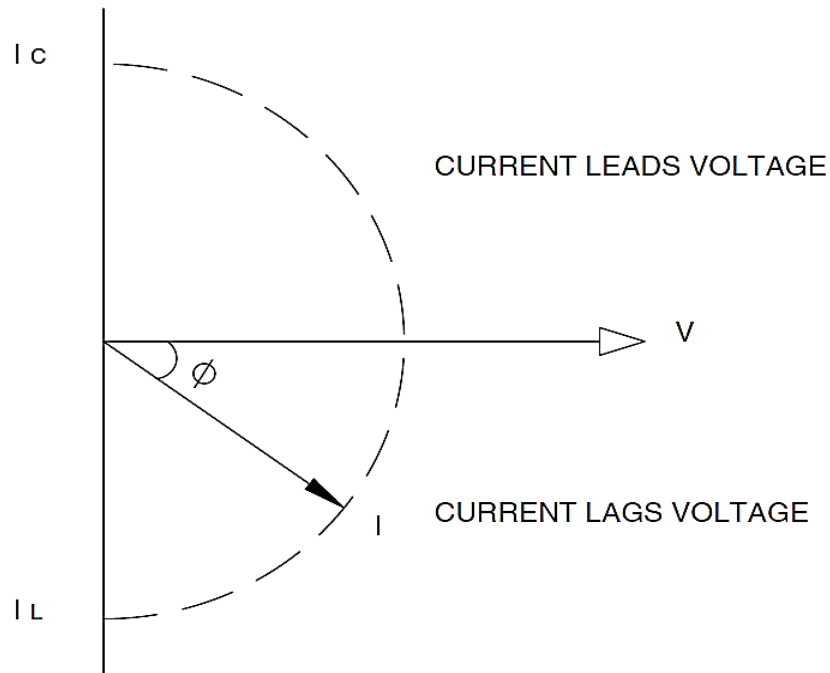


Figure 3-8: Voltage and current phase angle

In other words, the power triangle diagram in Figure 3-9 can describe $\cos \phi$, where it is also located between the active power and apparent power. The power triangle diagram shows that the reactive power is proportional to the power angle. For instance, if the reactive power Q or current I_Q is small, the power angle also is small and results in a high $\cos \phi$, but if the reactive power increases, the angle increases, which tends to a low $\cos \phi$.

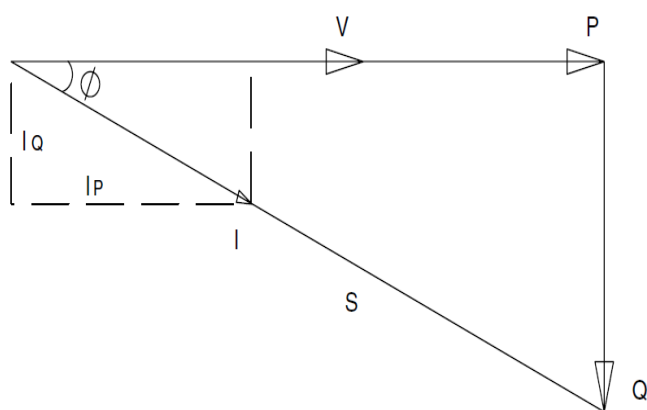


Figure 3-9: Power triangle diagram

Consequently, it can be understood that the active and reactive power have a significant role in determining $\cos \phi$ because the power factor can also be expressed as $\frac{P}{P+jQ}$. The active power and reactive power can affect the behaviour of the power factor. The active power and reactive power have a proportional relationship to the active current I_p and reactive current I_q that is shown in Equations (3-11) and (3-12).

$$P = V \times I_p \quad \text{where} \quad I_p = I \times \cos \phi \quad (3-11)$$

$$Q = V \times I_q \quad \text{where} \quad I_q = I \times \sin \phi \quad (3-12)$$

Since in the induction motor the ratio of active and apparent power must have a value higher than 0.8, the reactive power or current can have a significant responsibility for maintaining this ratio, which is known as $\cos \phi$ or the power factor [7]. However, power factor distortion is related to the harmonic distortion, in which the THD of the voltage and current affects the induction motor's power factor.

The power factor distortion is expressed in Equation (3-13) and the total harmonic distortion in the voltage and current is presented in Equations (3-14) and (3-15).

$$PF_{dist} = \frac{1}{\sqrt{1 + THD_V^2} \sqrt{1 + THD_I^2}} \quad (3-13)$$

$$THD_V = \frac{\sqrt{(V_2^2 + V_3^2 + V_4^2 + \dots)}}{V_{T1}} \times 100 \quad (3-14)$$

$$THD_i = \frac{\sqrt{(I_2^2 + I_3^2 + I_4^2 + \dots)}}{I_{S1}} \times 100 \quad (3-15)$$

where $(I_2^2 + I_3^2 + I_4^2 + \dots + I_n^2)$ and $(V_2^2 + V_3^2 + V_4^2 + \dots + V_n^2)$ are harmonics, and I_{S1} and V_{T1} are the fundamental voltage terminal and stator current.

These values compute the total harmonic distortion of the voltage (THD_v) and motor current (THD_i) in percentage. The power factor distortion equation will be applied when there is either distorted voltage or distorted current. Then, the THD_i or THD_v or even both can be accommodated into the equation and so obtain the power factor distortion. As a result, in the case of non-sinusoidal voltage and motor current waveforms, the true power factor will be represented by the power factor distortion times the power factor displacement, but if the voltage and motor current waveforms are sinusoidal, only the power factor displacement is considered.

3.6. Impact of Low Power Factor in Electrical Systems

A low power factor in the induction motor, particularly at no-load or light-load, indicates a high demand for reactive current to support leakage and magnetizing reactance. This demand is much higher than for the active current (as there is no mechanical load), which shows that the load is more inductive [100].

Inductive load produces excess current that is alternately stored in the magnetization reactance and regenerated back to the line with each AC cycle.

A low power factor also provides low efficiency since the input power is proportional to the power factor. Therefore, although a low power factor does not affect the performance of the motor as the power factor characteristics are the result of the motor design, it affects power grid systems more [19] as a low power factor creates a penalty charge for industrial factories.

Utility companies require a suitable grid power factor near unity because a low power factor in grid systems draws a high current and generates heat and thus huge losses. Moreover, a high current requires a change in the size of conductors with high capacity, which can be a huge cost. In addition, a low power factor causes a voltage drop and so reduces the quality of power in the grid systems. Consequently, determining the operating power factor of induction motor at different load leads to compensate the low power factor [101].

3.7. Power Factor Correction of Induction Motor

Correcting the low power factor of the induction motor not only prevents penalty charges, but also creates a high quality of power in electrical grid systems. The point of common coupling, which is a point between a utility and a customer, is an important point for power factor correction because at this point multiple electrical loads are connected and the utility monitors the low power factor at this point to apply the penalty charge. Therefore, the power factor has a significant role and must be corrected at this point. Since the loads of induction motors in many cases vary, industrial customers are always responsible for monitoring and correcting the power factor toward unity at any loading condition [18].

This correction requires an amount of reactive power that can be generated by capacitors. Methods of power factor correction are described in Figure 3-10. It can be seen that there are several approaches to correct the power factor of the induction motor. An individual capacitor at each induction motor is one basic method and is usually suitable for a fixed motor load. Using a single capacitor bank in group induction motors is another method for power factor correction that is also appropriate for a fixed motor load. Automatic power factor correction using a capacitors bank with a reactive power controller is a common method in terms of the power factor correction of induction motors at PCC points. To provide a high performance power factor correction at any loading condition, using a combination of all techniques as a hybrid method is more efficient.

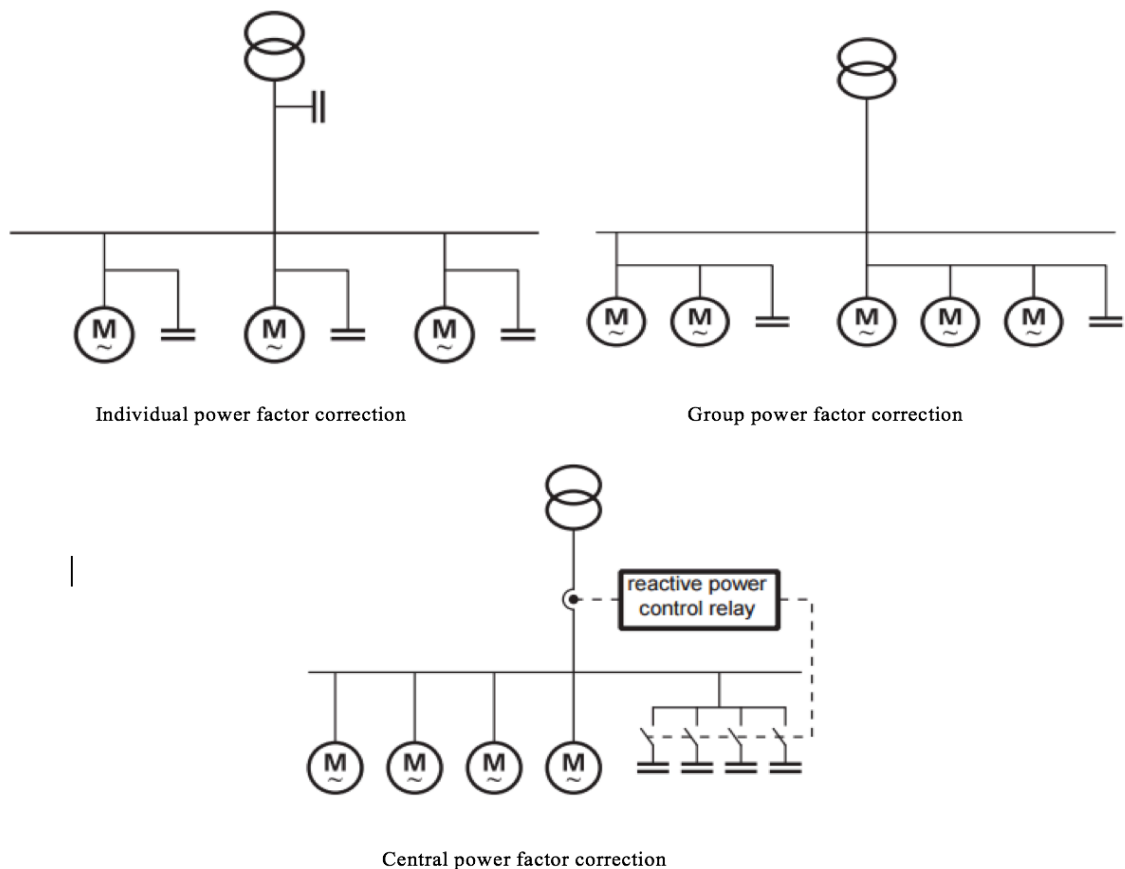


Figure 3-10: Methods of correcting power factor of induction motors

It is understood that adding the required reactive power at the right times enables the correction of the power factor of induction motors to the target value at any loading point. A capacitor is one of the significant electrical components to generate reactive power. Controlling the amount of required reactive power at any loading point is important because under- or over-correction produces many issues since under-sizing absorbs more reactive current from the grid and over-sizing generates more reactive current than the motor requires and backs to the grid. Over-sizing also causes the capacitor current to be higher than the magnetizing current of the induction motors and in such a situation self-excitation will occur.

To find the optimum value of the required reactive power or size of the capacitor, a power factor correction formula can be applied as shown in Equation (3-16), which requires three values including the input power, initial power factor and target power factor.

$$Q_c = P \left(\frac{\sqrt{1 - \cos^2 \phi_1}}{\cos \phi_1} - \frac{\sqrt{1 - \cos^2 \phi_2}}{\cos \phi_2} \right) \quad (3-16)$$

where Q_c is the value of reactive power compensation in VAR, P is the input power in W, $\cos \phi_1$ is the initial or operating power factor, and $\cos \phi_2$ is the new power factor. In Figure 3-11, the power triangle indicates that ϕ_1 and Q_1 are the old values and ϕ_2 and Q_2 are the new values. By obtaining the value of Δ_Q where Δ_Q is $Q_c = (Q_1 - Q_2)$, the required reactive power can be determined [4].

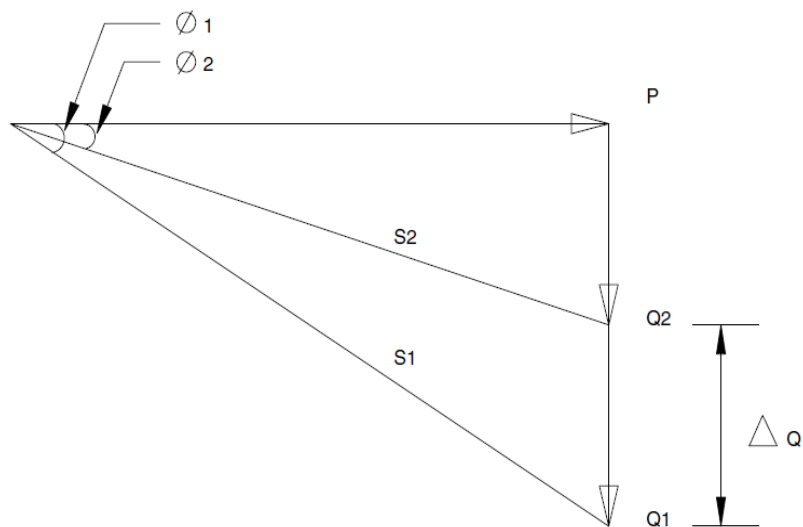


Figure 3-11: Power factor correction diagram

In this equation, the old value of the power factor and input power at any load from no-load to full-load and over-load can be determined by several approaches. The first is to calculate the power factor by online measurement of the voltage and current with the angle or input power. The second is direct measurement of the power factor by a measurement device. The third uses MATLAB/Simulink to model the induction motor and measure the power factor.

3.8. Power Factor Determination of Induction Motor

The zero crossing method and instantaneous power method are techniques that can compute the power factor from voltage and current measurement waveforms. In the zero crossing method, a zero crossing sensor is needed to detect the distance between the voltage and current waveforms [14]. In the instantaneous power method, measurement of the average power is required. Both methods will be explained in the following sections.

3.8.1. Zero Crossing Method

From Figure 3-12, in the zero crossing method the distance between the voltage and current waveforms indicates the angle between the voltage and current waveforms,

so the cosine angle will be the power factor. Using the displacement method, measurement of the supply voltage and the motor current waveforms is required.

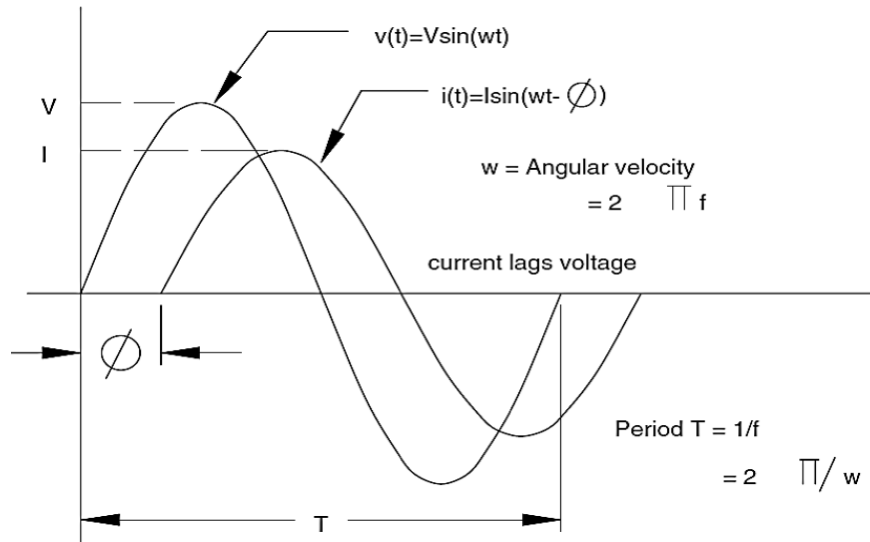


Figure 3-12: Phase angle measurement between voltage and current waveforms

Also, a zero crossing sensor is necessary to distinguish the differences between voltage and current waveforms. Then, by considering the voltage as a reference (constant) and the motor current as a displacement current from zero crossing, the power factor can be obtained by Equation (3-17).

$$PF = \cos\left(\frac{\pm\Delta t}{T} \times 360^\circ\right) \quad (3-17)$$

where $\pm\Delta t$ is the distance between the voltage and current waveforms, T is a period and 360° is one period of the cycle.

3.8.2. Instantaneous Power Method

Another method to determine the power factor is instantaneous power measurement. Indeed, from the zero crossing time displacement, the power factor can also be

calculated via instantaneous power measurement. In this method, measuring both the synchronized supply voltage and motor current waveforms and their multiplication in point by point provide the instantaneous power that utilizes the average power (\bar{P}). Then, the motor power factor is expressed by Equation (3-18).

$$PF = \frac{\bar{P}}{V * I} \quad (3-18)$$

where \bar{P} is the average active power, V is the RMS voltage supply and I is the RMS motor current. The zero crossing and instantaneous power method requires both voltage and current waveforms in order to evaluate the power factor from no-load to full-load condition.

3.8.3. Direct Measurement Method

Several types of electrical device such as a power factor meter, clamp meter, oscilloscope and power analyser can be applied for direct power factor measurement. An oscilloscope is usually used for small induction motors in the laboratory. A power factor meter is also used in industry to indicate the power factor of the induction motor. A power analyser is a powerful device that is able to measure and record all components, including voltage, current, power factor and harmonics, at one second intervals.

3.9. Experimental Work

In this study, three different induction motors with ranges of 250 W, 10 HP and 100 HP are considered in order to measure and evaluate the behaviour of the power factor versus motor load. The 250 W and 10 HP induction motors are taken from the

laboratory. Both are coupled to the DC generator. A volume button, which is connected to the torque sensor, is used to control the motor load. Two types of measurement device can be used to measure the components.

One is a normal meter to measure the voltage, current and input power at any possible point while the load is increasing gradually, then to calculate the power factor. Another is a power analyser, which is able to measure and record all components from no-load to full-load and over-load at one-second intervals [102]. In these cases, due to its high performance, a power analyser is connected to the induction motors and records the voltage, current, power factor and harmonics.

Figure 3-13 shows the experimental set-up.

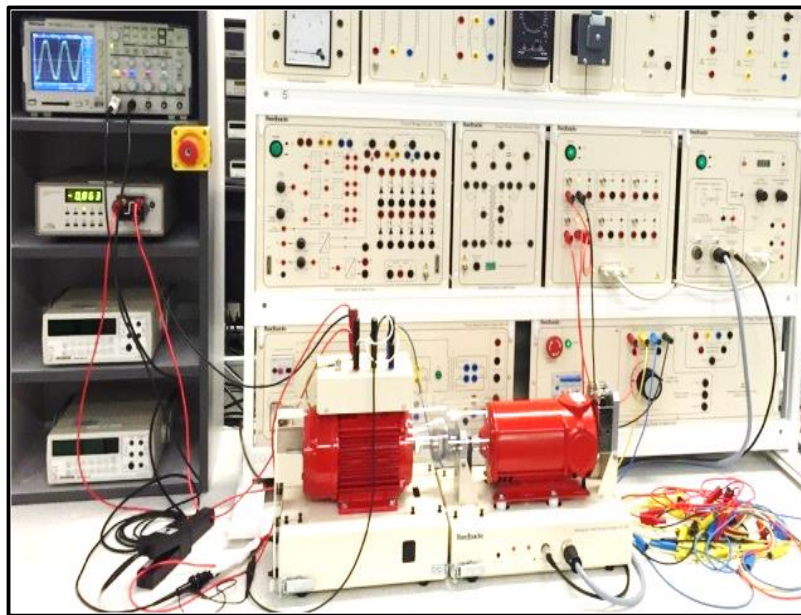


Figure 3-13: Experimental set-up of induction motor

In addition, a three-phase induction motor with a power rating 100 HP is taken from a stone-cutting factory (stone-cutting machine). Measurement took place when the operator gradually moved the blade for cutting the stone by variable volume from no-load to full-load and over-load. A Unipower (UP-2210) power analyser was used to measure and record all components for the three phases, including voltage,

current, active and reactive power, power factor and harmonics. The power analyser stored all components at 6-second intervals and provided 30 measurement points from no-load to full-load and over-load conditions. To connect the power analyser, the motor is shut down for half an hour. The measurement process took an hour. Table 3-1 shows the specifications of the considered induction motors.

Table 3-1 Specifications of considered induction motors

Nameplate data	IM (250 W)	IM (10 HP)	IM (100 HP)
Nominal Voltage	380 V	380 V	380 V
Frequency	50 Hz	50 Hz	50 Hz
Nominal Current	0.6	29	139
Rated Power	250W	10HP	100 HP
Rated Speed	2770 RPM	765 RPM	990 RPM
Rated Power Factor	0.85	0.8	0.82
Nominal efficiency	0.71	0.85	0.92

MATLAB/Simulink is valuable software that is able to model the induction motor with the required electrical components and then measure the power factor at the desired loading points. Figure 3-14 indicates a three-phase 100 HP induction motor with the same specifications as induction motors used in industry, as modelled by MATLAB/Simulink. A torque meter is used to increase the motor load step by step. Then, a simulated power factor meter measures the power factor from no-load to full-load and over-load conditions.

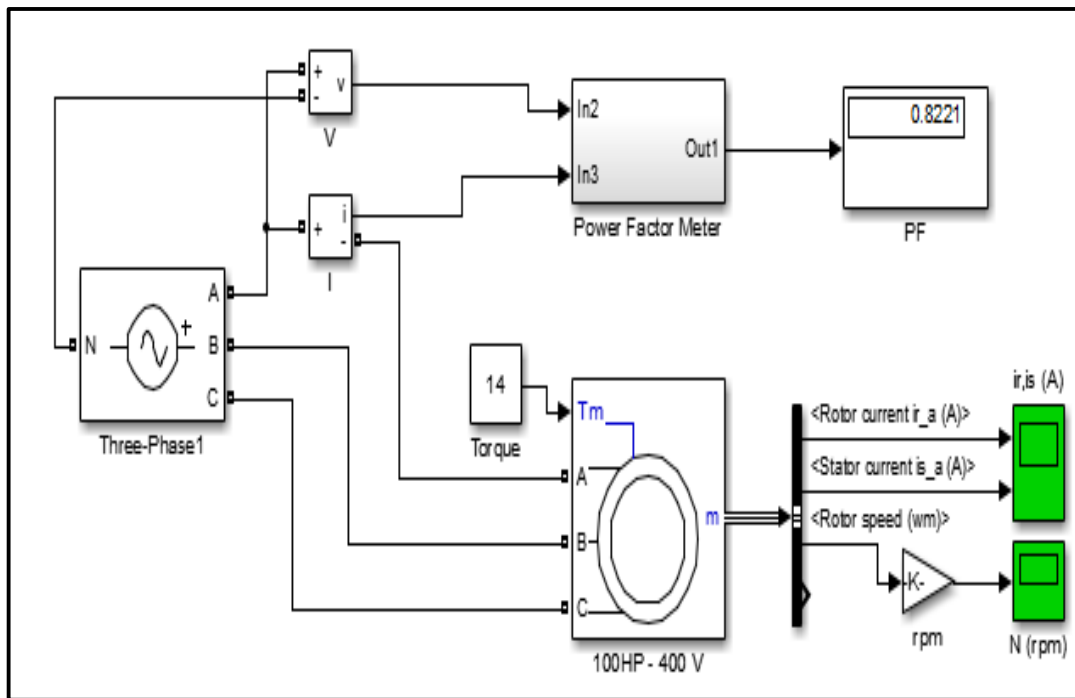


Figure 3-14: Simulation of induction motor by MATLAB/Simulink

It is understood that the operating power factor of the induction motor at any loading condition from no-load to full-load and over-load must be determined. Determination of the operating power factor helps to obtain the required reactive power for creating a new power factor at the desired loading points. The zero crossing method and instantaneous power method enable the power factor to be obtained by measuring the voltage and current waveforms or average power.

It is observed that the measurement devices including the power factor meter and power analyser indicated a good solution to determine the power factor versus load. In addition, modelling of the induction motor in MATLAB/Simulink introduced another way to determine the power factor at any loading point. However, those approaches had limitations in their measurements. For instance, in the zero crossing and instantaneous power method, measurement of the voltage and current waveforms with a sensor is required. In MATLAB/Simulink, the parameters of the equivalent

circuit are required to model the induction motor, and finding these parameters is difficult.

In the practical work, it is shown that the power factor meter installed in the induction motor by the manufacturer creates a reading problem due to numerical fluctuation. The power analyser is shown to be able to measure and record the power factor versus load accurately. However, to connect it, the induction motor must be switched off, but it is sometimes not possible to shut down the induction motor for power factor measurement.

In this thesis, a new technique will be presented in order to solve the recent problems and obtain the power factor at any desired loading point with high accuracy. The procedure of this technique is demonstrated and followed by a flow chart in Figure 3-15. In this technique, adding some input data including the measured voltage, current, and input power from no-load to full-load is the first step. In the second step, the motor load via the power measurement method will be calculated. In the third step, the power factor needs to be obtained from the measured voltage, current and input power. In the fourth step, the obtained load and power factor will be considered as the x and y axis respectively. The fifth step considers the proposed methods, including MCMD, Kriging, regression, ANN and SVR, for estimating the power factor at any desired loading point from no-load to full-load and over-load conditions. The last step makes a comparison, and then presents the best method with the highest accuracy. The theory of the proposed methods will be presented in the next chapter.

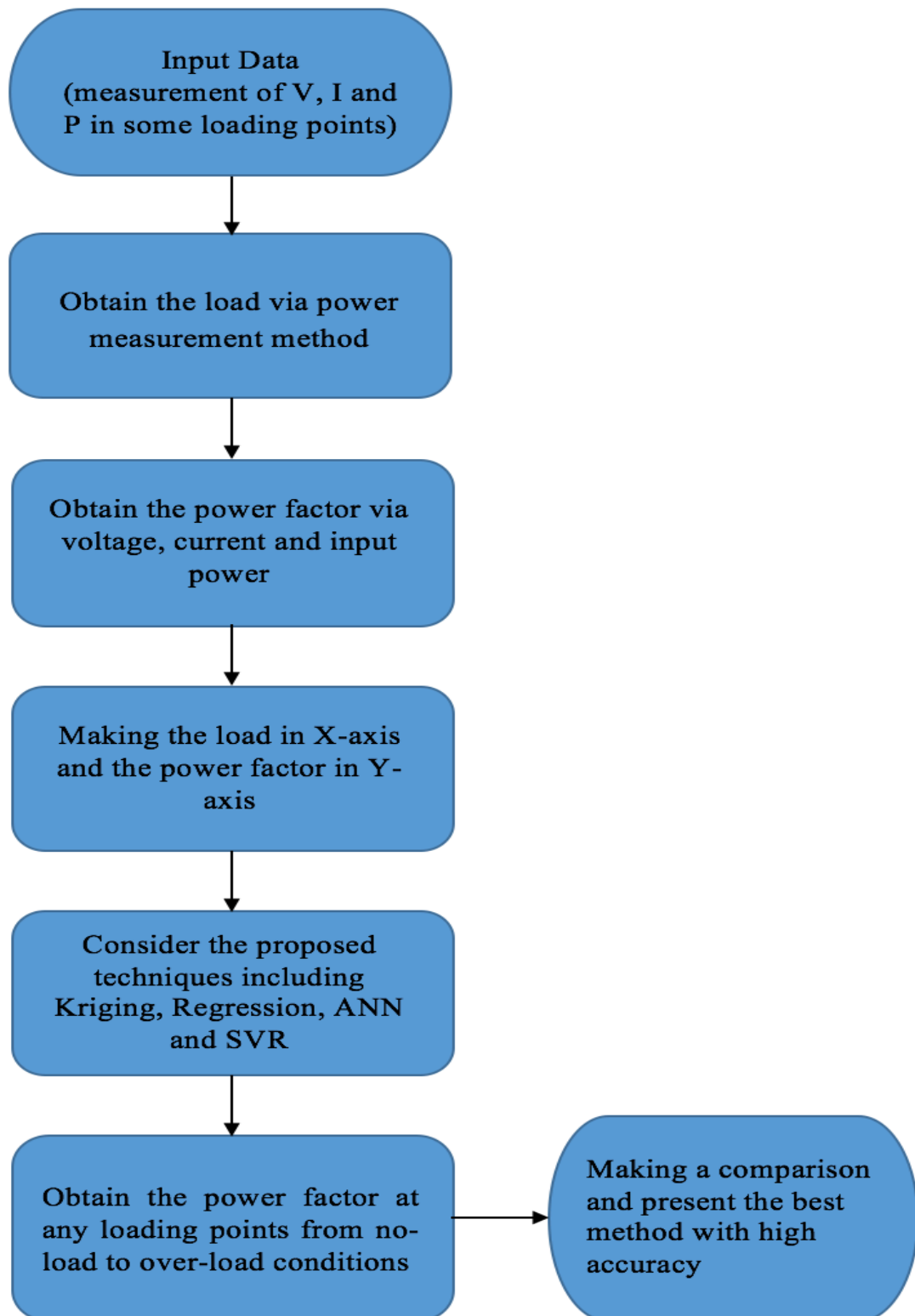


Figure 3-15: The main flowchart of estimating power factor of induction motor

3.10. Summary

In this chapter, the theory of the power factor in induction motors and the results of experimental work indicated that variation of the motor load produced different power factors from no-load to full-load and over-load conditions. Since the power factor must be maintained at unity as previously discussed, determining the power factor against load is required. In this chapter, the experimental studies indicated that measurement devices created restrictions in terms of wiring connection, such that the motor had to be shut down, or needed control of the motor load for power factor measurement, which is not easy. Therefore, estimation techniques using some measured points are suggested to determine the power factor against input power at every loading point. In the next chapter, the estimation techniques will be introduced in detail.

Chapter 4: Estimation Techniques

4.1. Introduction

In this chapter, the theory of the proposed techniques, including a method using the measured current and manufacturer's data, Kriging, regression, an artificial neural network and support vector regression, will be described in detail. The method using measured current presents a simple equation to predict the power factor. The other methods are statistical and intelligent techniques that are able to create a mathematical model, and then determine the power factor at any desired loading point from no-load to full-load and over-load conditions.

4.2. Method Using Measured Current

In this method, a simple technique was developed by [14] in order to estimate the power factor based on a numerical equation with measurement of the current and some information from the manufacturer's data. In this technique, two components need to be considered. The first is the nominal power factor from the data sheet or the nameplate of the motor in order to calculate the nominal reactive current. The second is measurement of the current at any loading from no-load to full-load conditions. Then, by using the proposed Equation (4-1), the power factor can be estimated at any measured point of loading.

$$PF = \cos\phi = \sqrt{1 - \sin^2\phi} = \sqrt{1 - \left(\frac{I_{rnom}}{I_m}\right)^2} \quad (4-1)$$

In the trigonometry, the basic relationship between the sine and cosine will be obtained by the Pythagorean identity as $\sin^2\phi + \cos^2\phi = 1$. Therefore, $\cos\phi$ can be written as $\cos\phi = \sqrt{1 - \sin^2\phi}$ and is able to solve the $\cos\phi$ in math as well [103].

Since the power factor in the case of sinusoidal waveforms can be named as $\cos \phi$, the proposed equation is able to solve $\cos \phi$ with this theorem, where $\sin^2 \phi$ would be converted in to the $(\frac{I_{rnom}}{I_m})^2$ according to Equation (4-4).

In the induction motor, the motor current (I) in Equation (4-2) is divided into two components, the active current and reactive current. The active current in Equation (4-3) is used for useful work and it has a linear correlation with the mechanical resistance from no-load to full-load [11]. The reactive current in Equation (4-4) is magnetization current and is used in magnetization reactance. If the magnetization current or reactive current is assumed to be constant, the power factor can be estimated by Equation (4-1).

$$I = \sqrt{I_{Active}^2 + I_{reactive}^2} \quad (4-2)$$

$$I_{active} = I \cos \phi \quad (4-3)$$

$$I_{reactive} = I \sin \phi \quad (4-4)$$

Therefore, by considering this assumption, the nominal reactive current can be obtained by the nominal power factor using Equation (4-5), where I_{rnom} is the nominal reactive current, PF_{nom} is the nominal power factor, and I_m is the measured current from no-load to full-load.

$$I_{rnom} = I_m \sin (\cos^{-1} PF_{nom}) \quad (4-5)$$

The proposed equation with current measurement is a good idea to predict the power factor of the induction motor against load, since the load can be determined by the

measured current method as well. The computation of this method will be done with MATLAB programming with the following outline.

- Considering measured current values from no-load to full load conditions as input
- Considering the nominal power factor which can be found from the motor nameplate
- Computing the nominal reactive current via the nominal power factor
- Putting the measured current and nominal reactive current into the developed equation
- Computing the motor load via the measured current method
- Obtain the power factor at the measured current
- Obtain the power factor versus load.

This technique has advantages and disadvantages. The main advantage is that it is able to determine the power factor at the measured current by considering only the nominal reactive current because, otherwise, to obtain the power factor, measurement of the voltage, current and active power is required synchronously, while in the proposed method only measurement of the current is necessary. Therefore, this method simplifies the power factor determination because, for measurement of the required components, the induction motor must be switched off in order to connect the measurement device and the motor cut-off may create a cost for the user.

The disadvantage is that this method is only able to estimate the power factor by assuming that the reactive current of the induction motor at any loading condition is constant. Assumption of a constant reactive current and using the nominal reactive current may produce high error compared with real measurement because, in

practice, at operation time the reactive current may not be constant when the load is changing from no-load to full-load. In addition, obtaining the power factor at every loading point in this method may be difficult since measurement of the current at any loading point from no-load to full-load conditions with a normal device is difficult due to numerical fluctuation.

Moreover, this technique considers $\cos\phi$, which is the cosine angle between the voltage and current, which mainly provide the displacement power factor. However, in present of harmonics, this technique is not able to obtain the power factor distortion and so may also provide errors compared with real power factor measurement. In this research, the main goal is to implement the proposed technique with the developed equation in three different sizes of induction motor in order to present the positive and negative performance. Then, a technique will be presented to enhance and improve the technique of power factor estimation. In the next section, the Kriging method is described in detail.

4.3. Kriging Method

Kriging is a geostatistical approach that produces a predicted surface from a separate set of points. The fundamental theory of this method was developed in 1960 by Georges Matheron, a French mathematician. Kriging is a kind of interpolation technique that constructs a model and predicts unknown values between observed points. In this method, assumptions are based on the distance and direction between sample points with a spatial autocorrelation. This method can give the best performance when the correlation and direction of the dataset are clear [25, 24].

In the Kriging method, two tasks are important to make a prediction. One is variography in order to describe the spatial structure of the data. The other is applying a semivariogram model to predict unknown values at different locations.

In the first task, the variogram function indicates the statistical dependence values, which is called spatial autocorrelation of values. The spatial autocorrelation quantifies the assumed points that are closer and more alike than values that are farther apart. To quantify the spatial autocorrelation, structure analysis or variography must be considered by a graph of an empirical semivariogram computed with Equation (4-6) for all pairs separated by distance h .

$$\gamma(h) = \frac{1}{2N(h)} \sum_{i=1}^{N(h)} [z(x_i) - z(x_i + h)]^2 \quad (4-6)$$

where $\gamma(h)$ is a semivariogram for number N of pairs that are separated by distances, $z(x_i)$ is the observed value at x point, and $z(x_i + h)$ is the observed value that is located at distance (h) from x . To compute the semivariogram, initially the square of two points with distance is necessary. To generalize the difference in the values of the two points, all points with distances will be considered.

Since each pair at different locations are at some distance, plotting all pairs in the form of x and y axes is unmanageable. Therefore, instead of plotting each pair, all pairs can be plotted by computing the average semivariogram for all pairs of locations. The graph of the empirical semivariogram comprises the averaged semivariogram values on the y -axis and the distance on the x -axis. The plot is shown in Figure 4-1. Figure 4-2 is an example with eleven locations to indicate how the empirical semivariogram will be obtained. In this figure, the red point is an unknown value that must be estimated. Black points are known values. Dashed lines are the distance between all known locations. Solid lines are the distance between an unknown point and all known points [104, 105].

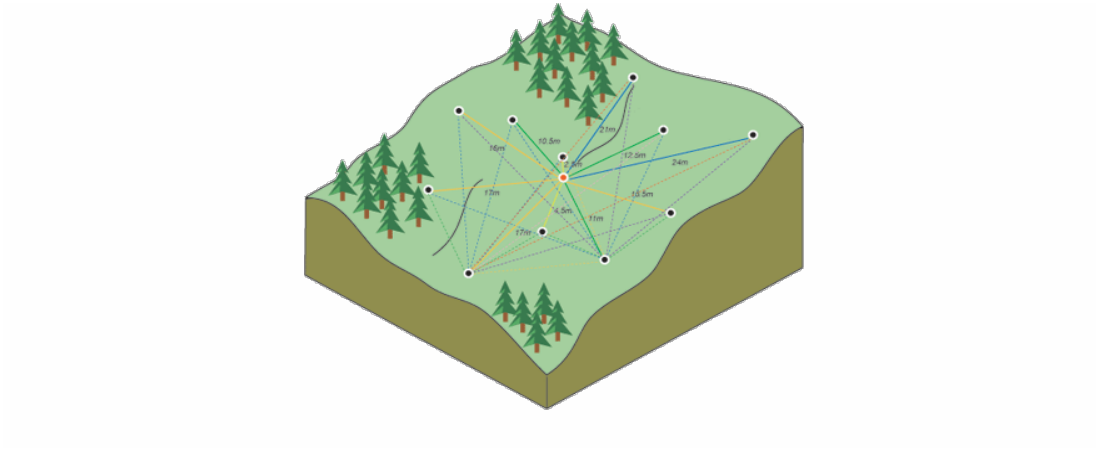


Figure 4-1: Illustration of an unknown point surrounded by known points [105]



Figure 4-2: Example of empirical semivariogram graph [105]

- **Semivariogram models**

The next task is to fit a model to the points forming the empirical semivariogram for prediction. Indeed, semivariogram modelling is a good solution to obtain a suitable model because the main application of Kriging is to estimate the required values at un-sampled locations. Although the empirical semivariogram creates direction in the spatial autocorrelation of the dataset, it does not provide any information on all distances. Therefore, a semivariogram model needs to be fitted to the empirical semivariogram. There are many semivariogram models in Kriging, including

spherical, circular, exponential, linear and Gaussian. These are illustrated in Figure 4-3.

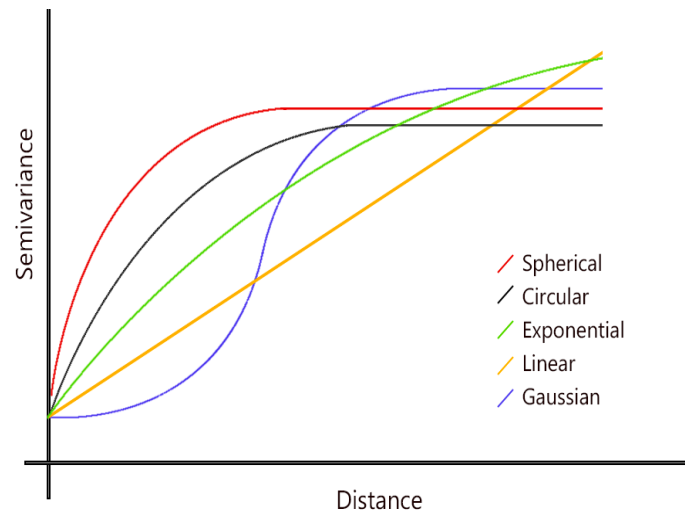


Figure 4-3: Semivariogram models [106]

In the Kriging, a properly selected semivariogram model indicates a high level of prediction, in particular when the model is similar to the dataset. The proposed model predicts all unknown points in different locations. Each model is designed to fit different applications with more accuracy [107]. Semivariogram models are described by three parameters: range, sill, and nugget. Range is the distance by which the observed location is separated. Locations farther apart than the range set cannot be autocorrelated. The value at which the model reaches the range on the y-axis is named the sill. A partial sill is the sill minus the nugget. The nugget is the value that represents the starting point of the dataset.

Theoretically, at zero separation distance the value of the semivariogram is zero. However, with a small separation distance, the semivariogram indicates the nugget, which will be greater than zero. Figure 4-4 illustrates the parameters of the semivariogram model.

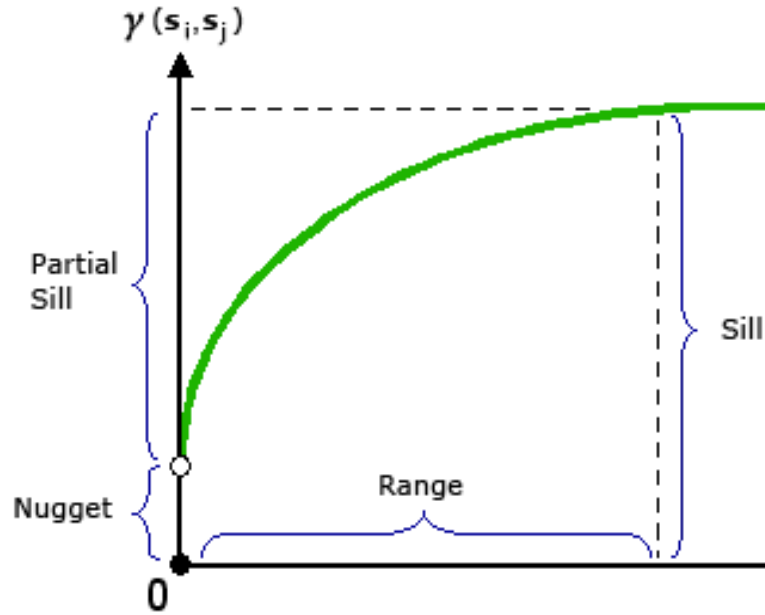


Figure 4-4: Characteristics of semivariogram model [107]

As previously mentioned, there are many different semivariogram models. The equations for these mathematical models are as follows:

$$\text{Exponential} \quad \gamma(h) = c_0 + c \left(1 - \exp\left(\frac{-3h}{a}\right) \right) \quad h > 0 \quad (4-7)$$

$$\text{Gaussian} \quad \gamma(h) = c_0 + c \left(1 - \exp\left(\frac{-h^2}{a^2}\right) \right) \quad h > 0 \quad (4-8)$$

$$\text{Spherical} \quad \gamma(h) = c_0 + c \left(\frac{3h}{2a} - \frac{1}{2} \left(\frac{h}{a} \right)^3 \right) \quad 0 < h < a \quad (4-9)$$

$$\text{Linear} \quad \gamma(h) = c_0 + c \left(\frac{h}{a} \right) \quad 0 < h < a \quad (4-10)$$

$$\text{Circular} \quad \gamma(h) = c_0 + c \left(1 - \frac{2}{\pi} \cos^{-1} \left(\frac{h}{a} \right) + \sqrt{1 - \frac{h^2}{a^2}} \right) \quad h > 0 \quad (4-11)$$

where c_0 is the nugget, c is the partial sill at which levelling takes place, h is the distance between variables and α is the range that represents the maximum distance in the x -axis of the semivariogram model. The key point of Kriging is applying a suitable semivariogram model to provide high output accuracy in the desired application. For this study, among the semivariogram models, selecting the exponential model is more applicable since it is similar to the power factor curve. Therefore, in Equation (4-2), c is replaced as the rated power factor at maximum load (m_{PF}), h is the distance between all load points, α is replaced as the maximum load (m_L), $\gamma(h)$ is the semivariogram of the exponential model.

There are two types of Kriging, ordinary and universal, that can be selected based on the quality of correlation and trend of the data as well as the relationship between paired points in different locations. In ordinary Kriging, it is assumed that the spatial autocorrelation is directly deployed by the semivariogram and there is no trend in the observed points [108]. In the universal type, it is assumed that not only is the presence of the spatial autocorrelation between points necessary, but also that there will be a trend in the data. Therefore, Kriging is combined with a 1st or 2nd order polynomial. In this case, ordinary Kriging will be described by Equation (4-6), where Kriging estimates the unknown values based on nearby observed values at surrounding locations. Obtaining the weight of each observed point and unknown point requires the error of a predicted value to be minimised.

$$\hat{Z}_{(S_0)} = \sum_{i=1}^N W_i Z_{(S_i)} \quad (4-12)$$

where $Z_{(S_i)}$ is the observed value at the i_{th} location, W_i is an unknown weight for the observed value at the i_{th} location, S_0 is the prediction location, and N is the number of observed values. Using this equation, first of all the calculation of weights w_i is important. To obtain w_i , Kriging requires the use of a semivariogram. This is a function that relates the semivariance of the data points to the distance that separates them. A Lagrange matrix will be applied to obtain the weights of the observed values. In the Lagrange matrix, two main vectors are needed. One is the obtained values of semivariance $\gamma(h)$ and the other is the distance between the observed value and the point that will be estimated. Then, the Lagrange multiplier matrix can be expressed in Equation (4-13).

$$\begin{bmatrix} w_1 \\ w_2 \\ \vdots \\ w_n \\ \lambda \end{bmatrix} = \begin{bmatrix} \gamma_{11} & \gamma_{12} & \dots & \gamma_{1n} & 1 \\ \gamma_{21} & \gamma_{22} & \dots & \gamma_{2n} & 1 \\ \vdots & \vdots & \ddots & \vdots & \vdots \\ \gamma_{m1} & \gamma_{m2} & \dots & \gamma_{mn} & 1 \\ 1 & 1 & \dots & 1 & 0 \end{bmatrix}^{-1} \cdot \begin{bmatrix} \gamma_{10} \\ \gamma_{20} \\ \vdots \\ \gamma_{n0} \\ 1 \end{bmatrix} \quad (4-13)$$

In Lagrange multiplication, w_i is ($m \times 1$ matrix) the weight of actual and estimated points, which is unknown, γ_h is ($m \times n$ matrix) the output of the semivariogram function, and γ_{no} is a vector ($m \times 1$) between the unknown loading points and observed loading points. Thus, from the obtained values of w_1, w_2, \dots, w_n and λ (where λ is useful in calculating the variance), the unknown point can be estimated by Equation (4-14).

$$Z_{S_0} = w_1 S_1 + w_2 S_2 + w S_3 + \dots w_n S_n \quad (4-14)$$

where w_i is the weight between an estimated point and observed points, S_i is the observed points. Then, multiplying the observed points by the obtained weights, the target point at a desired location is estimated. In the Kriging algorithm, a loop function has been applied in order to estimate any unknown points in the desired location. In this project, the Kriging method will be applied in different sizes of induction motor, small, medium and large (250 W, 10 HP and 100 HP), in order to estimate their power factor at any desired loading point. The steps of the algorithm are as follows:

- Compute the distance between each pair of points in the x -axis and make it as 4×4 vectors.
- Compute the distance between all x -axis points and a point needs to be estimated.
- Create an empirical semivariogram model
- Select an appropriate function, and then insert the obtained parameters from the computed distances in the x -axis
- Put in the results obtained by the function, and the results of the distance between all x -axis points and a given point need to be estimated in the Lagrange matrix
- Create a loop function to iterate the algorithm in order to obtain the next desired points.

4.4. Regression Method

Regression is a statistical technique that is widely used in prediction and forecasting. Regression was developed by Francis Galton in 1877. In the technique, regression predicts the relationship between variables and contributes to understanding how a dependent variable reacts when each independent variable is constant or varying [109, 110, 111]. The basis of regression is determining the relationship between one or more independent values in the x -axis, and one or more dependent values in the y -axis by obtaining their coefficients [112]. The main equation of regression can be expressed in Equation (4-15).

$$y_i = f(x_i, \beta) + \varepsilon_i \quad i = 1, 2, \dots, n \quad (4-15)$$

where y_i is the number of observations of dependent values, x_i is the number of predictor variables related to y_i , β is the coefficient of regression, f is the regression function that is explained in the next section. Therefore, β multiplied by x_i provides an estimated value \hat{y}_i . The difference between y_i and \hat{y}_i is ε_i . Now, by obtaining the value of β and ε_i with a new set of x_i , the values of y_i will be determined. Creating a fitting model requires the sum of squares of the residuals to be minimised [25, 26]. Least squares is a common approach in regression in order to find the coefficients (β) and minimise (the sum of squared residual) the differences between known values and the fitted values. To obtain the coefficients, therefore, the equation can be converted into matrix form as in Equation (4-16).

$$[Y] = [X][\beta] + [\varepsilon] \quad (4-16)$$

where $[Y]$ is an $n \times 1$ vector of dependent variables, $[X]$ is an $n \times m$ matrix of estimators (Vandermonde matrix), with one column for each estimator and one row for each observation. $[\beta]$ is an $m \times 1$ vector of unknown parameters to be predicted. $[\varepsilon]$ is an $n \times 1$ vector of independent variables and indicates the error between the observed and estimated values. Hence, converting Equation (4-15) to Equation (4-16), the coefficient will be obtained in Equation (4-17).

$$\beta = (X^T X)^{-1} X^T Y \quad (4-17)$$

4.4.1. Goodness of Fit

In the statistical methods, indicating the goodness of fit is important because it can show the fitness of the model. R^2 , which is the square of correlation between the observed values and the predicted values, can be an indicator to show the fitness of methods [113, 114]. R^2 is defined as the ratio of the sum of squares of regression (SSR) and the total sum of squares (TSS). It is expressed in Equations (4-18) to (4-21).

$$R^2 = \frac{SSR}{SST} = 1 - \frac{SSE}{SST} \quad (4-18)$$

$$SSE = \sum_{i=1}^n (y_i - \hat{y}_i)^2 \quad (4-19)$$

$$SSR = \sum_{i=1}^n (\hat{y}_i - \bar{y}_i)^2 \quad (4-20)$$

$$SST = SSR + SSE \quad (4-21)$$

R^2 can take values of 0 and 1. A value closer to 1 provides a greater proportionality to the model. It is observed that increasing the number of degrees in the model provides a greater R^2 . However, the fit may not improve in a practical sense. To avoid this situation, the adjusted R^2 , which is indicated in Equation (4-22), must be considered in (4-23).

$$\text{Adjusted } R^2 = 1 - \frac{SSE(n-1)}{SST(v)} \quad (4-22)$$

$$v = n - m \quad (4-23)$$

In Equation (4-23), v indicates the number of independent pieces of information involving the n data points that are required to calculate the sum of the square, n is the number of values and m is the number of fitted coefficients. The adjusted R^2 is the best indicator of the quality of the fit. It can be a value less than one or equal to one. A value closer to 1 indicates a better fit. Root mean square error (RMSE) can be used to indicate the standard error of the fit and the standard error of the regression, which are defined in Equation (4-24), where the mean square error (MSE) is obtained by E/v .

$$RMSE = S = \sqrt{MSE} \quad (4-24)$$

4.4.2. Linear and Non-linear Regression Models

Regression can be described in two types including a linear regression and non-linear regression model, shown in Figure 4-5. Linear regression provides a linear model between the independent variable (x) and dependent variable (y).

In linear regression, the model can be obtained by using a linear predictor function, where the model is named a linear model. Non-linear regression provides a non-linear model by a function which is a combination of model parameters and variables [114]. In both linear and non-linear regression, there are many functions that can be selected based on the model data. The regression models are described as follows.

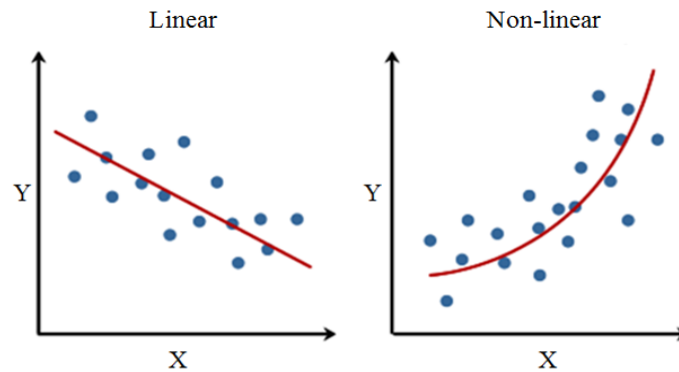


Figure 4-5: Linear and non-linear regression models [114]

4.4.2.1. Exponential Model

An exponential function is used to provide a linear or non-linear model to fit in the dataset model. The linear and non-linear functions are presented in Equations (4-25) and (4-26). These functions can be used when the change rate of quantities is proportional to the initial quantities. In these equations, a , b , c and d are the coefficients of the exponential that are estimated by the least squares method. These functions can only produce a fixed model after obtaining the coefficients. Both equations are unable to provide flexible models because in these functions there is no adjustable parameter.

$$y = ae^{bx} \quad (4-25)$$

$$y = ae^{bx} + ce^{dx} \quad (4-26)$$

4.4.2.2. Gaussian Model

The Gaussian model is another use of a regression function to provide a desired model fitting to the data model. In this function, a is the amplitude, b is the location, and c is related to the peak width. n is the number of peaks for fitting where $1 \leq n \leq 8$. In this function, it is possible to produce several models by changing the peak value from 1 to 8. Adjusting the peak value manually indicates the flexibility of this function in terms of creating an exact fitting model to the data points. This function is more applicable in cases where the input model is similar to the Gaussian shape.

$$y = \sum_{i=1}^n a_i e^{\left[-\left(\frac{x-b_i}{c_i}\right)^2\right]} \quad (4-27)$$

4.4.2.3. Power Series Model

In this function, only two terms can provide linear and non-linear models. These are indicated in Equations (4-28) and (4-29), where a , b and c are the coefficients. The power series is only able to create two models in linear and non-linear form, in which the first term in Equation (4-28) is a linear function and the second term in Equation (4-29) is a non-linear function. In these functions there are no adjustable parameters to regulate the existing model. Once its coefficients are obtained by least squares, it will produce a fixed model.

$$y = ax^b \quad (4-28)$$

$$y = ax^b + c \quad (4-29)$$

4.4.2.4. Polynomial Model

The polynomial model is also a very common use of regression in which the relationship between the dependent variable in the y -axis and independent variable in the x -axis is modelled by the number of degrees. Polynomial regression also provides a model fitting to a linear and non-linear model from datasets by adjusting the polynomial order. The main equation of the polynomial is presented in Equation (4-30).

$$y = \sum_{i=1}^{n+1} \beta_i x^{n+1-i} \quad (4-30)$$

where $n + 1$ is the polynomial order, and n is the polynomial degree where $1 \leq n \leq 9$. The order provides the number of coefficients for fitting. The degree indicates the highest power of the estimator variable. In polynomial regression, the polynomial degrees have significant roles in terms of fitting the linear and non-linear models. If the polynomial degree is ($n = 1$), this represents a linear model. If the polynomial degree is ($n = 2, 3$), this indicates non-linear models, quadratic and cubic models respectively. Third-degree polynomials are described in Equation (4-31).

$$y = \beta_1 x^3 + \beta_2 x^2 + \beta_3 x + \beta_4 \quad (4-31)$$

Polyfit and *polyval* are substantial functions in statistical MATLAB tools. The *polyfit* (p) function is used to obtain the coefficients for a polynomial of degree (n). It can also be described as $p = \text{polyfit}(x, y, n)$, in which x is an observed point and determined as an independent value. y is an observed value and is determined as a

dependent value. n is a degree of polynomial that specifies the polynomial power of the coefficient in p . p obtains the polynomial coefficients by using the least squares procedure and selecting the value of the degree (the length of p is $n + 1$) [26]. In the *polyfit* procedure, an independent value requires the formation of a Vandermonde matrix with $n + 1$ columns. *Polyfit* solves the polynomial coefficients with $p = V/y$ as expressed in Equation (4-32).

$$\begin{pmatrix} p_1 \\ p_2 \\ \vdots \\ p_n \end{pmatrix} = \begin{pmatrix} x_1^{n+1} & x_1^n & \dots & 1 \\ x_2^{n+1} & x_2^n & \dots & 1 \\ \vdots & \vdots & \ddots & \vdots \\ x_n^{n+1} & x_n^n & \vdots & 1 \end{pmatrix}^{-1} \begin{pmatrix} y_1 \\ y_2 \\ \vdots \\ y_n \end{pmatrix} \quad (4-32)$$

Polyval is a function that evaluates p at query points. The function can be described as $y = polyval(p, x)$, in which the y output is the polynomial coefficient of degrees and evaluated at query points x . Therefore, combining both functions with the required numbers of degrees can predict values at unknown points with significant accuracy. The steps of the algorithm are outlined as follows:

- Inserting the load and the power factor data as the x -axis and y -axis
- Putting the x -axis and y -axis data in a Vandermonde matrix
- Using the *polyval* technique to obtain the polynomial coefficients
- Using the *polyfit* technique to place the obtained coefficient in the points that need to be determined

Selection of the polynomial degree can be an effective solution for solving non-linear models. In the regression analysis, the polynomial function has the advantage that it is not too complicated due to the flexibility in data. In addition, the fitting process is simple and the polynomial degree at any term can provide the desired models. The main disadvantage of this function is that a high degree creates instability in the model and it diverges outside the range. Of the aforementioned functions, however, polynomial regression is more flexible and can be applied in different cases for prediction and forecasting. In this project, polynomial regression is applicable and more powerful than other functions for the estimation of the power factor because the initial power factor curve in all induction motors is exponential. Selecting different polynomial degrees can provide the best fitting for each model.

Although a two-term exponential function can be used in this application, this may not provide a high performance in the output result, since there is no adjustable parameter to regulate the best fitting. In addition, in a two-term power series function only one model can be obtained and also it is not possible to adjust the new model into the dataset model. The Gaussian function is flexible and can produce several models by selecting different numbers of peaks. However, it is not appropriate in the case of power factor estimation, since the existing model is different from the power factor curve. As a result, this analysis demonstrates that using a polynomial function can provide better performance compared with other functions. The proposed method will be implemented in three different power factors of induction motors and the results will be presented in the next chapter.

4.5. Artificial Neural Network Method

An artificial neural network is a novel computation method that is able to predict the output responses from complex systems.

The idea of such a network arises from the biological neural network that constitutes the human brain. A biological neural network is a series of interconnected neurons where each connection between neurons can transmit a signal to other neurons and therefore provide an output. A neuron is constituted of dendrites and an axon. These are connected via synapses, which are responsible for transmitting the signal from the dendrites to the axon terminals. The neuron and synapse may have a weight that is able to increase or decrease the strength of the signals sent downstream. Further, they may have a threshold to evaluate the signal if it is below or above it [115, 116].

Hence, it was possible to simulate an artificial neural network with a model as in Figure 4-6. In this model, X is the input where each line considers a column as X_1 . w is a coefficient of the input vector and can also be called a weight. It times to the input vector in order to indicate the strength of the signal. All input vectors with their weights are summed. This summation, before going to the output, will be taken into a different process that is called an activation function in order to determine whether the output is right or not. In this structure, the aim is to train the neurons in order to specify the matrix weight by the input data, and then provide an optimal output. In general, an artificial neural network in terms of learning is divided into fixed and adaptive networks, where in a fixed network the weight is constant, but in an adaptive network the weight is variable (a learning network). The adaptive network can be divided into two categories, supervised and unsupervised learning. In supervised learning, the ideal output can be obtained by training the sample points that have been considered as input.

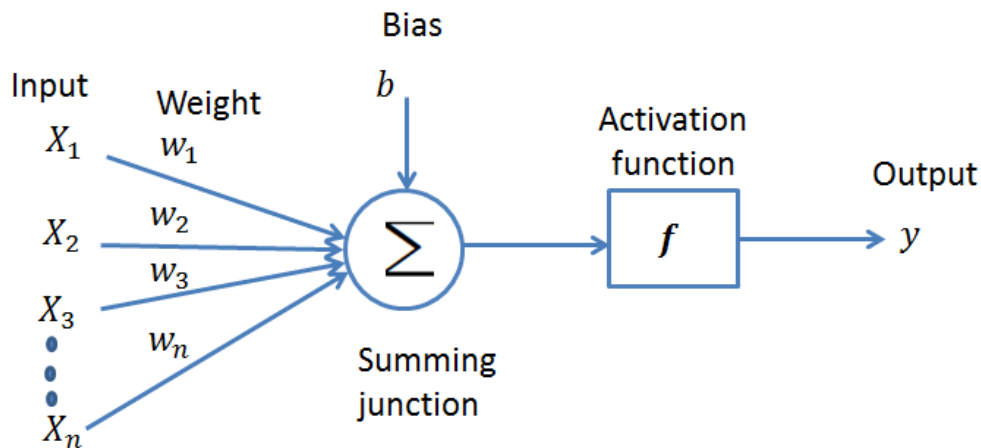


Figure 4-6: Simplified mathematical model of real nerve [116]

However, in unsupervised learning, the output data will be given without considering the input data. In fact, its aim is to discover an interesting structure, a process which is sometimes named knowledge discovery. In this learning, it has not been indicated what the desired output is for each input, unlike in supervised learning. Supervised learning is used in the case of a regression problem, while unsupervised learning is considered to solve the problem of clustering data into the group. In the case of supervised learning, the artificial neural network acts like a body nerve and can provide a supervised learning ability so that by receiving signals from the input, it is able to create the output. To obtain the desired output, the weight needs to be changed each time. Since the topology of the brain is much more complicated, it is not possible to deploy this topology as the same as modelling a biological neural network [117].

Therefore, a simpler method for this arrangement is considered. One of the most commonly suggested models for modelling the connection and agreement of neurons is Multi-layer Feedforward (MLF), which will be described in the next section.

- **Multi-layer Feedforward**

Multi-layer feedforward is the most popular network pattern and is associated with back propagation (BP). It is used in prediction and forecasting applications by having two vector variables of which one is the estimator and the other is the target. Figure 4-7 shows the feedforward structure which is taken from the main neural network structure (Figure 4-6), where the main neural network takes several inputs and obtains one output, while the feedforward structure takes one input and provides one output as well. As can be seen from Figure 4-7, the feedforward network structure is constituted by a hidden layer and an output layer. The hidden layer supplies the input for the output layer; its number is flexible and can be increased manually. In addition, there are two differentiable transfer functions in this structure. One is located in the hidden layer with sigmoid functions. The other is located in the output layer with a linear transfer function. Such structure is able to learn non-linear relationships between input and output vectors. The linear output layer is most commonly used to solve non-linear regression problems [118, 115].

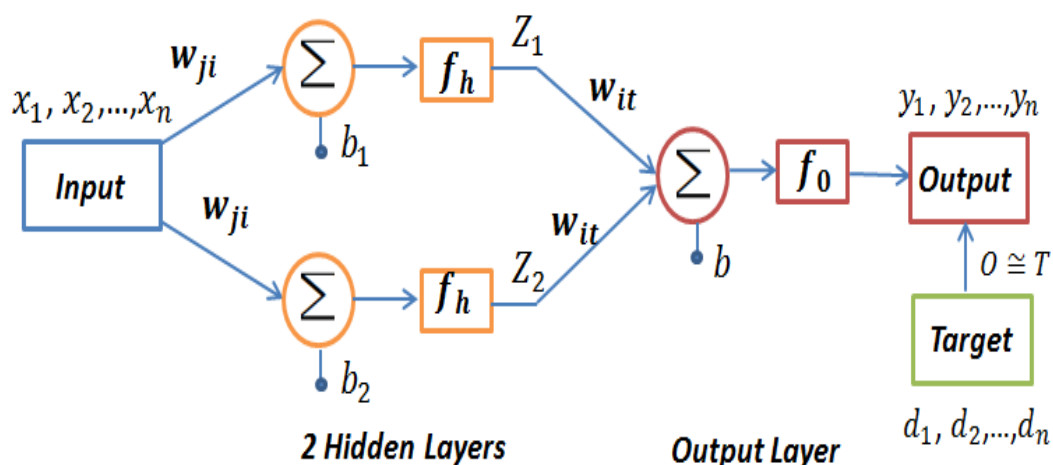


Figure 4-7: Structure of Multi-layer Feedforward with 2 hidden layers [118]

In the feedforward network, the sample values in the x -axis are considered as input $x_j (j = 1, 2, \dots, n)$, and the sample values in the d -axis $d_t (t = 1, 2, \dots, n)$ are considered as the target. The output network will be obtained as $y_t (t = 1, 2, \dots, n)$. The hidden layer, which supplies the input for the output layer, is considered as $z_i (i = 1, 2, \dots, n)$. w_{ij} is a weight between each two connected neurons of the input and hidden layers, and w_{it} is a weight between the hidden layer and output layer. Finally, by using an optimization technique with a back-propagation algorithm, the weights are updated, and then the error between the output and target will be minimised. The next section presents the minimization process with the back propagation algorithm.

- **Back Propagation Algorithm**

This algorithm was introduced by Rumelhart and McClelland in 1985 and is mostly used in feedforward neural networks. The idea of the back propagation algorithm in a multi-layer feedforward function is to adjust the weights of each neuron in order to obtain optimal values in the input by a forward and backward process. Back propagation is one of the supervised learning methods in which the input values are observed and the output of each sample will be predicted. In the back propagation algorithm, the function of each neuron takes the sum of weights in the input of the considered neurons and provides output. However, if the obtained outputs are not similar to the target values, the algorithm back propagates the output to the input and creates a new weight to obtain outputs closer to the targets. This process continues until the outputs achieve the target values. This process is named minimization. An error function in Equation (4-33), which is also named the sum of squared error (SSE), is used through the back propagation algorithm for this minimization.

$$E(w) = \frac{1}{N} \sum_{i=1}^N (y_i - d_i)^2 \quad (4-33)$$

Here, w represents the set of all weights in the network, y_i is the output of the feedforward structure that needs to be obtained, and d_i is the target value which is observed. To compute y_i , two steps are required. The first step is obtaining hidden layer z_i by Equation (4-34), where w_{ji} are the weights between each two connected neurons between the input and hidden layer, x_j is the training value located as inputs, and f_h is a sigmoid function which is indicated in Equation (4-35).

$$z_i = f_h(w_{ji}x_j) = f_h(\text{net}_j) \quad 1, 2, \dots, n \quad (4-34)$$

$$f_h(w_{ji}, x_j) = \frac{1}{1 + \exp(-w_{ji}, x_j)} \quad (4-35)$$

The second step is to obtain the output of all neurons in the output layer by Equation (4-36), where w_{it} is the weight between each two connected neurons between the hidden layer and output layer, z_i is the hidden layer, and f_0 is a linear transfer function in the output layer.

$$y_t = f_0 \sum_{j=0}^n w_{it} z_i = \text{net}_t \quad 1, 2, \dots, n \quad (4-36)$$

There are various methods, including gradient descent, the Newton method and Marquardt–Levenberg, for updating the weights in order to minimise the error function. Among these methods, gradient descent is the simplest and one of the most common methods for error minimization. In the gradient descent method, the delta

rule is a significant technique to update each weight and can be expressed in Equations (4-37) and (4-38).

$$\Delta w_{it} = w_{it}^{new} - w_{it}^c = -\rho_0 \frac{\partial E}{\partial w_{it}} \quad (4-37)$$

$$\Delta w_{ji} = w_{ji}^{new} - w_{ji}^c = -\rho_h \frac{\partial E}{\partial w_{ji}} \quad (4-38)$$

where this equation is the partial derivative of the error function with respect to each of the weights in the hidden and output layers and ρ is the learning rate parameter. If ρ is small, the search path will approximate the gradient path, but convergence will be very slow due to the large number of update steps needed to reach a local minima. On the other hand, if ρ is larger, convergence will be very fast, but the algorithm will not reach a minimum. In the feedforward neural network, the complete procedure for updating the weights can be summarised as follows:

- Initialize all weights and refer to them as current weights w_{ji}^c and w_{it}^c .
- Set the learning rates ρ_0 and ρ_h to small positive values
- Select an input pattern x^k from the training set and propagate it through the network, thus generating hidden and output units based on the current weight settings.
- Use the desired target, d^n , associated with x^n , and employ Equation (4-37) to compute the output layer weight changes Δw_{it}
- Update all weights according to $w_{it}^{new} = w_{it}^c + \Delta w_{it}$ and $w_{ji}^{new} = w_{ji}^c + \Delta w_{ji}$ for the output and hidden layers respectively.
- Test for convergence

This step will be done by an error function (4-33). If convergence is met, stop; otherwise, set $w_{it}^c = w_{it}^{new}$ and $w_{ji}^c = w_{ji}^{new}$ and go to step 3. However, back propagation may not be able to find the solution. In such cases, reinitializing or using more hidden layers can be tried.

In this project, the neural network toolbox from MATLAB programming is used to estimate the power factor curve of the considered induction motors at different loading points. This tool is made to solve the fitting problem between a dataset of numeric inputs and a set of numeric targets. The main aim of this tool is that after selecting the input data, it trains the network and evaluates its performance using mean squared error and regression analysis. Then, it produces a model fitting the dataset model. In this tool, a two-layer feedforward network with sigmoid hidden neurons and linear output neurons is considered to solve the fitting problem. Using a gradient technique called a back propagation algorithm involves performing computations backward through the network [119]. In MATLAB programming, neural network design has four primary steps as follows:

1. Collect data

In this step, the input data must be presented by two vectors where one vector is the estimator and the other is the target. Then, they must be divided into three subsets. The first is the training set which is used for the gradient and updating the weights and biases. It normally selects 70% of all data. The second is the validation set. It is used to measure the network generalization and is responsible for stopping training when the generalization is improved. It is usually 15% of all the data. The third is the test set, which is used to provide an independent measure of network performance during and after training. It will not have any effect on the training. It is used to compare the different models and plot the test set error during the training process. It

to is usually 15% of the data. The division of data into subsets can be done either manually or randomly by the defined functions described in the tool.

2. Create and configure the network

After data collection, the next step is to create the multi-layer feedforward network. The feedforward network constitutes two layers, a hidden and an output layer with a number of neurons. The number of neurons in the hidden layer can be added manually. When the network has been created, it has to be configured. The configuration steps include demonstrating the input and target data, setting the size of the input and output to match the data, and selecting settings for processing the inputs and outputs to provide satisfactory performance. The configuration step is normally done automatically when the selected training function is called.

3. Initialize the weights and biases

Before training the network, the weights and biases must be initialized. The configured network automatically initializes the weights. Configuration is a process setting the network input, output and target sizes, and also setting the weight initialization to match the input and target data.

4. Train the network

After initialization of the weights and biases, the multi-layer feedforward network can be trained for non-linear regression. The process of training involves the values of weights and biases of the network in order to optimise the network performance. The performance function in the feedforward network is the mean squared error (MSE), which is the average squared error between the network outputs and the target outputs that are expressed in Equation (4-33). To train the multi-layer feedforward networks, any standard numerical optimization technique can be used to

optimise the function. These optimization methods use the gradient of the network performance with respect to the network weights. The gradient is computed using a technique called back propagation that involves backward computation through the network. The computation of back propagation is derived using the delta rule. In MATLAB programming, a training algorithm is applied to compute the gradient by performing calculations backward through the network. Gradient descent and Levenberg–Marquardt are the most common algorithms in the case of non-linear regression due to their fast computation [119].

It is understood that the artificial neural network is one of the significant intelligent techniques that is able to generalize and create a desired model. In reality, in this method a mathematical structure is considered with some parameters that need to be adjusted. In this structure, a learning or training algorithm will be introduced to optimise and find the parameters. This learning process is similar to the human brain, in which the data has been analysed by weakness and strength between the neural cells of the brain. This weakness and strength in the mathematical structure is defined and modelled by adjusting a parameter, which is known as weighting.

Artificial neural networks are different types. The first is Multi-layer Feedforward (MLF), which is a simplified model and the most commonly used in neural networks. In MLF, some measured values are required for the network (input layer) as a training sample. For updating weights, the error between the predicted and actual output values is back propagated via the network. Minimising the error of the desired and predicted values will be done by the back propagation algorithm. The back propagation (BP) algorithm with the gradient descent method is used in MLF and is able to minimise the error between the inputs and targets data and provide the desired model.

The second type is the radial basis function. This is similar to the MLF, but the RBF concentrates more on processing of the input neurons and allows faster data processing. In the neural network, both MLF and RBF try to improve the structure of the neural network in which the estimation error is mainly concentrated. In other words, in the neural network there will be another specific type, called support vector machine regression. This type concentrates on reducing empirical risk. The structure of the SVM is similar to the MLF. The only differences are in the learning style. In this project, support vector machine regression will be used for estimating the power factor curve as well. The theory of this technique is described in the next section.

4.6. Support Vector Regression Method

The study indicates that the conventional estimation methods provide high error and also poor performance in many applications. Artificial intelligence is the newest method for prediction with high accuracy. In the recent development of artificial intelligence, the neural network was one of the most common methods. However, this method showed weaknesses in performance, such as the requirement to control the parameters, difficulty ensuring stable results and so on. Due to such weaknesses, better methods have been designed to improve the neural network. The support vector machine (SVM) is one of the supervised learning methods that are able to solve the recent problems. SVM can be applied for classification and regression. In this project, for model prediction, regression is the main focus [51]. In this method, the regression is named support vector regression (SVR). The theory of SVR was developed by Vapnik in 1997. It is known as one of the significant techniques in terms of solving regression problems [120, 121].

The structure of support vector regression is similar to the SVM. In contrast, the SVR tries to fit a line or curve to the data by minimising the cost function. The SVR

developed a new technique to solve the fitting problems and minimise the error as well. The main structure of SVR is presented in Figure 4-8, where x is the input data, $K(x_i, x)$ is the kernel function, $\alpha_i^+ - \alpha_i^-$ are support vector coefficients, b is bias, and y is the output.

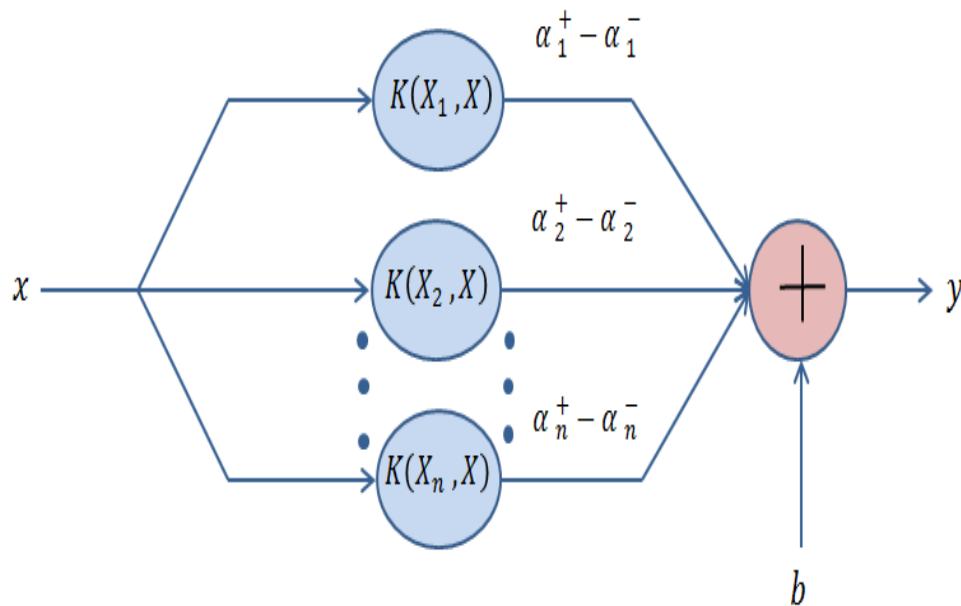


Figure 4-8: Support vector regression structure

As can be seen from Figure 4-9, the strategy of SVR is to construct a hyperplane in high-dimensional space with consideration of constraints in order to create a boundary for data points with upper and lower bounds. The distance between the hyperplane and upper bound or lower bound is measured by ϵ . The distance between the upper and lower bound is measured by $\frac{1}{2} \|w\|^2$. In reality, $\|w\|^2$ is proposed as a regularization term or the flatness of the function that needs to be minimised.

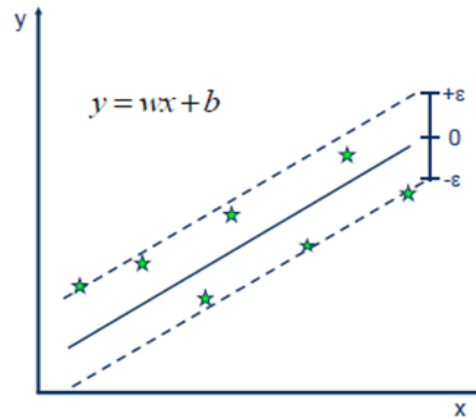


Figure 4-9: Hyperplane with upper and lower bounds [122]

The main aim of this technique is to minimise the margin by a loss function and place the hyperplane close to as many of the data points as possible. SVR can only act in a linear way, but by mapping the main space into the high-dimensional space, it can construct a set of hyperplanes close to all the data points to solve a non-linear model. In SVR, the set of training data includes predictor variables and observed values are considered. The main goal of this technique is to find a function $f(x)$ that deviates from y_i by a value no bigger than ε at each training point of x . In the next section, the mathematical formulation of SVR in linear and non-linear conditions will be explained in detail.

4.6.1. Linear Support Vector Regression

Suppose a set of training data is $D = \{x_i, y_i\}_i^n$ where x_i is the predictor variable, y_i is the observed value, and n is the number of observations. Then, the linear function can be expressed in Equation (4-39), where x is predictor variables, w is a parameter to measure the hyperplane location between the margin, and b is named bias and indicates the starting points of the hyperplane [122].

$$f(x) = xw + b \quad (4-39)$$

Ensuring its flatness, $f(x)$ would be found by minimal norm value $\|w\|^2$, which can also be indicated as $(w'w)$. This is formulated as a convex optimization problem to minimise $\frac{1}{2} w'w$ by subjecting it to all residuals having a value less than ϵ , which is presented in $|y_i - (x_i w + b)| \leq \epsilon$. However, this function is not able to solve these constraints for all points because, as can be seen from Figure 4-10, the points which are outside the tube create errors. Therefore, in such a condition, slack variables (ξ_i^+, ξ_i^-) for the points which are far from the tube need to be introduced because the slack variables allow regression errors to exist up to values of ξ_i^+ and ξ_i^- . Locating the slack variables in an objective function is known as a primal formula, which is shown in Equation (4-40).

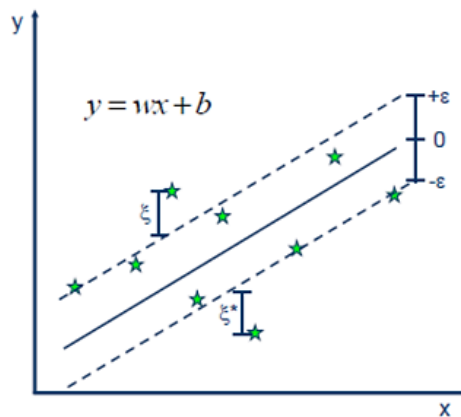


Figure 4-10: Hyperplane with a point out of margin target [122]

Minimise:

$$J(w) = \frac{1}{2} w'w + C \sum_{n=1}^N (\xi_i^+ + \xi_i^-)$$

Subject to:

$$\forall_i: y_i - (x_i w + b) \leq \epsilon + \xi_i^+ \tag{4-40}$$

$$\forall_i: (x_i w + b) - y_i \leq \epsilon + \xi_i^-$$

$$\forall_i: \xi_i^+ \geq 0$$

$$\forall_i: \xi_i^- \geq 0$$

C is a box constraint that determines the trade-off between the flatness of $f(x)$ and the amount up to which deviations larger than ε are tolerated. The positive or negative slack variables that control the penalty are imposed on the points that are located outside the epsilon margin and contribute to prevent overfitting. The linear ε -insensitive loss function $L_\varepsilon(f(x), y)$ is defined to ignore the errors of the points that are located within the margin [52]. The loss function is described as follows:

$$L_\varepsilon = \begin{cases} 0 & \text{if } |y - f(x)| \leq \varepsilon \\ |y - f(x)| - \varepsilon & \text{otherwise} \end{cases}$$

A Lagrange dual formulation is introduced to solve the optimization problem previously described. Indeed, in mathematical optimization, the minimization problem can be viewed by the primal and the dual problems, in which the solution to the dual problems provides a lower bound to the solution of the primal problem. The values of the primal and dual problems do not need to be equal and the difference is named the duality gap. However, when the problem is convex and it satisfies a constraint qualification condition, the solution of the dual problem provides the optimal solution to the primal problem. To obtain the dual formula, a Lagrange function introducing multipliers including α_i^+ and α_i^- for each data points x_i is used. The dual formula can be expressed in Equation (4-41).

$$L(a) = \frac{1}{2} \sum_{i=1}^N \sum_{j=1}^N (\alpha_i^+ - \alpha_i^-)(\alpha_j^+ - \alpha_j^-) x_i x_j + \varepsilon \sum_{i=1}^N (\alpha_i^+ + \alpha_i^-) + \sum_{i=1}^N y_i (\alpha_i^- - \alpha_i^+) \quad (4-41)$$

Subject to the constraints:

$$\sum_{i=1}^N (\alpha_i^+ - \alpha_i^-) = 0$$

$$\forall_i : 0 \leq \alpha_i^+ \leq C$$

$$\forall_i : 0 \leq \alpha_i^- \leq C$$

The w parameter can be described completely by a linear combination of the training points using Equation (4-42).

$$w = \sum_{i=1}^N (\alpha_i^+ - \alpha_i^-) x_i \quad (4-42)$$

Moreover, for obtaining the value of \mathbf{b} , two main parameters are required. One is w , which is obtained from Equation (4-42) and the other is S (support vector), which can be considered by a constraint. Therefore, b can be determined in Equation (4-43).

$$b = \frac{1}{|S|} \sum_{i \in S} [y_i - w' - x_i - \text{sign}(\alpha_i^+ - \alpha_i^-) \varepsilon] \quad (4-43)$$

$$S = \{i \mid 0 < \alpha_i^+ + \alpha_i^- < C\}$$

The support vectors lead to the prediction of new values using the function in Equation (4-44). The Karush–Kuhn–Tucker (KKT) complementarity conditions are optimization constraints that are required for computing the optimal solutions. In linear regression, the conditions are described in Equation (4-45).

$$f(x) = \sum_{i=1}^N (\alpha_i^+ - \alpha_i^-) (x_i, x) + b \quad (4-44)$$

KKT condition

$$\forall_i: \alpha_i^+ (\varepsilon + \xi_i^+ - y_i + x_i w + b) = 0$$

$$\forall_i: \alpha_i^- (\varepsilon + \xi_i^- + y_i - x_i w - b) = 0$$

$$\forall_i: \xi_i^+ (C - \alpha_i^+) = 0$$

$$\forall_i: \xi_i^- (C - \alpha_i^-) = 0$$

These conditions show that all the data points inside the epsilon tube have Lagrange multipliers with $\alpha_i^+ = 0$ and $\alpha_i^- = 0$. If these coefficients are not zero, the corresponding value is named the support vector.

4.6.2. Non-linear Support Vector Regression

The support vector regression method is also able to solve non-linear problems. Selecting an appropriate non-linear function with the Lagrange dual formulation that was previously described provides a great solution in non-linear models. From Figure 4-11, a non-linear regression model can be mapped in high-dimensional feature space. Then, using an appropriate kernel function with the form of $G(x_1, x_2) = \langle \varphi(x_1), \varphi(x_2) \rangle$ is able to provide the solution, where $\varphi(x)$ is a transformation that maps x to the high-dimensional space. Three kernel functions are expressed by Equations (4-45) to (4-47).

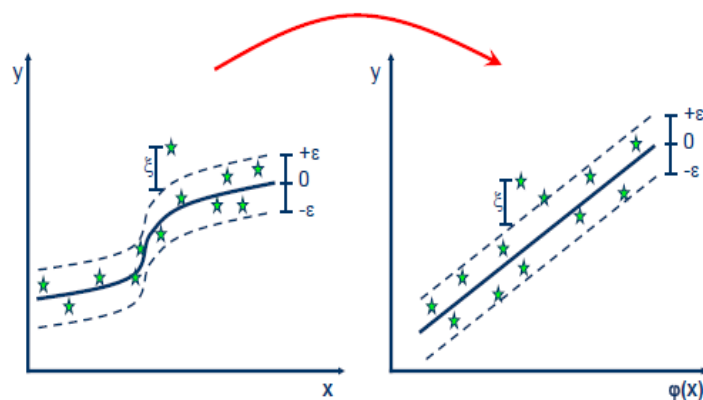


Figure 4-11: Mapping non-linear model into the feature space [122]

Linear (dot product) $G(x_j, x_k) = x_i x_j$ (4-45)

Gaussian $G(x_j, x_k) = \exp\left(-\frac{1}{2\sigma^2} \|X_i - X_j\|\right)$ (4-46)

Polynomial $G(x_j, x_k) = (1 + x_i x_j)^q$, where q is {2,3,..} (4-47)

The dual formula in non-linear regression replaces the predictors (x_i, x_j) . Then non-linear regression obtains the coefficients, which are minimised by a loss function in Equation (4-48).

$$L(a) = \frac{1}{2} \sum_{i=1}^N \sum_{j=1}^N (\alpha_i^+ - \alpha_i^-)(\alpha_j^+ - \alpha_j^-) G(x_i, x_j) + \varepsilon \sum_{i=1}^N (\alpha_i^+ + \alpha_i^-) - \sum_{i=1}^N y_i (\alpha_i^+ - \alpha_i^-)$$

Subject to

$$\sum_{j=1}^N (\alpha_i^+ - \alpha_i^-) = 0 \tag{4-48}$$

$$\forall_i : 0 \leq \alpha_i^+ \leq C$$

$$\forall_i : 0 \leq \alpha_i^- \leq C$$

The new value is predicted by the function in Equation (4-49).

$$f(x) = \sum_{i=1}^N (\alpha_i^+ - \alpha_i^-) G(x_i, x) + b \tag{4-49}$$

KKT condition

$$\forall_i: \alpha_i^+(\varepsilon + \xi_i^+ - y_i + f(x_i)) = 0$$

$$\forall_i: \alpha_i^-(\varepsilon + \xi_i^- + y_i - f(x_i)) = 0$$

$$\forall_i: \xi_i^+(C - \alpha_i^+) = 0$$

$$\forall_i: \xi_i^-(C - \alpha_i^-) = 0$$

In the support vector regression, quadratic programming is used to find the multipliers including α_i^+ and α_i^- for each data point x_i . Quadratic programming is the mathematical technique to solve the optimization problem, and it involves minimising the objective function subject to bounds. In this case, the *quadprog* function with a trust-region-reflective algorithm from MATLAB programming is used to solve bound-constrained problems.

In the proposed method, it is understood that w and b are two important parameters that can be found by a regularized empirical risk function. In this function, $C \sum_{n=1}^N L_\varepsilon(f(x), y)$ is measuring the empirical risk errors and $\frac{1}{2} w'w$ is a regularization term or the flatness of the function that needs to be minimised for simplification of the model. Parameter C is the capacity of the SVR that decides the trade-off between the regularization term and the empirical risk. ε is the size of the hyper-dimensional cylinder that covers the function with the training data points. Indeed, SVR performs linear regression in high-dimensional feature space using ε -insensitive loss, and at the same time tries to reduce the model's complexity by minimizing $w'w$. The minimization can be determined by introducing slack variables ξ_i^+, ξ_i^- $i = 1, \dots, n$ since ε -insensitive loss is equal to slack variables. The parameters C and ε are set by the designer during the training step for optimising the slack variables.

The w will be obtained by applying quadratic programming to determine the alpha for each data point x_i . b is obtained by Equation (4-44), which involves the designed C , ε and the support vectors.

In the case of a non-linear model, the model will be mapped in the feature space by a suitable kernel function. There are several kernel functions to solve the non-linear problem. In this study, a radial basis function (RBF) is used in this case, where σ is the dispersion coefficient, and it will be designed manually. The Karush–Kuhn–Tucker (KKT) conditions are used to optimise the constraints, and then find the optimal solutions.

These conditions state that all data points inside the epsilon tube have Lagrange multipliers with $\alpha_i^+ = 0$ and $\alpha_i^- = 0$. If these coefficients are not zero, the corresponding value will be named a support vector. Therefore, multiplying of the obtained w to the support vectors gives the new y . In this approach, MATLAB programming is used for computation with the following steps.

- Select the data as the x -axis and y -axis in the column
- Define a hyperplane with high-dimensional space by designing the parameters including epsilon ε and C
- Define the loss function with the considered constraints for minimization
- Define the kernel function and design the sigma based on assumptions
- Obtain the support vector coefficients with quadratic programming
- Compute bias (b) by the obtained support vector coefficients and other parameters
- Insert the desired x -axis points (load points) to find the desired y -axis points (desired power factor values)

Support vector regression has several strengths and weaknesses. The strengths are firstly that it can be trained easily and provides good generalization in theory and practice. It works well with a little training and creates the globally best model, unlike a neural network. It is able to scale well to high-dimensional data. In addition, the trade-off between the hyperplane and points failing to meet the target margin can be controlled explicitly. The weaknesses are the need to design the parameters C , but selecting an appropriate kernel function and finding its coefficient are the main weaknesses. Table 4-1 indicates the advantages and disadvantages of the considered methods explained in this chapter.

Table 4-1 The main features and issues of proposed methods

Methods	Advantages	Disadvantages
MCMD	<ul style="list-style-type: none"> • PF against load can be estimated by only measured current • It only needs nominal reactive current and measured current from no-load to full/over-load 	<ul style="list-style-type: none"> • It is not suitable in a large induction motor as reactive power changes via motor load
Kriging	<ul style="list-style-type: none"> • It can interpolate the unknown points and respond very well in a smooth model • There is no restriction on the number of input data 	<ul style="list-style-type: none"> • High distance between pair points provides low accuracy in predicting points • It causes overfitting at over-load conditions because it is not able to extrapolate the over-loading points
Regression	<ul style="list-style-type: none"> • It is able to make several models by polynomial degrees and provide the best fitting 	<ul style="list-style-type: none"> • A smaller number of sample points creates bad fitting • Polynomial degrees are not able to extrapolate the points at over-load
ANN	<ul style="list-style-type: none"> • Selecting proper hidden layers sorts out the overshooting problem at over-load condition 	<ul style="list-style-type: none"> • Needing large input data • A assumption percentage in selection of validation and testing data • Several running times are needed to create the best fitting • After closing and opening the program, all data will be deleted and again several running require • It is not very good in case of interpolation due to random selection of initializing the weights
SVR	<ul style="list-style-type: none"> • Good generalization • Works well with little training • Easily finds best model • Scales well in high-dimensional data • Controls the trade-off between complexity and errors • Identifies unseen points out of range • Provides an exact fitting model 	<ul style="list-style-type: none"> • Selects appropriate kernel function and designing the proper parameters. • Selection of C is tricky

4.7. Summary

In this chapter, the theory of the proposed techniques, including a method using the measured current and manufacturer's data, Kriging, regression, an artificial neural network and support vector regression, are described in detail. In the measured current method, a numerical equation requiring the nominal reactive current and measured current from no-load to full-load is considered. In the Kriging and regression, statistical procedures are followed by introducing appropriate functions that will be applied in both methods respectively. In the artificial neural network, the multi-layer perceptron structure is presented. A back propagation algorithm with gradient descent methods is used to train the data. In the support vector regression, a hyperplane with high-dimensional space is presented. Also, a loss function is used to minimise and obtain the coefficients.

Chapter 5: Results and Discussion

5.1. Introduction

In this chapter, the results of the measured power factor in the 250 W, 10 HP and 100 HP induction motors are presented. The results of the proposed methods, including a method using rgw measured current and manufacturer's data, Kriging, regression, an artificial neural network and support vector regression, which are implemented in the considered induction motors, will be described separately. The results of the proposed methods in the induction motors will be compared in order to substantiate the performance of the support vector regression method.

5.2. Results of Measured Power Factor

From the practical work, the measured power factors of 250 W, 10 HP and 100 HP induction motors from no-load to full-load and over-load are indicated in Figures 5-1, 5-2 and 5-3. It can be seen that the power factor in the three different induction motors changes exponentially from no-load to full-load and over-load conditions. Moreover, Figures 5-4, 5-5 and 5-6 illustrate the total harmonic distortion (THD) of the voltage and current in the considered induction motors.

It is observed that the THD_i and THD_v in these induction motors are less than 4% and, according to the IEEE standard, if $THD_{i\&v}$ is less than 4%, power factor distortion will be approximately unity and only the high reactive power consumption affects the power factor. The results of the measured power factor of the 100 HP induction motor from MATLAB/Simulink are shown in Figure 5-7. It is observed that the MATLAB/Simulink results are approximately close to the online power factor measured by the power analyser. The measured results at any loading point in both practical and simulation work are indicated in Table 5-1. It is observed that the measured results of the simulation compared with real measurement produced an average error of about 3%.

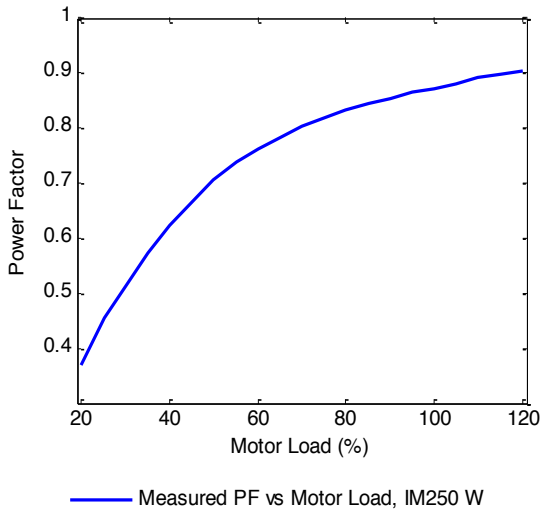


Figure 5-1: Measured PF of IM 250 W

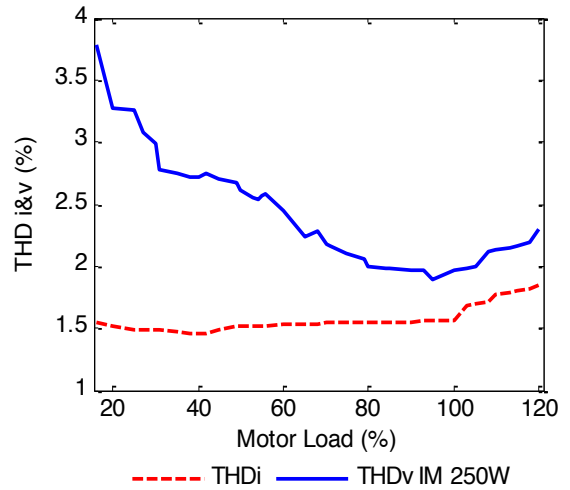


Figure 5-4: Measured THD of IM 250 W

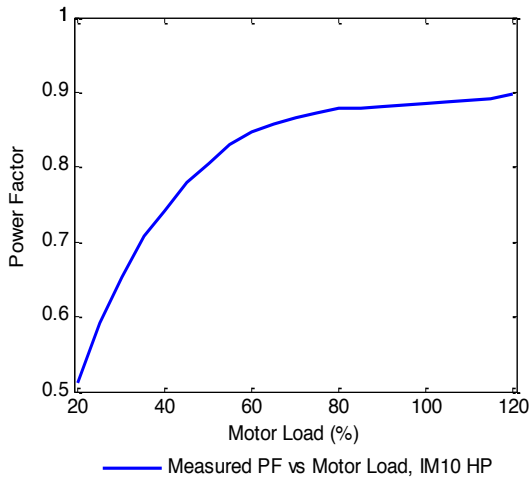


Figure 5-2: Measured PF of IM 10 HP

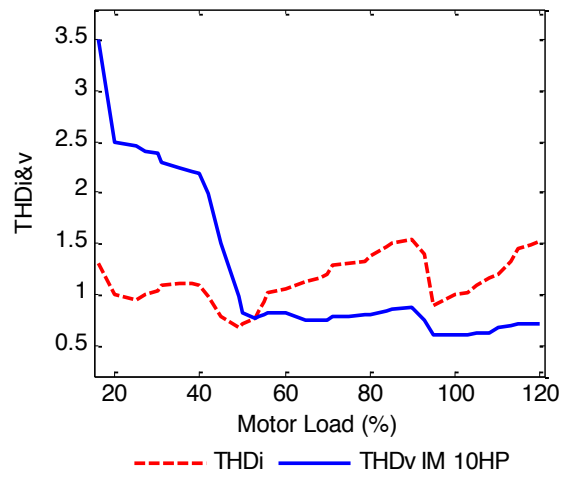


Figure 5-5: Measured THD of IM 10 HP

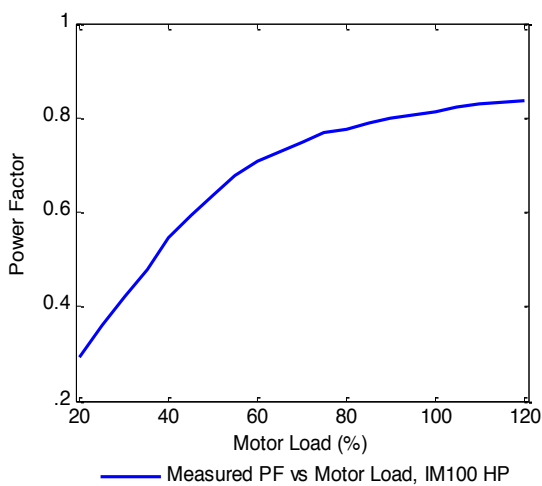


Figure 5-3: Measured PF of IM 100 HP

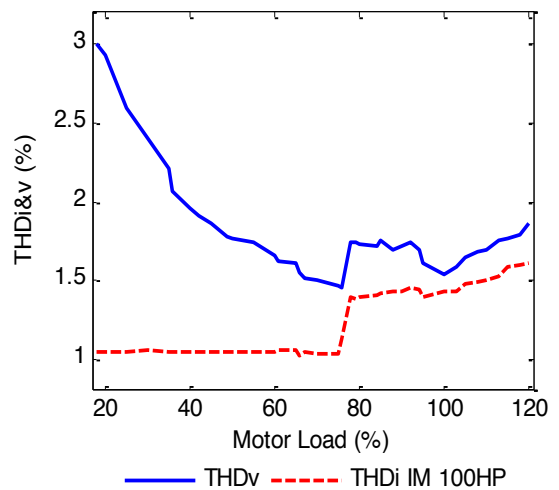


Figure 5-6: Measured THD of IM 100 HP

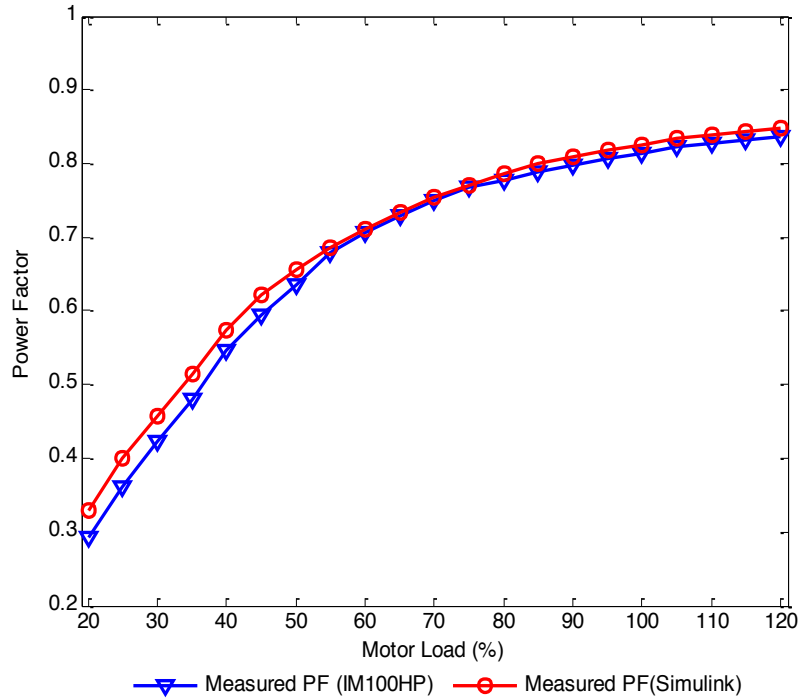


Figure 5-7: PF measurement by simulation and power analyser

Table 5-1 Measured PF of IM 100 HP using MATLAB/Simulink

Load (%)	Experimental (PF)	Simulation (PF)	APE (%)
20	0.294	0.329	10.811
25	0.360	0.400	9.975
30	0.422	0.458	7.882
35	0.480	0.515	6.796
40	0.547	0.574	4.824
45	0.594	0.623	4.689
50	0.636	0.656	3.094
55	0.678	0.685	1.109
60	0.707	0.711	0.591
65	0.729	0.734	0.627
70	0.750	0.754	0.531
75	0.768	0.771	0.428
80	0.777	0.786	1.157
85	0.788	0.799	1.426
90	0.798	0.810	1.531
95	0.806	0.818	1.503
100	0.814	0.826	1.416
105	0.822	0.834	1.439
110	0.828	0.84	1.429
115	0.832	0.844	1.422
120	0.837	0.848	1.297
MAPE: 3.046			

5.3. Results of Measured Current Method

It is understood that by measuring the motor current and using the nominal power factor from the nameplate of the induction motor, the power factor can be estimated at any loading. However, using this method produced errors. Since it works based on the nominal reactive current, it creates significant errors at many loading points because the reactive current is obtained from the nominal power factor and the nominal power factor provides a constant reactive current. However, in reality, the reactive current at no-load or light-load is not constant.

As can be seen from Figures 5-8, 5-9 and 5-10, the reactive current of the 250 W, 10 HP and 100 HP induction motors increase from no-load to full-load. The increase in the 250 W induction motor is quite small, at about 4 mA. In the 10 HP induction motor, there is a quite large variation of about 6A from no-load to over-load that produces a substantial error in the power factor estimation. Thus, this variation from no-load to full-load and over-load creates high errors in power factor estimation particularly in the medium and large induction motors due to the large magnetic field.

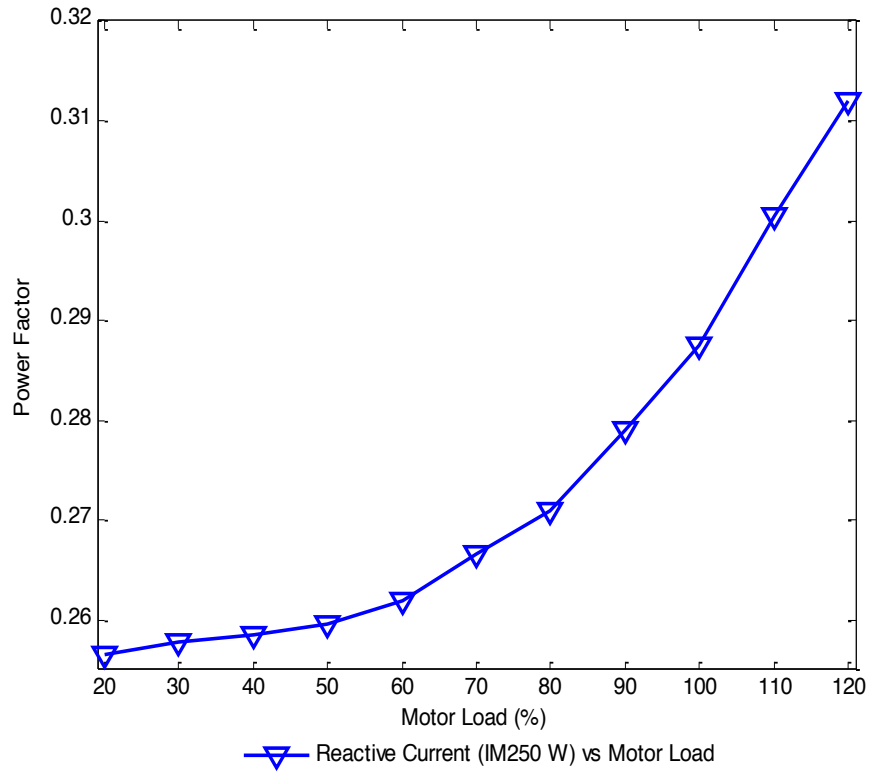


Figure 5-8: Measured reactive current in IM 250 W

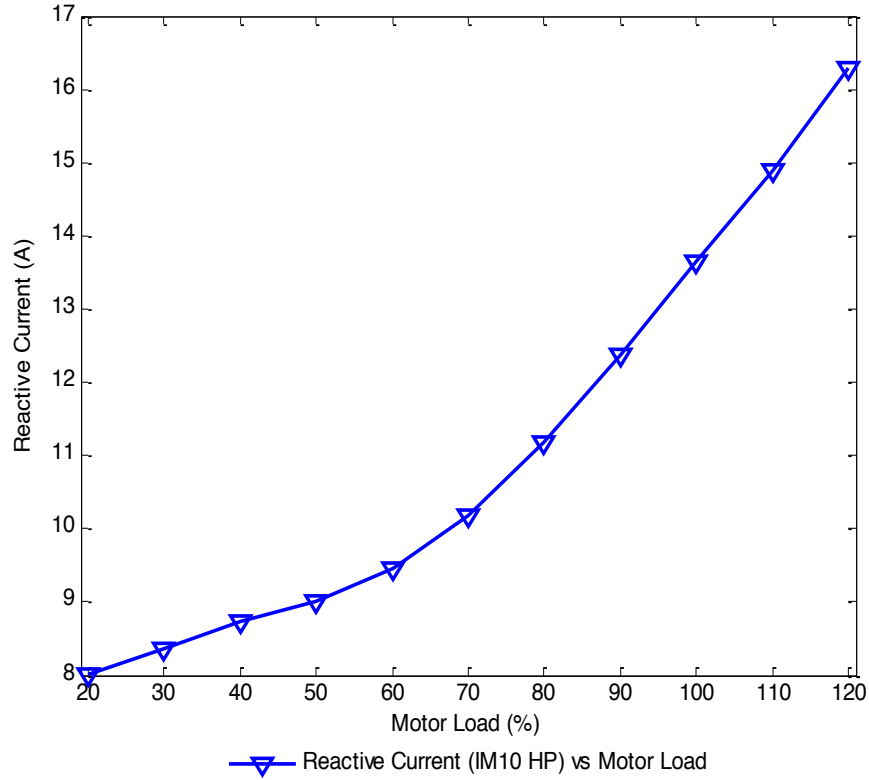


Figure 5-9: Measured reactive current in IM 10 HP

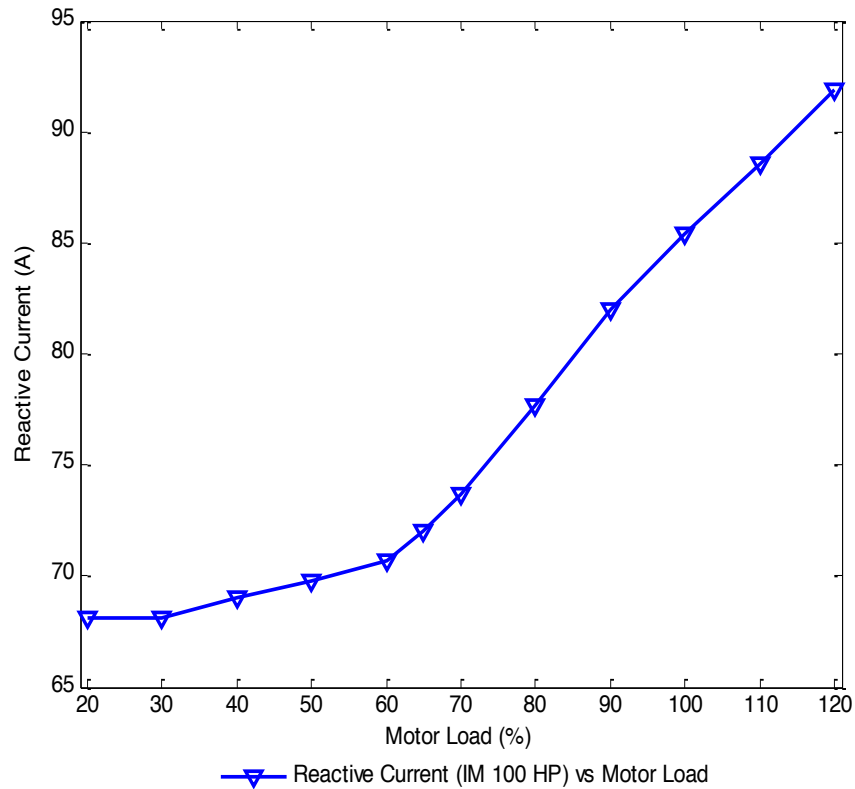


Figure 5-10: Measured reactive current in IM 100 HP

Figures 5-11, 5-12, and 5-13 indicate the estimated power factor of the 250 W, 10 HP and 100 HP induction motors from no-load to full-load conditions respectively. It can be seen that there are significant errors between the measured power factor and estimated power factor from no-load to full-load and over-load conditions. The error in the 250 W induction motor is low, but the errors in the 10 HP and 100 HP induction motors are extremely high.

The low and high errors in the proposed induction motors are due to the different specifications with different sizes because the reactive current in the 10 HP and 100 HP induction motors produced higher variation from no-load to full-load than in the 250 W induction motor. This variation is the main cause of huge errors in the medium and large induction motors.

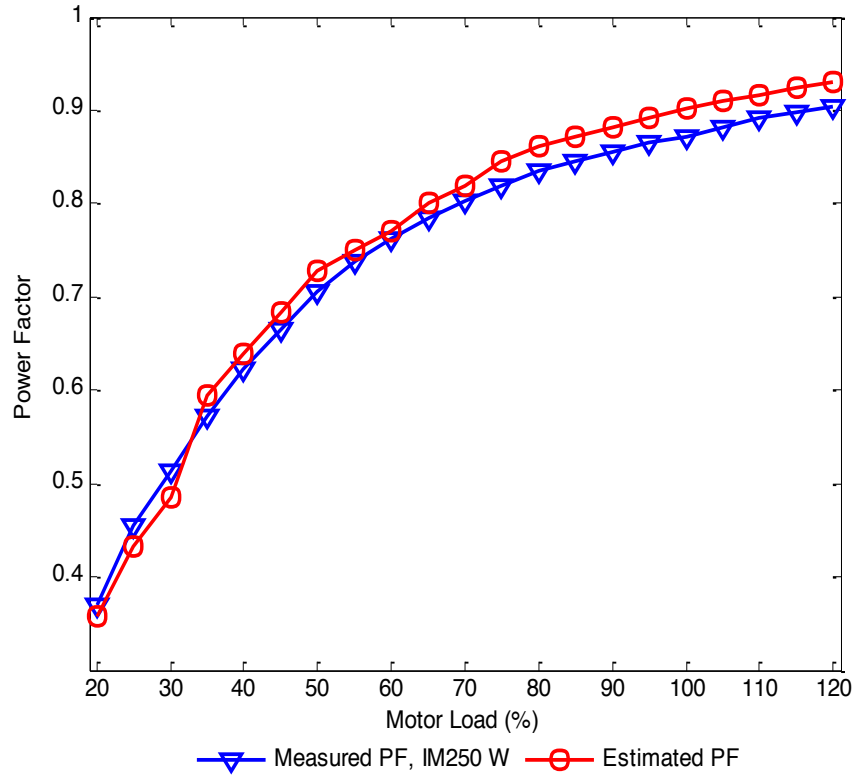


Figure 5-11: Estimated PF of IM 250 W using MCMD

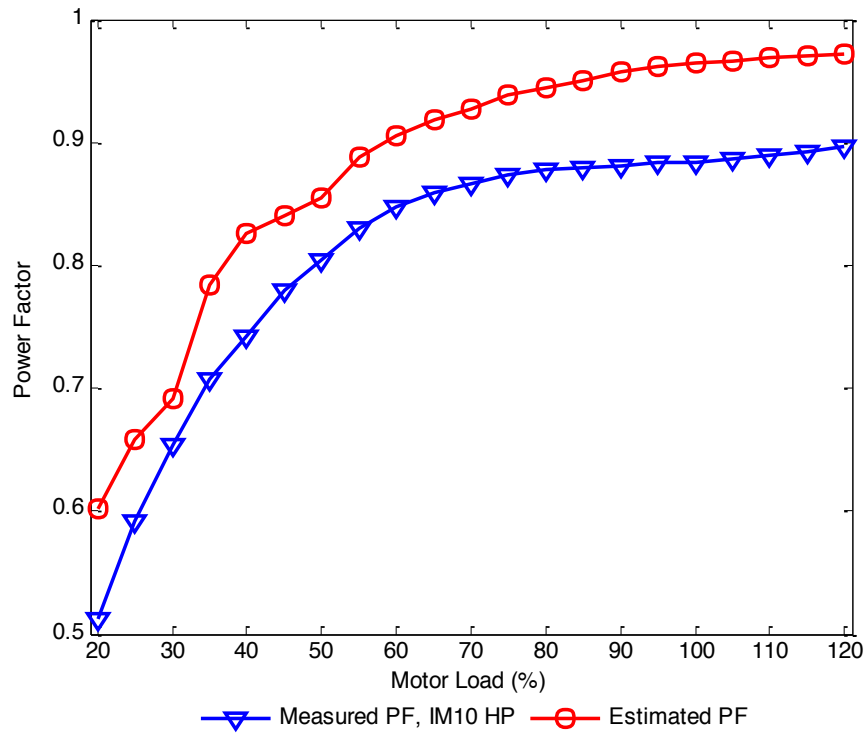


Figure 5-12: Estimated PF of IM 10 HP using MCMD

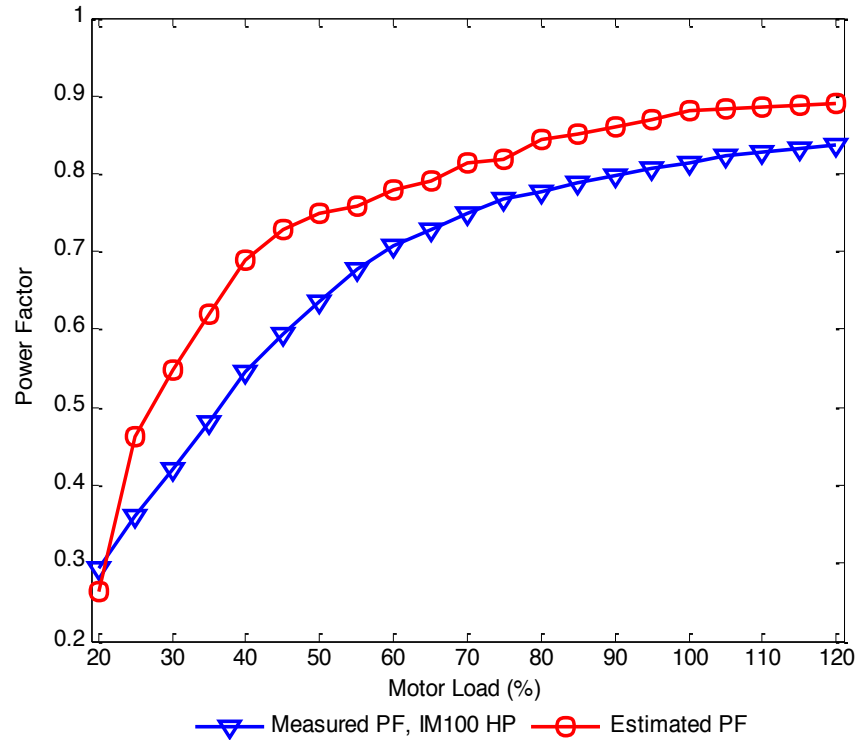


Figure 5-13: Estimated PF of IM 100 HP using MCMD

Table 5-2 indicates the error at any considered load point in percentage. It is observed that in the 250 W induction motor, the errors in the majority of load points are lower than 3%. Only the loads of 25 and 30 produced errors higher than 5%. However, in the 10 HP induction motor, the errors in many loads are between 6% and 8%, except for loads 20 and 25, which are 10% and 15%. In addition, in the 100 HP induction motor, the load from 25 to 50 produced higher errors of between 15% and 22%. The errors for the other load points are 7% and 11%. To obtain the error between the estimated points and measured points in percentage, the absolute percentage error (APE) in Equation (5-1) is used.

$$APE = \frac{\text{Estimated value} - \text{Measured value}}{\text{Estimated value}} \times 100 \quad (5-1)$$

Table 5-2 Estimated PF of IMs using MCMD from no-load to over-load

Load (%)	EPF (250 W)	APE (%)	EPF (10 HP)	APE (%)	EPF (100 HP)	APE (%)
20	0.357	3.612	0.601	14.870	0.265	11.040
25	0.432	5.045	0.659	10.276	0.462	22.073
30	0.485	5.983	0.691	5.483	0.548	23.067
35	0.594	3.571	0.784	9.823	0.619	22.418
40	0.639	2.660	0.825	10.044	0.690	20.774
45	0.683	2.548	0.840	7.110	0.729	18.607
50	0.729	3.224	0.855	5.965	0.749	15.066
55	0.749	1.508	0.887	6.503	0.760	10.757
60	0.770	0.922	0.906	6.414	0.779	9.315
65	0.800	2.012	0.919	6.552	0.791	7.827
70	0.818	1.931	0.927	6.540	0.814	7.924
75	0.844	2.926	0.939	6.998	0.819	6.298
80	0.861	3.101	0.944	7.023	0.844	7.905
85	0.871	2.917	0.950	7.483	0.851	7.404
90	0.881	2.962	0.958	8.018	0.861	7.310
95	0.892	3.049	0.961	8.136	0.871	7.421
100	0.902	3.405	0.964	8.299	0.881	7.539
105	0.910	3.197	0.9664	8.216	0.882	6.824
110	0.915	2.676	0.9686	8.115	0.885	6.430
115	0.924	2.901	0.9705	8.089	0.889	6.380
120	0.929	2.851	0.972	7.716	0.891	6.082
MAPE	-	2.964	-	7.984	-	11.355

Table 5-3 indicates the validity and accuracy of the method using the measured current in mean square error (MSE), mean absolute percentage error (MAPE) and accuracy. It is observed that MCMD produced an average error of about 2.964%, 7.984% and 11.355% in the 250 W, 10 HP and 100 HP induction motors respectively.

Table 5-3 Validity and accuracy of MCMD

Method	Validity	IM 250 W	IM 10 HP	IM 100 HP
MCMD	MSE	5.20E-04	5.00E-03	7.2E0-3
	MAPE	2.964	7.984	11.355
	Accuracy	97.036%	92.016%	88.645%

As a result, this method only worked well in the small induction motor due to the very small reactive current variation, which can approximately be considered constant.

However, this method is not reliable in estimating the power factor of medium and large induction motors because of the high reactive current variation, which produces high errors. In this research, statistical methods and intelligent techniques are implemented in different ranges of induction motors including 250 W, 10 HP and 100 HP in order to determine the power factor against motor load properly. These methods need to add three inputs, namely the voltage, current and input power, at a few points from no-load to full-load, as shown in Table 5-4.

5.4. Result of Kriging Method

The results of the Kriging method show that the estimated power factor in the 250 W, 10 HP and 100 HP induction motors are very close to the measured power factor from no-load to full-load conditions. However, the results at over-load conditions are far from the measured points. This is because Kriging is an interpolation technique and is not able to extrapolate the over-loading points. Figures 5-14, 5-15 and 5-16 illustrate the estimated power factor of the considered induction motors from no-load to full-load and over-load conditions, where the blue and red line show the measured and estimated power factor against load respectively. Table 5-4 illustrates the values of the estimated power factor and the errors between the measured and estimated points in percentage at the desired load points. In the 250 W induction motor, the errors at the majority of load points are less than 0.2%. Only the loads of 20 and 25 produced high errors of 1.309% and 0.980%. In the 10 HP induction motor, the minimum and maximum errors were presented at loads of 25 and 90, which were 2.248% and 0.057% respectively. Moreover, from load 65 to 100, the errors were less than 3%. In the 100 HP induction motor, the Kriging produced errors of less than 3% at many load points. The errors of 1.111% and 0.025% at loads 35 and 95 indicated the minimum and maximum.

However, the errors in the three induction motors from full-load to over-load increased to 12%. Therefore, the results confirmed that the Kriging in the 100 HP induction motor indicated low errors at many loads compared with the 250 W and 10 HP induction motors.

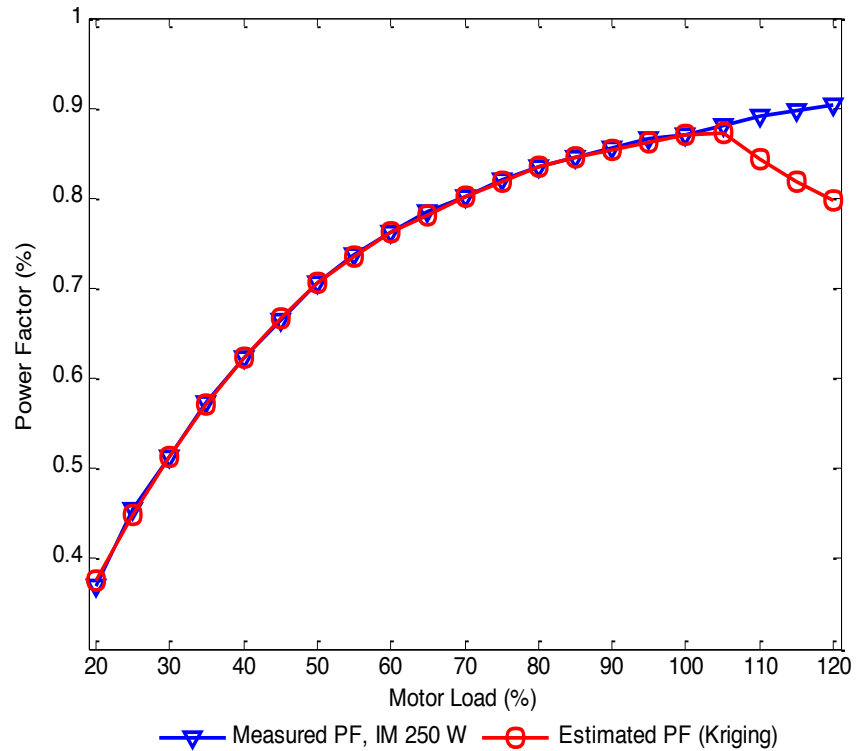


Figure 5-14: Estimated PF of IM 250W using Kriging

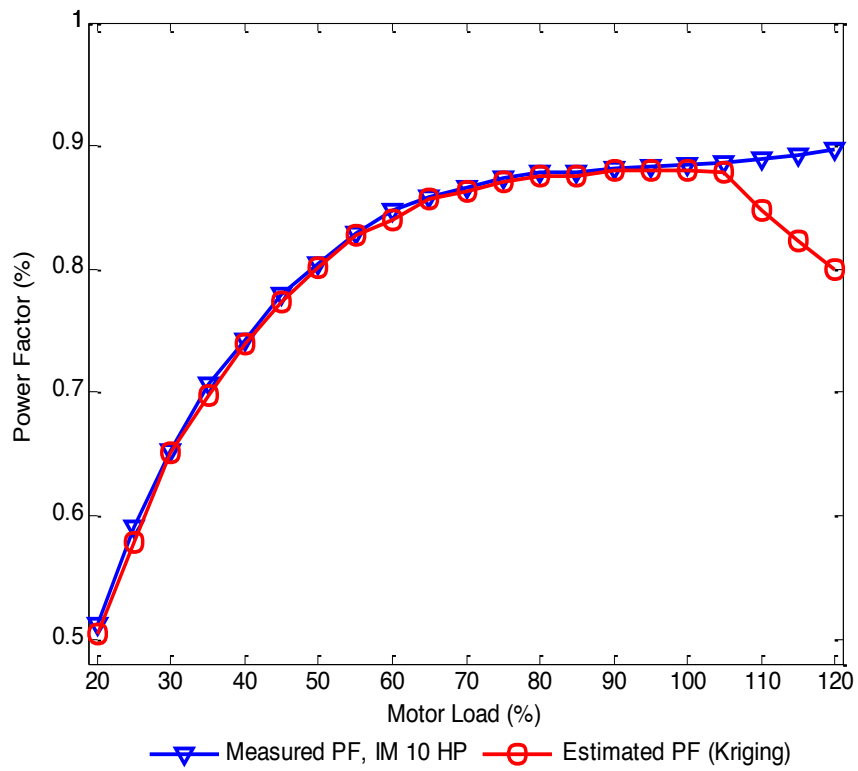


Figure 5-15: Estimated PF of IM 10HP using Kriging

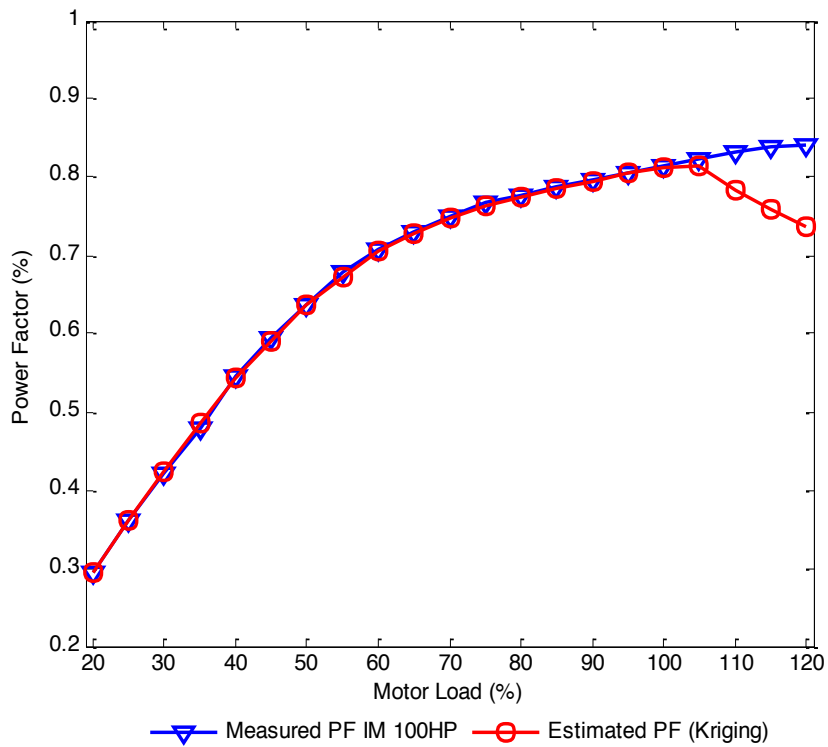


Figure 5-16: Estimated PF of IM 100HP using Kriging

Table 5-4 Estimated PF of IMs using Kriging from no-load to over-load

Load (%)	EPF (250 W)	APE (%)	EPF (10 HP)	APE (%)	EPF (100 HP)	APE (%)
20	0.375	1.309	0.504	1.620	0.294	0.061
25	0.450	0.980	0.578	2.248	0.361	0.104
30	0.514	0.034	0.651	0.426	0.424	0.407
35	0.571	0.190	0.698	1.280	0.485	1.111
40	0.623	0.090	0.740	0.367	0.542	0.744
45	0.666	0.088	0.773	0.956	0.589	0.759
50	0.707	0.150	0.801	0.437	0.636	0.043
55	0.735	0.493	0.827	0.303	0.671	0.945
60	0.762	0.191	0.840	0.942	0.706	0.134
65	0.781	0.428	0.856	0.279	0.727	0.218
70	0.802	0.023	0.863	0.362	0.748	0.210
75	0.818	0.218	0.870	0.326	0.763	0.658
80	0.834	0.020	0.876	0.235	0.775	0.285
85	0.845	0.047	0.876	0.374	0.786	0.196
90	0.853	0.215	0.881	0.057	0.795	0.319
95	0.862	0.359	0.880	0.392	0.806	0.025
100	0.870	0.157	0.881	0.375	0.812	0.302
105	0.873	0.943	0.878	0.965	0.814	1.141
110	0.844	5.306	0.848	4.682	0.784	5.734
115	0.819	8.735	0.822	7.818	0.759	9.437
120	0.797	11.745	0.799	10.847	0.737	12.477

Although the Kriging method performed well in power factor estimation at unknown points from no-load to full-load conditions, the strategy of Kriging is geostatistical, where the computing distance between one unknown point and surrounding observed points is required. A high interval between two points creates a complexity with high errors. Table 5-5 illustrates the evaluation of the validity and accuracy of Kriging. MSE and MAPE are used to indicate the quality of the estimator and measure the prediction accuracy respectively. In this table, it is shown that Kriging can be a good estimator from no-load to full-load conditions and provided a satisfactory accuracy of 99% for the three different sizes of induction motors. However, it was not a good estimator at over-load conditions because it produced high error at each point from full-load to over-load, in which the errors indicated were between 6% and 7% for the proposed induction motors.

Table 5-5 Validity and accuracy of Kriging method

Method	Validity	IM 250 W	IM 10 HP	IM 100 HP
Kriging	MSE	2.46E-03	1.13E-03	2.46E-03
	MAPE	3.488	3.3615	0.194
	Accuracy	96.509%	99.351%	96.20%

Although this method mostly provided good performance from no-load to full-load conditions, in general, using this method is not reliable for modelling because only the distance between each observed pair of points and also the interval between observed points and a point that requires to be estimated are used to find a solution. A small interval between these points means the estimating point becomes more accurate.

5.5. Results of Regression Method

Polynomial regression, which works based on the relationship between the independent variable x and the dependent variable y , provides a weight value between variables which is known as a polynomial coefficient. Polynomial regression requires a few observed values of x and y . In this case, some points of the motor load and power factor are considered as x and y . The coefficients between the two values need to be predicted because the predicted coefficient multiplied by the independent values in the x -axis leads to obtaining the unknown values in the y -axis. The accuracy of an unknown point depends on the number of polynomial orders; by increasing the order, the coefficient will be increased. Increasing the coefficients or orders makes the function more powerful, thus reducing the errors and creating a model with high fitness. The predicted coefficients within the 4th order in the 250 W, 10 HP and 100 HP induction motors are presented in Table 5-6.

Table 5-6 Obtained coefficients of polynomial degrees in considered IMs

IMs	Orders	β_1	β_2	β_3	β_4	β_5
250W	1st order	0.0060	0.3310	-	-	-
	2nd order	-8.77E-05	0.0166	0.086	-	-
	3rd order	7.85E-07	-2.29E-4	0.0239	-0.0163	-
	4rd order	-9.65E-10	1.017E-06	-2.48E-04	0.0260	-0.0224
10HP	1st order	0.0062	0.3770	-	-	-
	2nd order	-1.212E-4	0.0195	0.131	-	-
	3rd order	1.415E-06	-3.544E-4	0.0298	0.0341	-
	4rd order	-1.056E-08	3.74E-06	- 5.20E-4	0.034	8.79E-3
100HP	1st order	0.0063	0.2498	-	-	-
	2nd order	-9.09E-05	0.0173	-0.0121	-	-
	3rd order	4.88E-07	- 1.8E-04	0.0220	-0.079	-
	4rd order	1.33E-08	-2.74E-06	8.74E-05	0.0133	0.0108

In the regression method, increase of the coefficients provides a desired model very close to the observed power factor curve. In this method, the 1st, 2nd, 3rd and 4th orders are tried and it is observed that the 4th order indicated the best fitting model in the proposed induction motors. The fitness of the existing models in the induction motors is presented in Table 5-7. The residual models of the polynomial degrees in the induction motors are shown in Figures 5-17, 5-18 and 5-19.

Table 5-7 Fitness of polynomial degrees in considered IMs

Regression	Fitness	IM (250 W)	IM (10 HP)	IM (100 HP)
1 st order	SSE	0.03628	0.1129	0.0367
	R-square	0.8798	0.7493	0.8855
	Adjusted R-square	0.8627	0.7134	0.8691
	RMSE	0.07199	0.127	0.0724
2 nd order	SSE	0.00158	0.01002	7.9E-04
	R-square	0.9948	0.9778	0.9975
	Adjusted R-square	0.993	0.9703	0.9967
	RMSE	0.01623	0.04086	0.01144
3 rd order	SSE	2.17E-05	3.60E-04	2.36E-04
	R-square	0.9999	0.9992	0.9993
	Adjusted R-square	0.9999	0.9987	0.9988
	RMSE	0.002081	0.008479	0.006866
4 th order	SSE	2.05E-05	3.47E-05	2.90E-05
	R-square	0.9999	0.9999	0.9999
	Adjusted R-square	0.9999	0.9998	0.9998
	RMSE	0.002263	0.002946	0.002691

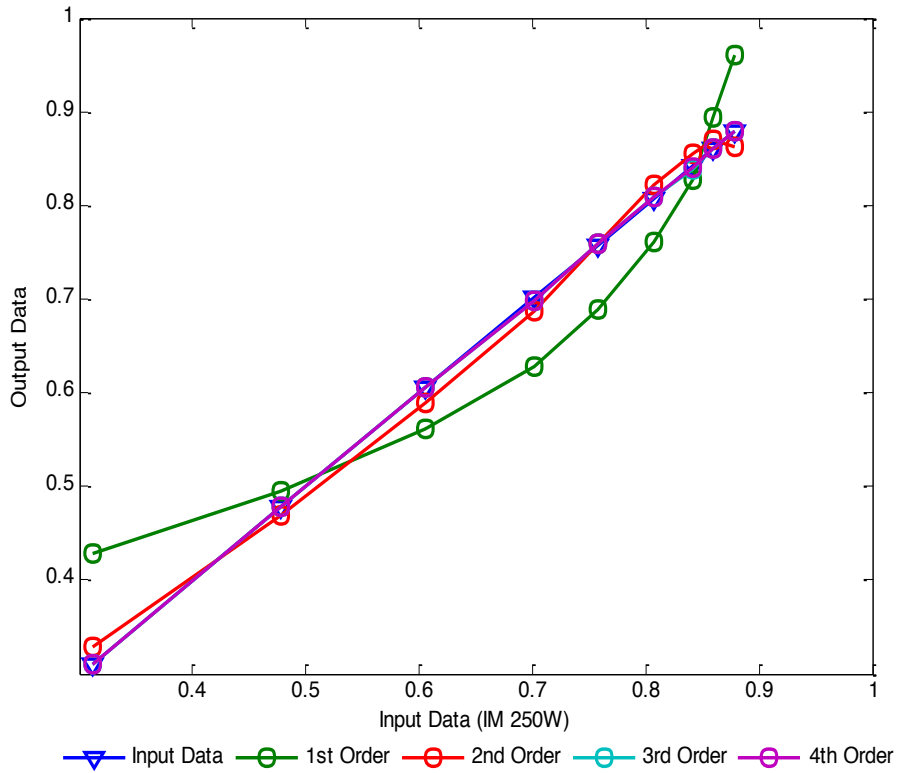


Figure 5-17: The residual models of the polynomial degrees in IM 250 W

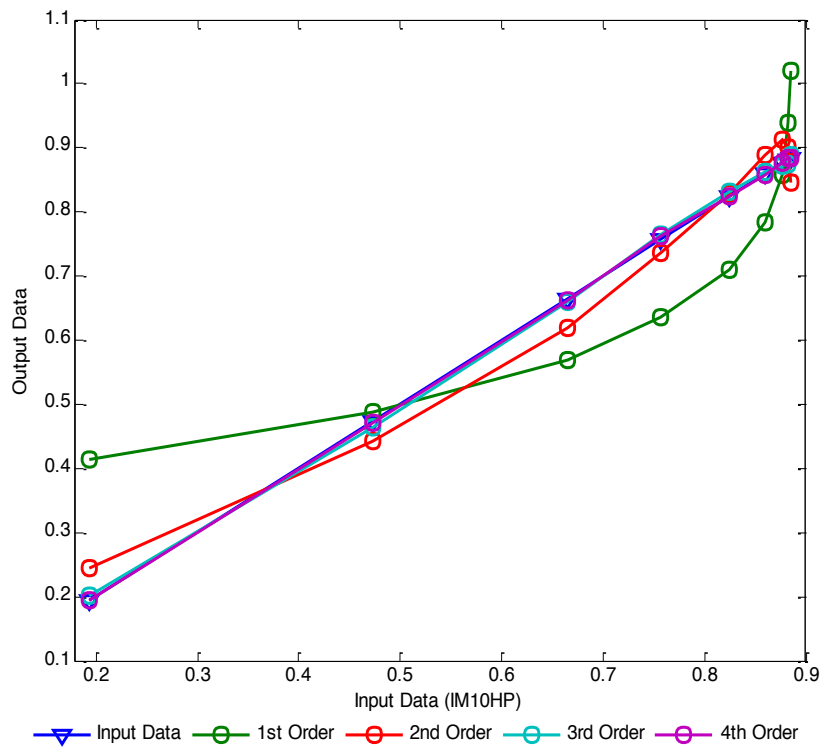


Figure 5-18: The residual models of the polynomial degrees in IM 10 HP

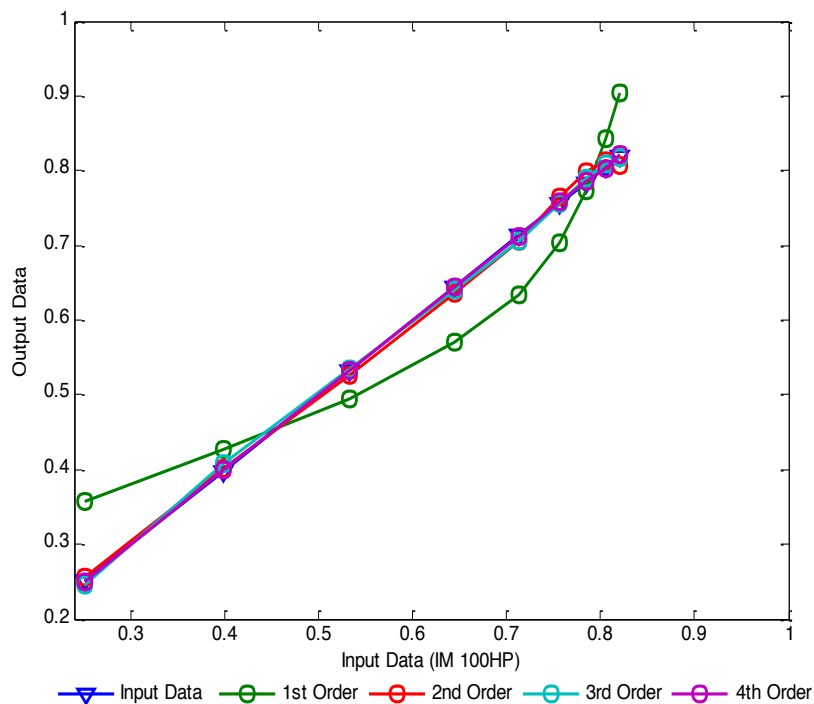


Figure 5-19: The residual models of the polynomial degrees in IM100 HP

The power factor of induction motors at unknown points is estimated based on the different existing polynomial degrees models. Figures 5-20, 5-21 and 5-22 indicate the estimated power factor in the induction motors by the 1st, 2nd, 3rd and 4th orders. The results show that the 1st and 2nd orders in the three induction motors produced high errors. However, the 3rd and 4th orders obtained satisfactory results very close to the measured power factor from no-load to full-load conditions. Although the number of orders is proportional to the number of independent values in the x -axis and the last order provides high performance in terms of best fitting, in such cases the 4th order performed very well, with lower average error in estimating the unknown power factor of induction motors from no-load to full-load conditions. Although polynomial regression can provide a high performance from no-load to full-load condition, in these cases, polynomial regression with any degree is not able to extrapolate over-load points very well and produces a dramatic drop in the results

from full-load to over-load conditions. The error results of the proposed induction motors from no-load to over-load are indicated in Table 5-9.

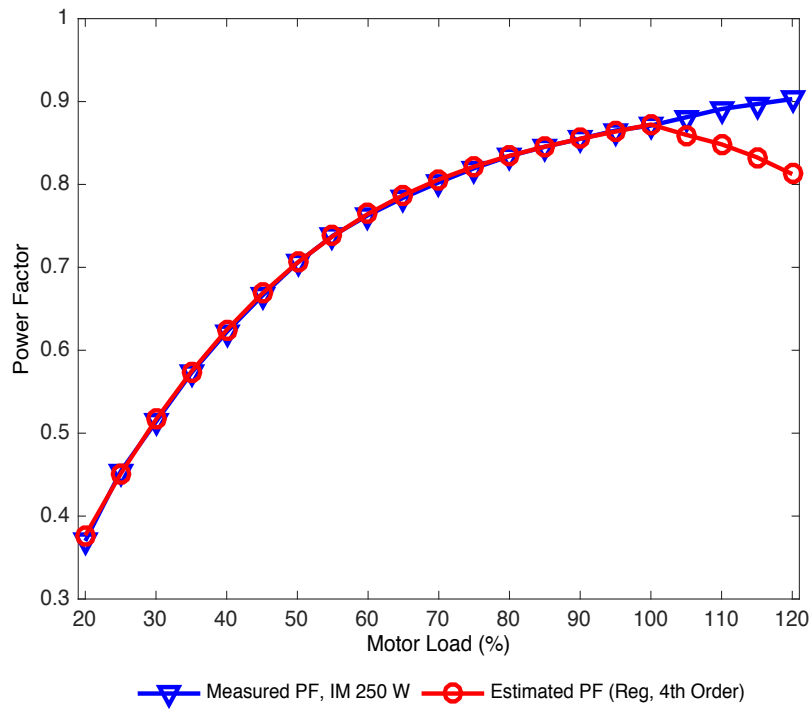


Figure 5-20: Estimated PF of IM 250W using regression

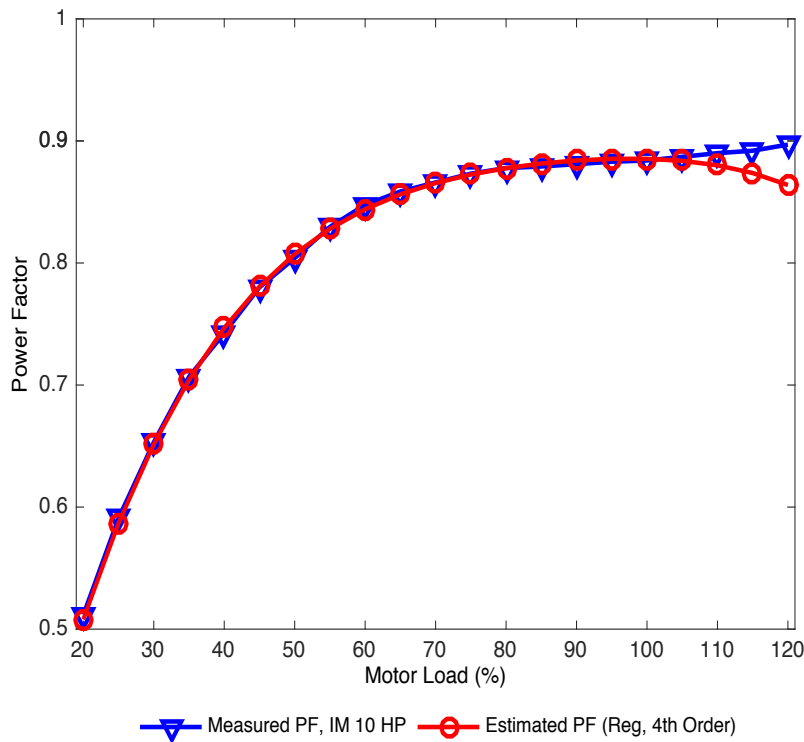


Figure 5-21: Estimated PF of IM10HP using regression

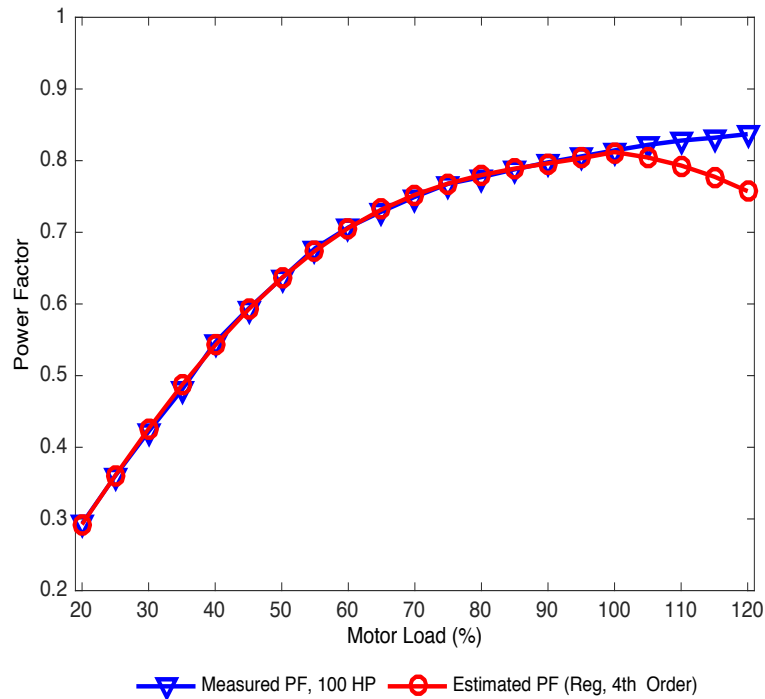


Figure 5-22: Estimated PF of IM100 HP using regression

Table 5-8 presents the estimated power factor of the considered induction motors with the percentage errors at every single loading point from no-load to full-load. It is observed that in the 250 W induction motor, the highest error is 1.849% at a load of 20 and the lowest error is 0.016% at a load of 90. The errors from loads of 20 to 45 are higher than 0.6%. However, at other load points the errors are less than 0.5%. In the 10 HP induction motor, loads of 20 and 25 created the highest errors of 0.750% and 0.735% respectively. The errors at many loads are less than 0.2%. Moreover, in the 100 HP induction motor, the minimum error is indicated at a load of 50 with about 0.07% and a load of 35 produced the maximum error of 1.389%. The errors for the majority of load points are less than 0.3%.

Table 5-8 Estimated PF of IMs using regression from no-load to over-load

Load (%)	EPF (250 W)	APE (%)	EPF (10 HP)	APE (%)	EPF (100 HP)	APE (%)
20	0.377	1.857	0.508	0.750	0.292	0.445
25	0.451	0.554	0.587	0.735	0.361	0.208
30	0.517	0.638	0.652	0.266	0.426	0.954
35	0.575	0.365	0.704	0.363	0.487	1.389
40	0.625	0.448	0.747	0.583	0.542	0.765
45	0.668	0.404	0.781	0.085	0.592	0.214
50	0.706	0.014	0.807	0.411	0.636	0.070
55	0.737	0.109	0.828	0.187	0.674	0.529
60	0.764	0.157	0.844	0.432	0.706	0.116
65	0.787	0.356	0.856	0.273	0.732	0.396
70	0.806	0.410	0.866	0.056	0.752	0.385
75	0.822	0.243	0.873	0.080	0.768	0.055
80	0.835	0.072	0.878	0.011	0.780	0.366
85	0.846	0.071	0.882	0.271	0.789	0.126
90	0.856	0.070	0.884	0.343	0.796	0.174
95	0.864	0.081	0.885	0.266	0.803	0.315
100	0.872	0.160	0.885	0.153	0.812	0.286
105	0.860	2.466	0.884	0.530	0.804	2.145
110	0.848	5.0210	0.880	1.681	0.793	4.197
115	0.833	7.722	0.874	3.572	0.778	6.542
120	0.813	11.138	0.864	5.847	0.757	9.515

The comparison results in this table indicate that the 4th order polynomial regression obtained results with errors less than 1% at many loading points in the 250 W, 10 HP and 100 HP induction motors. However, it is shown that the estimated power factor at over-load conditions produced large errors from full-load to over-load, where the errors in the 250 W induction motor were from 2.466% to 11.138%. In the 10 HP induction motor, the minimum and maximum errors observed were 0.530% at full-load and 5.847% at over-load respectively. In the 100 HP induction motor, the errors gradually increased from 2.145% to 9.515% and the maximum load indicated the highest error.

Table 5-9 presents the validity and accuracy of polynomial regression within four orders in the three induction motors. MSE, MAPE and accuracy are used to show the performance of the 1st, 2nd, 3rd and 4th orders. It is observed that the 4th order

performed very well compared with the 1st, 2nd and 3rd orders and it produces high accuracy in the three induction motors, with values of about 99.60%.

Table 5-9 Validity and accuracy of regression results

IMs	Validity	Polynomial Regression			
		1st order	2nd order	3rd order	4th order
250 W	MSE	0.0049	8.01E-04	1.38E-05	7.60E-06
	MAPE	8.0028	2.4461	0.3765	0.3418
	Accuracy	91.972	97.554	99.623	99.658
10 HP	MSE	0.0123	0.0033	2.24E-04	7.88E-05
	MAPE	11.7005	5.219	1.178	0.5945
	Accuracy	88.3	94.781	98.822	99.4055
100 HP	MSE	0.0041	5.80E-04	5.37E-05	2.65E-04
	MAPE	9.7205	2.0519	0.88	0.9697
	Accuracy	90.280	97.95	99.12	99.030

Table 5-10 presents the average errors with a comparison between MCMD, Kriging and regression. It is observed that the proposed methods in the 250 W induction motor produced errors of less than 4%, where the error in MCMD is 3% and in the Kriging and regression methods is 3.5%. However, MCMD creates high errors of more than 8% in the 10 HP and 100 HP induction motors, while the errors of both Kriging and regression in the 10 HP induction motor and in the 100 HP induction motor are 3% and 2%, 4% and 3% respectively. Therefore, from this table it can be seen that regression in the 10 HP and 100 HP induction motors reduced the errors and performed very well compared with the MCMD and Kriging methods.

Table 5-10 Validity and accuracy of all the proposed methods

IMs	Validity	Methods		
		MCMD	Kriging	Regression (4 th)
250 W	MSE	5.20E-04	2.46E-03	7.60E-06
	MAPE	2.964	3.488	0.3418
	Accuracy	97.036	96.509	99.658
10 HP	MSE	5.00E-03	1.13E-03	7.88E-05
	MAPE	7.984	3.3615	0.5945
	Accuracy	92.016	96.637	99.4055
100 HP	MSE	7.2E0-3	2.46E-03	2.65E-04
	MAPE	11.355	3.790	0.969
	Accuracy	88.645%	96.205%	99.030%

5.6. Results of Artificial Neural Network

In the artificial neural network, three kinds of samples are needed as inputs, namely training, validation and testing data. In these cases, 9 input data are selected, of which 5 points are as training, 2 points as testing and 2 points as validation. The training values are presented to the network and the network is adjusted according to its error. The validation is used to measure network generalization and stop training when the generalization has improved. Testing provides an independent measure of network performance during and after training.

In addition, selecting the number of hidden layers and the least squares algorithm are important in order to fit the inputs and targets. Once the parameters have been selected, the algorithm can be run. The results in Figure 5-23 indicate that the neural network is not able to provide great results with one running time because the algorithm needs to run several times in order to back propagate the output and update the weights. In these cases, in order to verify the best results, 10 running times are considered for testing. It is observed that in the three different case studies more or fewer running times are required to create the best model with the lowest error. For example, in the 250 W induction motor with 10 running times, running five indicated a better model. However, for the 10 HP and 100 HP induction motors, running six and eight times provided high performance.

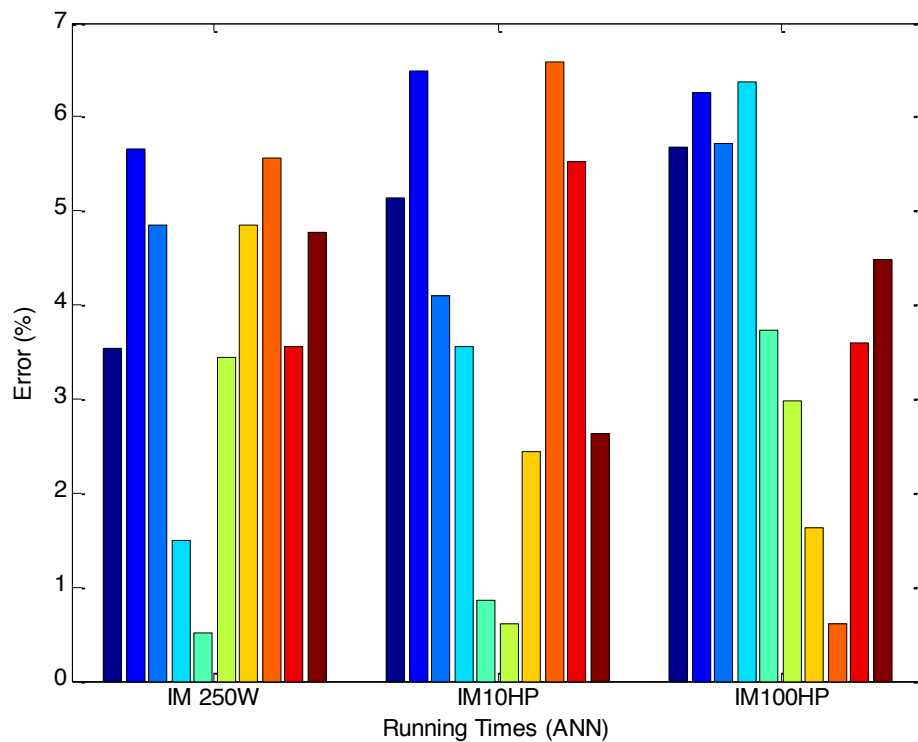


Figure 5-23: Error results of ANN considering IMs within 10 running times

Tables 5-11, 5-12 and 5-13 indicate the selected input data and progress results with the considered running times in these induction motors. Figures 5-24, 5-25 and 5-26 illustrate the residual error of training, validation and testing in the 250 W, 10 HP and 100 HP induction motors. In these figures, the regression plot is used to show the relationship between the outputs of the network and the targets; if the training were perfect, the network outputs and the targets would be exactly equal. However, if the network is not sufficiently accurate, the network can be initialized again and each time the network parameters will be changed and produce different solutions. Increasing the number of hidden neurons and using a different training function can be a good solution to create better generalization.

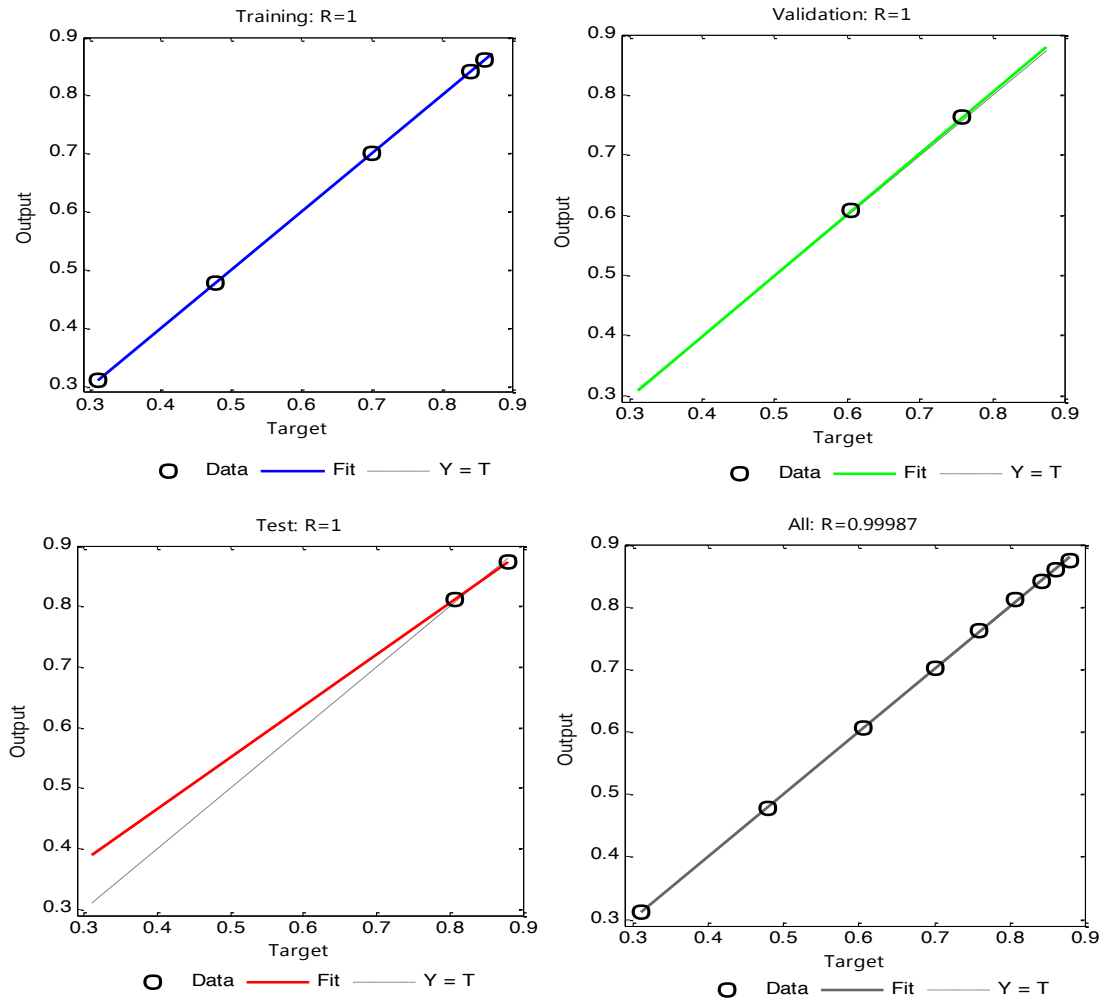


Figure 5-24: Fitness of ANN in IM 250 W

Table 5-11 Selected input data and progress results (IM 250W)

NN Training Progress (IM 250W)	
Number of inputs points	9
Number of training points	5
Number of validation points	2
Number of testing points	2
Number of neurons in the hidden layer	2
Number of epochs	14
Least square algorithm	L-M
Performance (MSE)	2.35E-06
R-Squared	0.99987
Elapsed Time (s)	0.6127

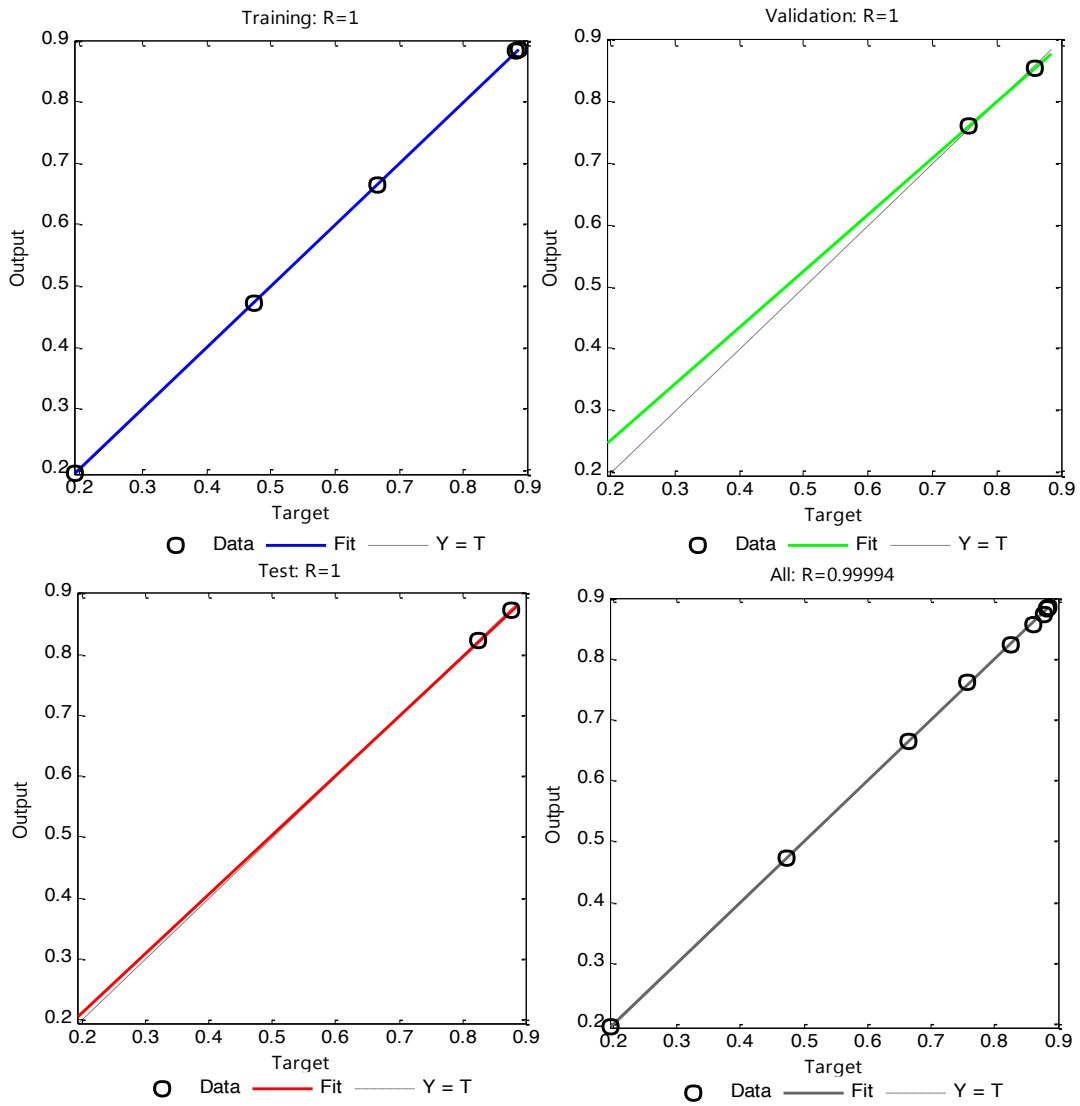


Figure 5-25: Fitness of ANN in IM 10 HP

Table 5-12 Selected input data and progress results (IM 10 HP)

NN Training Progress (IM 250W)	
Number of input points	9
Number of training points	5
Number of validation points	2
Number of testing points	2
Number of neurons in the hidden layer	2
Number of epochs	10
Least square algorithm	L-M
Performance (MSE)	7.01E-06
R-Squared	0.99994
Elapsed Time(s)	1.679

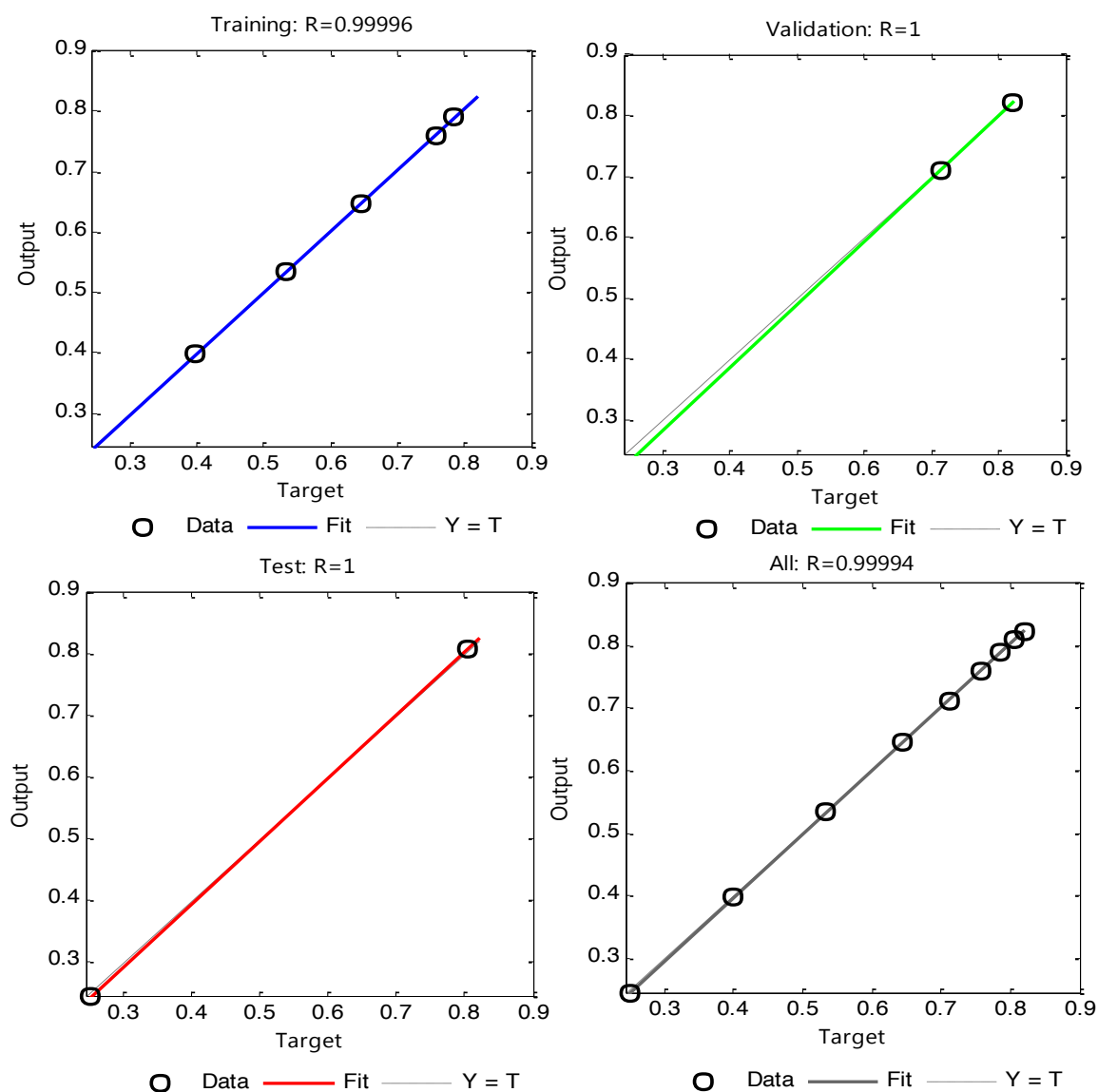


Figure 5-26: Fitness of ANN in IM 100 HP

Table 5-13 Selected input data and progress results (IM 100 HP)

NN Training Progress (IM 100HP)	
Number of input points	9
Number of Training points	5
Number of validation points	2
Number of testing points	2
Number of neurons in the hidden layer	2
Number of epochs	10
Least square Algorithm	L-M
Performance (MSE)	1.06E-06
R-Squared	0.99994
Elapsed Time(s)	0.268

In the artificial neural network, the predicted model based on some observed values estimated the power factor at any desired loading point. Figures 5-27, 5-28 and 5-29 indicate the estimated power factor of the 250 W, 10 HP and 100 HP induction motors from no-load to full-load and over-load conditions. It is observed that the estimated results in the three induction motors are very close to the measured power factor. Although this method provided high performance from no-load to over-load conditions, several running times need to be applied in each case in order to achieve the best results.

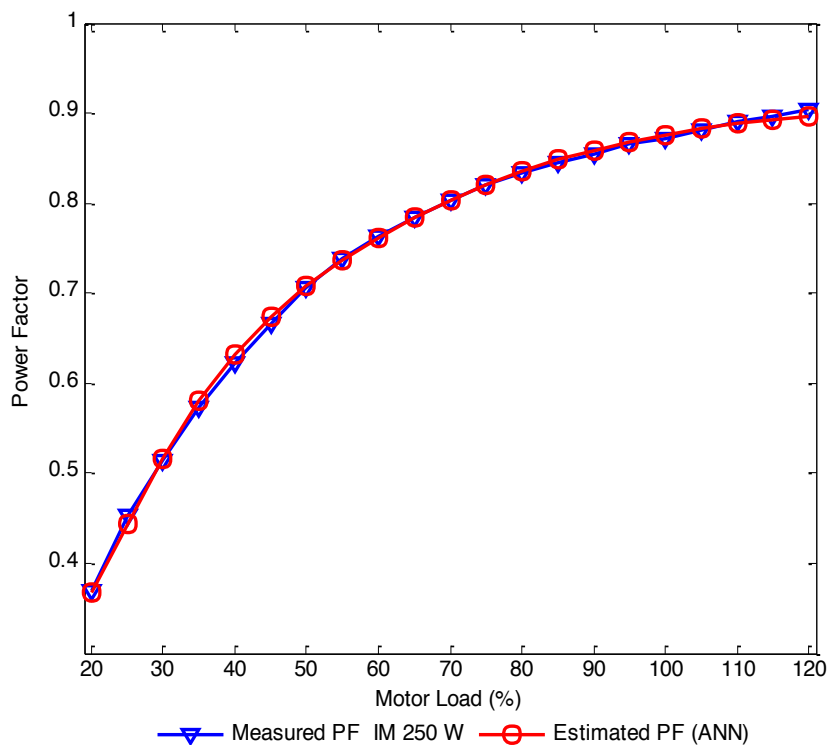


Figure 5-27: Estimated PF of IM 250 W using ANN

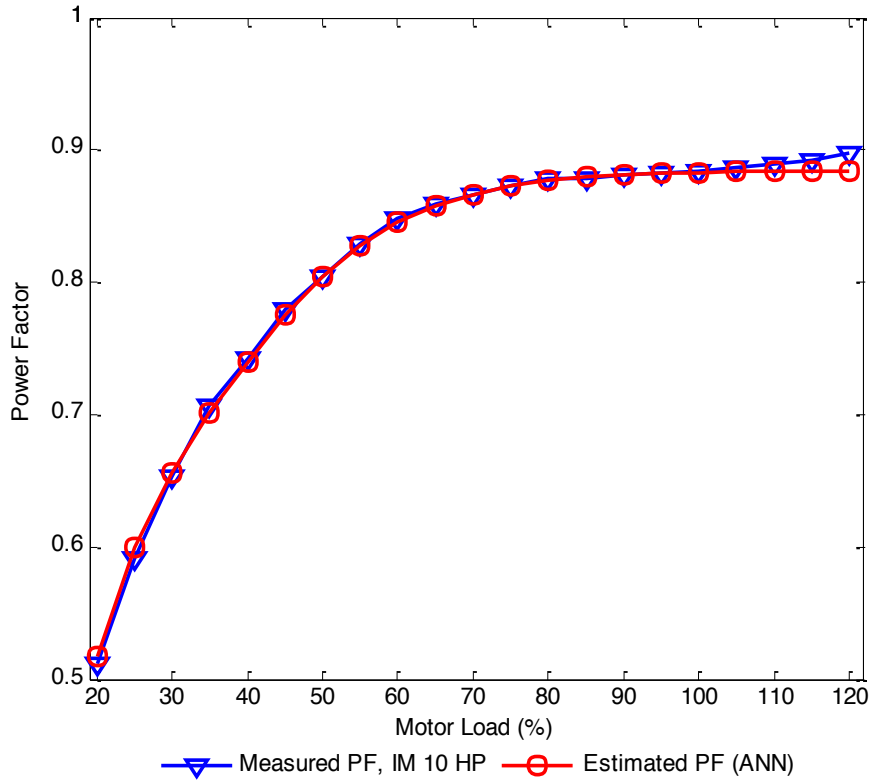


Figure 5-28: Estimated PF of IM 10 HP at using ANN

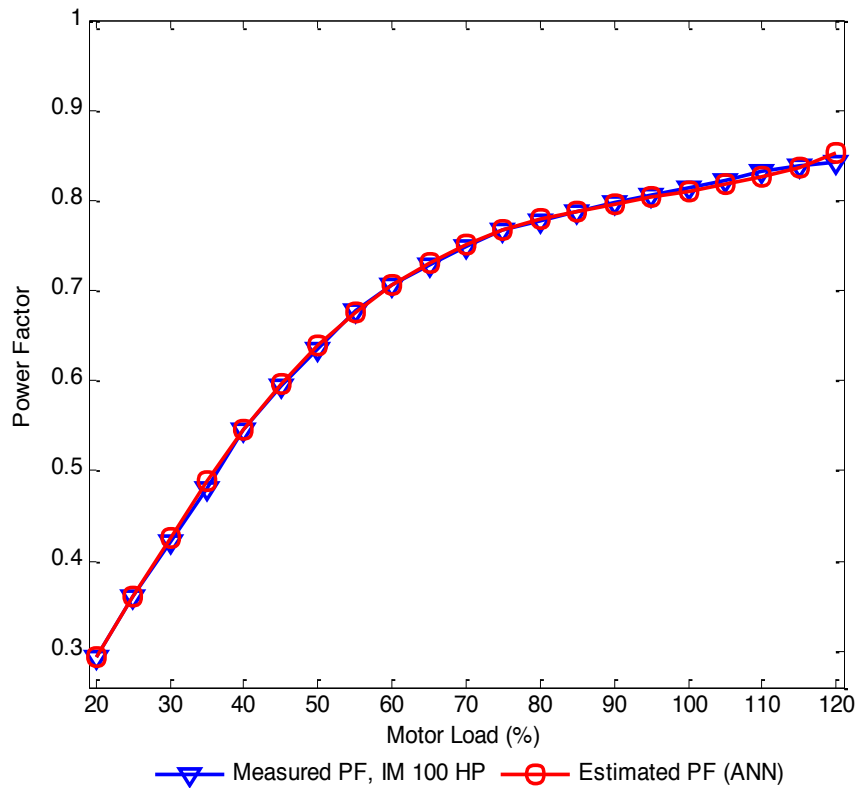


Figure 5-29: Estimated PF of IM 100 HP using ANN

Table 5-14 indicates the estimated power factor of the proposed induction motors with errors from no-load to full-load and over-load conditions. In the 250 W induction motor, the error from loads of 35 to 45 is approximately 1%. However, the highest error is indicated at a load of 25 at 2.391%. The error from loads of 50 to 100 is between 0.1% and 0.5%, except for a load of 65, at which the error is the lowest at about 0.026%. The errors from no-load to full-load gradually increased from 0.2% to 0.72%. In the 10 HP induction motor, the load of 20 presented the highest error of 1.577%. The lowest error was produced at a load of 40 with 0.013%. At other loads, the errors produced are less than 0.5%.

In over-load conditions, the errors also increased from 0.57% to 1.43%. In the 100 HP induction motor, the load of 35 shows the biggest error of about 1.650%, while the load of 60 generated the lowest error of 0.028%. The error at loads of 25, 70, 75, 80 and 90 are approximately 0.1%. In addition, at loads of 20, 40, 55 and 65 the error indicated is about 0.2%. Loads of 45 and 95 indicated errors of 0.378% and 0.302% respectively. The loads of 105 and 115 produced errors of 0.6% and loads of 110 and 120 indicated errors of 0.23% and 1.9% respectively. It is observed that ANN not only produced great results from no-load to full-load, but also produced satisfactory results from full-load to over-load conditions.

Therefore, the ANN using a back propagation algorithm is able to determine the unknown values, which are outside the observed points. Even though the ANN presented acceptable results from no-load to full/over-load conditions, it had difficulty in catching these results because several running times need to be applied in order to obtain the best results, and also closing the program deletes the obtained results, such that again several new running times are needed to catch best model. This was a major problem as it required more time.

Table 5-14 Estimated PF of IMs using ANN from no-load to over-load

Load (%)	EPF (250 W)	APE (%)	EPF (10 HP)	APE (%)	EPF (100 HP)	APE (%)
20	0.367	0.708	0.520	1.577	0.293	0.260
25	0.443	2.391	0.594	0.538	0.359	0.107
30	0.517	0.542	0.653	0.077	0.426	0.851
35	0.580	1.276	0.701	0.827	0.488	1.650
40	0.632	1.520	0.742	0.013	0.545	0.253
45	0.673	1.158	0.778	0.322	0.596	0.378
50	0.708	0.325	0.807	0.310	0.640	0.577
55	0.737	0.163	0.829	0.048	0.676	0.218
60	0.762	0.118	0.846	0.189	0.707	0.028
65	0.784	0.026	0.858	0.047	0.731	0.292
70	0.804	0.149	0.867	0.058	0.751	0.166
75	0.821	0.134	0.872	0.126	0.766	0.181
80	0.836	0.156	0.876	0.228	0.779	0.198
85	0.848	0.330	0.878	0.102	0.789	0.074
90	0.859	0.477	0.880	0.136	0.797	0.135
95	0.868	0.392	0.881	0.250	0.804	0.302
100	0.876	0.593	0.881	0.295	0.810	0.523
105	0.883	0.202	0.882	0.567	0.817	0.595
110	0.888	0.309	0.883	0.793	0.826	0.273
115	0.893	0.469	0.883	0.905	0.837	0.624
120	0.897	0.715	0.884	1.436	0.853	1.879

Table 5-15 indicates the validity and accuracy of the ANN by MSE and MAPE. MSE is used to measure the performance of the ANN. MAPE gives a measure of the prediction accuracy of the proposed method. The MSE in the considered induction motors presented values of 2.09E-05, 4.17E-05 and 4.18E-05, and the MAPE indicated was 0.5195%, 0.6135% and 0.599% separately, from no-load to over-load conditions.

Table 5-15 Validity and accuracy of the ANN

Method	Validity	IM 250 W	IM 10 HP	IM 100 HP
ANN	MSE	2.09E-05	4.17E-05	4.18E-05
	MAPE	0.520	0.6135	0.599
	Accuracy	99.48%	99.39%	99.401%

5.7. Results of Support Vector Regression

In the support vector regression, the load and power factor of the proposed induction motors at some points are determined as input data. The SVR based on these values constructed a hyperplane in high-dimensional space between the defined upper and lower bounds and created a model very close to the observed model. Selecting the Gaussian radial basis function and the parameters of SVR such as capacity (C), sigma and epsilon lead to make the model, where C is the capacity of the SVR; it is also known as a parameter regulator that determines the adjustment between the empirical risk and regularization term and tries to fit the model to the observed curve. Sigma is a dispersion coefficient of the Gaussian function, also known as the radial basis function (RBF).

Epsilon is the size of the dimensional cylinder which indicates the error in the ϵ -insensitive region and controls the width of the ϵ -insensitive zone. Therefore, the proper values of these parameters are able to provide a significant model fitting to the main model. In the literature, there are no general rules for choosing these parameters. Thus, this research presents the most common approach to find the best value of C and sigma. To design the parameters, assumptions need to be made. Epsilon can be adjusted based on the smoothness of the main model so that whenever the main curve is smooth, the value of epsilon will be smaller. Epsilon cannot be larger than the target value because then good results cannot be expected. In addition, epsilon cannot be zero because then overfitting would occur. Therefore, a small epsilon must be chosen. Capacity and sigma, which are the main parameters, can be selected based on considering interval values. For instance, in these cases sigma is tested from 5 to 50 within three values of capacity (20, 30 and 40).

Table 5-16 indicates the results in mean square error, in which capacity and sigma with the values of 30 and 25 provided the best model of the power factor for the three considered induction motors.

Table 5-16 Selection of SVR parameters for predicting model of PF in the IMs

C	Sigma	IMs 250 W	IMs 10 HP	IMs 100 HP
		Training MSE($10E-04$)	Training MSE($10E-04$)	Training MSE($10E-04$)
20	5	67.000	34.000	44.000
	10	37.000	19.000	22.000
	15	12.000	8.719	6.455
	20	1.528	2.184	0.939
	25	0.090	0.177	0.543
	30	0.041	0.892	0.439
	35	1.056	0.374	0.197
	40	2.624	0.098	0.091
	45	2.088	0.955	0.056
	50	0.682	1.768	0.041
30	5	67.000	34.000	44.000
	10	37.000	19.000	22.000
	15	12.000	8.715	6.455
	20	1.528	2.184	0.194
	25	0.074	0.028	0.045
	30	0.029	0.691	0.060
	35	0.361	0.474	0.210
	40	1.645	0.091	0.104
	45	2.669	0.142	0.452
	50	1.097	1.649	0.491
40	5	67.000	34.000	44.000
	10	37.000	19.000	22.000
	15	12.000	8.719	6.447
	20	1.528	2.180	0.938
	25	1.117	0.121	0.313
	30	0.205	0.518	0.507
	35	0.160	0.452	0.211
	40	1.458	0.076	0.131
	45	2.290	0.079	0.065
	50	1.333	0.990	0.047

Figure 5-30 indicates the mean absolute percentage error by selecting sigma from 5 to 50 with a fixed value of capacity of 30. In this figure, the results showed that selecting sigma with a value of 25 provides a better prediction model that is very close to the actual model of the power factor in the three considered induction motors.

The value of 25 also minimised the absolute percentage error to less than 1% in the three induction motors compared with other values. Therefore, this value is selected as an optimum value of sigma in the considered models.

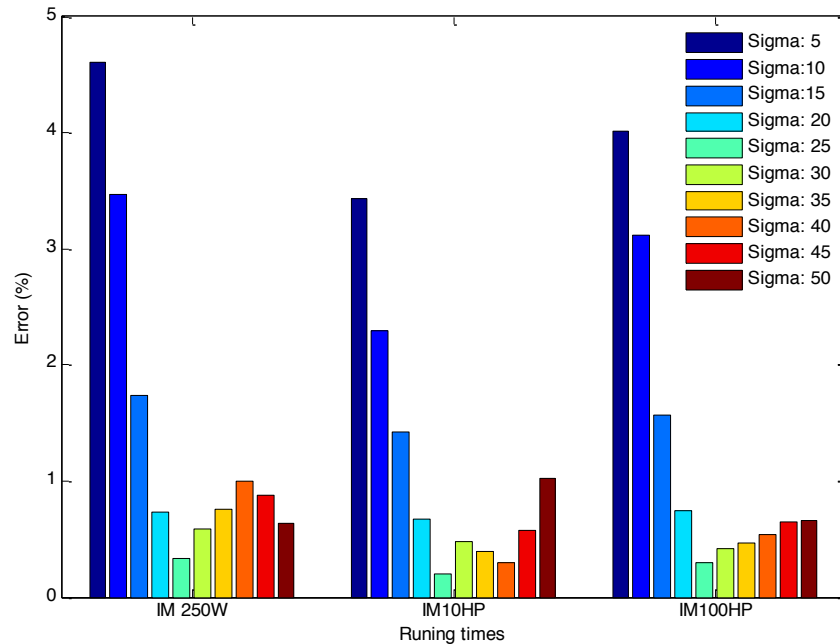


Figure 5-30: Observing the optimum value of sigma in the considered IMs

Table 5-17 shows the designed parameters including capacity, sigma and epsilon in the considered IMs. The epsilon in all models is assumed to have the small value of 0.00015 and the capacity is randomly assumed based on the designed sigma. Within the considered values, 25 in all models provided the optimum value.

Table 5-17 Designed SVR parameters in the IMs

Parameters	IM250 W	IM10 HP	IM100 HP
C	30	30	30
Sigma	25	25	25
Epsilon	0.00015	0.00015	0.00015

The results of the predicted models with the designed parameters can be seen in Figures 5-31, 5-32, and 5-33. From these predicted models, the unknown values of

the power factor of the considered induction motors from no-load to full/over-load conditions can be estimated as well.

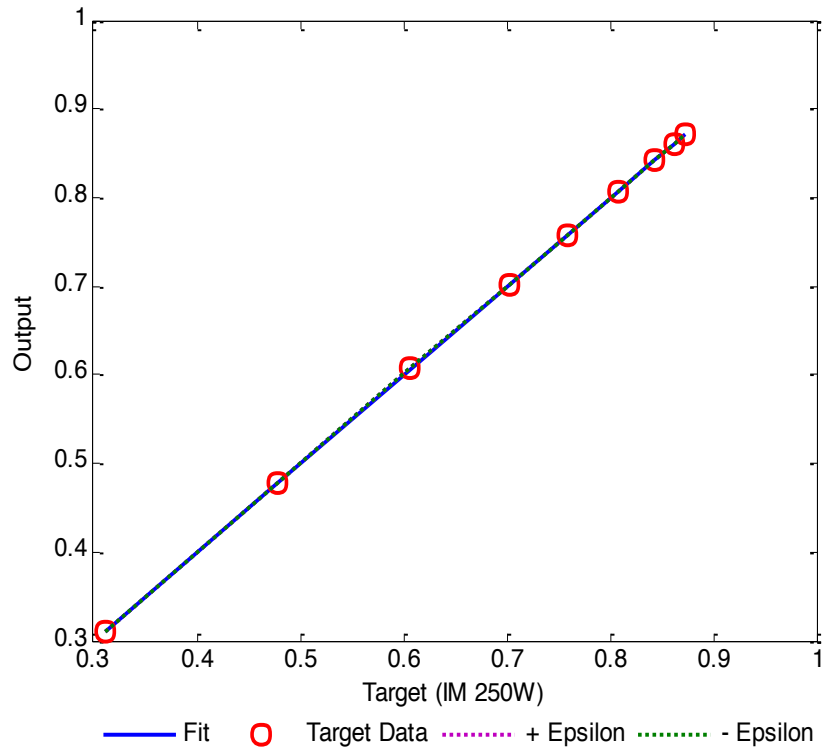


Figure 5-31: Residual model of SVR in IM 250 W

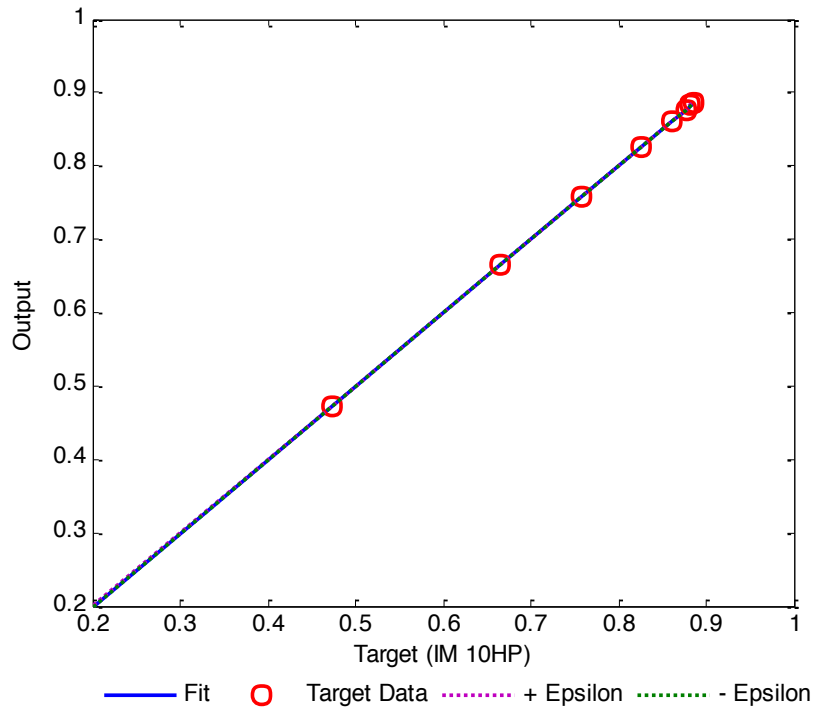


Figure 5-32: Residual models of SVR in IM 10 HP

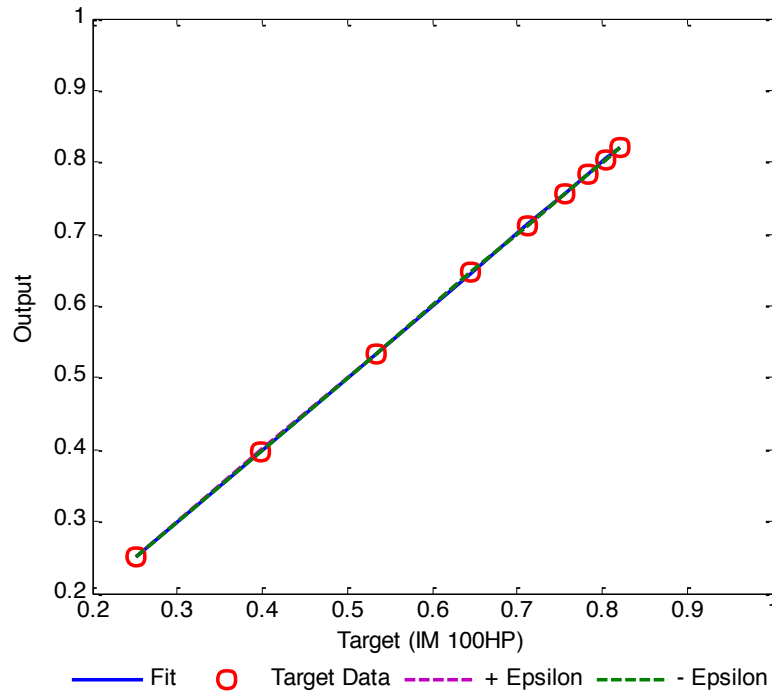


Figure 5-33: Residual model SVR in IM 100 HP

Table 5-18 presents the computed value of the correlation coefficient (R^2) and MSE in the considered power factor curve of the induction motors in order to verify the fitness of the models and performance of the SVR method. The trained models in the three induction motors produced R^2 very close to unity, which proved the best fitting. The root mean square error, which is the square of MSE, is used to measure the differences between the output and target values. It also represents the standard deviation between the observed and predicted model. This value in these cases is near zero, which also justified the performance of the SVR in terms of high fitness. The estimated power factors of the 250 W, 10 HP and 100 HP induction motors using SVR methods are presented in Figures 5-34, 5-35 and 5-36 respectively. It is observed that the estimated points in the considered induction motors are very close to the measured points, in which the blue line indicates the measured power factor and the red solid line illustrates the estimated power factor at the desired loading points from no-load to full-load and over-load conditions.

Table 5-18 Fitness of the models in IMs

Fitness	IM (250 W)	IM (10 HP)	IM (100 HP)
R-Square	0.99997	0.99998	0.99994
MSE	1.2E-06	1.36E-07	9.95E-07
RMSE	0.00110	0.00037	0.00100

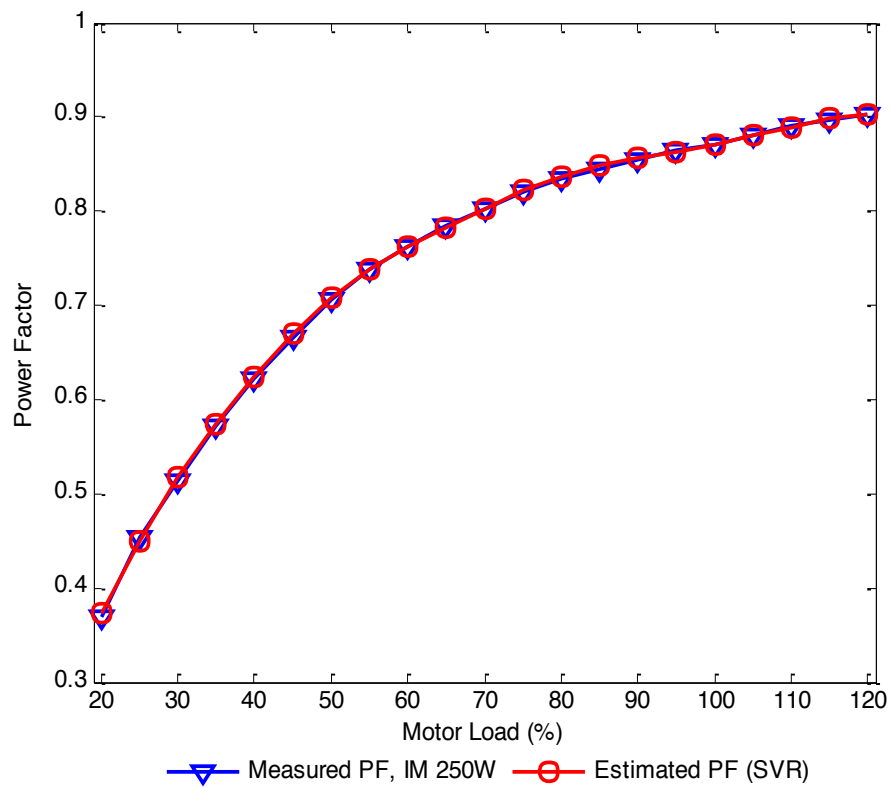


Figure 5-34: Estimated PF of IM 250W using SVR

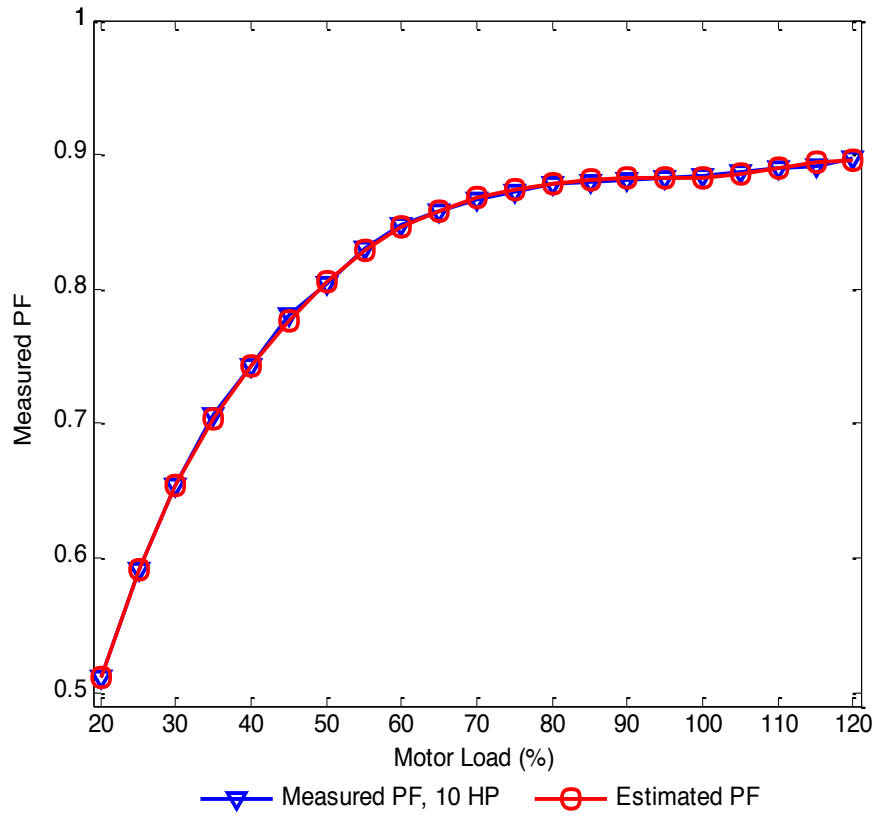


Figure 5-35: Estimated PF of IM 10 HP using SVR

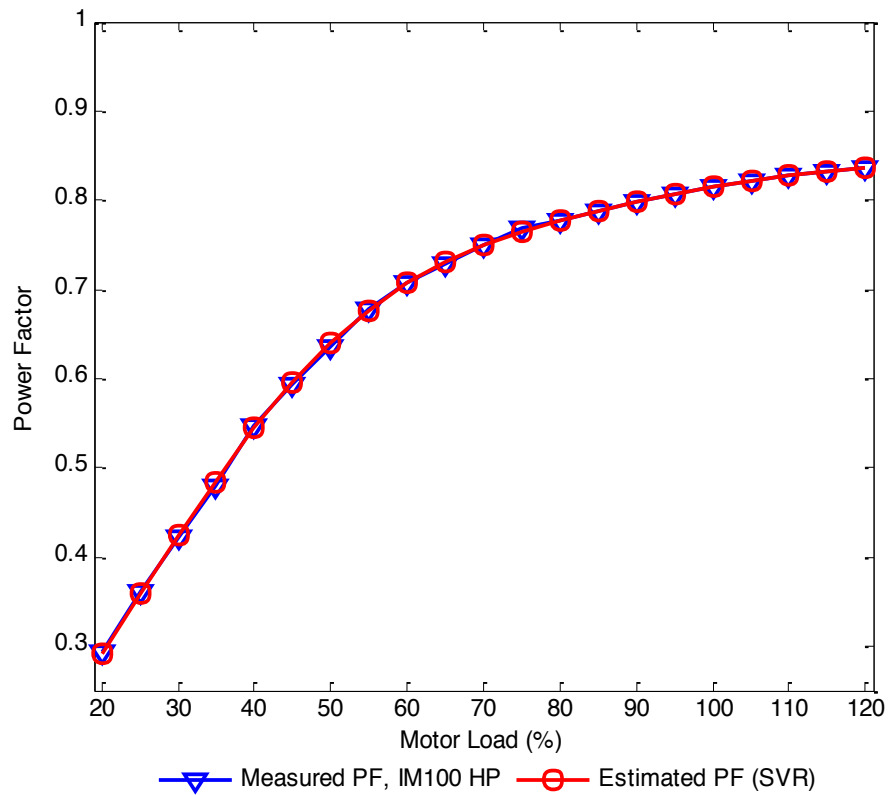


Figure 5-36: Estimated PF of IM 100 HP using SVR

Table 5-19 indicates the errors of the estimation results of the proposed induction motors from no-load to full-load conditions. In the 250 W induction motor, the errors from no-load to full-load are between 0.03% and 1.12%, where the minimum and maximum errors are indicated at loads of 100 and 20 respectively. From loads 20 to 50, the errors are high, approximately between 0.2% and 1.2%. However, the errors from loads 50 to 100 gradually decrease and indicate values of between 0.2% and 0.03%. In addition, the errors at over-load gradually increase from 0.14% to 0.18%, except for a load of 120, at which the error decreased to 0.011%. In the 10 HP induction motor, the highest error was produced at a load of 35 with 0.58%. The errors in their majority of loads are less than 0.2%. The loads of 115 and 120 produce similar errors of 0.28%. The loads of 105 and 110 generated errors of 0.160% and 0.034% respectively.

Table 5-19 Estimated PF of IMs using SVR from no-load to over-load

Load (%)	EPF (250 W)	Error (%)	EPF (10 HP)	Error (%)	EPF (100 HP)	Error (%)
20	0.374	1.122	0.511	0.157	0.291	0.963
25	0.450	0.979	0.592	0.152	0.358	0.530
30	0.518	0.734	0.654	0.138	0.398	0.075
35	0.577	0.763	0.703	0.583	0.424	0.495
40	0.628	0.940	0.743	0.040	0.486	1.316
45	0.671	0.849	0.777	0.373	0.544	0.515
50	0.707	0.283	0.806	0.248	0.595	0.202
55	0.738	0.081	0.829	0.072	0.639	0.501
60	0.763	0.039	0.846	0.201	0.676	0.222
65	0.784	0.038	0.858	0.047	0.710	0.423
70	0.803	0.112	0.867	0.115	0.731	0.301
75	0.820	0.085	0.874	0.057	0.751	0.133
80	0.835	0.060	0.879	0.091	0.766	0.261
85	0.846	0.106	0.881	0.250	0.778	0.116
90	0.855	0.035	0.882	0.125	0.788	0.038
95	0.863	0.243	0.882	0.113	0.797	0.038
100	0.871	0.034	0.883	0.136	0.806	0.012
105	0.880	0.148	0.886	0.158	0.814	0.049
110	0.890	0.157	0.890	0.034	0.822	0.061
115	0.899	0.178	0.895	0.279	0.828	0.048
120	0.903	0.011	0.895	0.279	0.838	0.107

In the 100 HP induction motor, loads of 20 and 40 presented the highest errors of 0.963% and 1.316%. The errors for loads of 30, 90, 95 and 100 indicated the lowest error at less than 0.07%. At the over-load condition, the errors produced at loads of 105 and 110 are 0.050% and 0.061%. However, the errors at loads of 115 and 120 are 0.050% and 0.107% respectively.

In summary, SVR in the three induction motors produced great results with overall errors less than 2% from no-load to full-load conditions. Although adjusting the SVR parameters is tricky, the SVR is able to estimate the power factor at unseen points and produces constant results with high performance from no-load to full-load and over-load conditions. Hence, the SVR method is not only faster but also more powerful, and performs with high accuracy in the estimation of unknown points between the observed points and unseen points in any models.

The validity of both the ANN and SVR are presented in Table 5-20 by the MSE, MAPE and accuracy. The SVR produced MSE in the considered induction motors of 5.18E-06, 3.16E-06 and 3.08E-06. In addition, it indicated MAPE of 0.2535%, 0.179% and 0.214% separately. Although the ANN provided similar results to those of SVR, several running times were required to initialize the network in order to achieve the best results.

Table 5-20 Validity and accuracy of the ANN and SVR

IMs	Validity	Methods	
		ANN	SVR
250 W	MSE	2.09E-05	5.18E-06
	MAPE	0.5195	0.2535
	Accuracy	99.480	99.750
10 HP	MSE	4.17E-05	3.16E-06
	MAPE	0.6135	0.179
	Accuracy	99.3865	99.820
100 HP	MSE	4.18E-05	3.08E-06
	MAPE	0.599	0.2135
	Accuracy	99.401	99.785

5.8. Obtaining Reactive Power Required to Improve Power Factor

In this study, the estimated power factor at any loading point between no-load and over-load conditions obtained the required reactive power to improve the power factor in unity. In the power factor correction equation, the active power, initial power factor and target power factor have the main roles in this computation. The target power factor is considered as one. The initial power factor and input power are obtained synchronously by modelling techniques. Tables 5-21, 5-22 and 5-23 show the obtained power, power factor, K , which is a ratio of the required reactive power at any loading point ($K = \tan \phi_1 - \tan \phi_2$), and the volt ampere reactive in the 250 W, 10 HP and 100 HP induction motors. Although the amount of required reactive power at some loading points is small, in large scales, particularly at points of common coupling, the amounts between each loading point will be high, so a capacitors bank with different values needs to be considered. Consequently, using the proposed technique not only selects the proper size of capacitors at different loading points, but is also able to estimate the required reactive power in the future plan so as to enhance the reliability and security of distribution systems.

Table 5-21 Estimated kVAR in IM 250 W

Load (%)	EPF	P (W)	K	VAR
20.00	0.374	55.600	2.478	137.789
25.00	0.450	69.500	1.987	138.116
30.00	0.518	83.400	1.653	137.901
35.00	0.577	97.300	1.416	137.764
40.00	0.628	111.200	1.240	137.835
45.00	0.671	125.100	1.104	138.161
50.00	0.707	139.000	0.999	138.885
55.00	0.738	152.900	0.916	140.014
60.00	0.763	166.800	0.848	141.443
65.00	0.784	180.700	0.791	142.934
70.00	0.803	194.600	0.741	144.228
75.00	0.820	208.500	0.697	145.371
80.00	0.835	222.400	0.660	146.731
85.00	0.846	236.300	0.629	148.740
90.00	0.855	250.200	0.606	151.569
95.00	0.863	264.100	0.586	154.675
100.00	0.871	278.000	0.565	157.028
105.00	0.880	291.900	0.541	157.789
110.00	0.890	305.800	0.513	157.005
115.00	0.899	319.700	0.488	156.103
120.00	0.903	333.600	0.476	158.629

Table 5-22 Estimated kVAR in IM 10 HP

Load (%)	PF	P (kW)	K	kVAR
20.00	0.511	1.660	1.682	2.792
25.00	0.592	2.075	1.361	2.825
28.00	0.654	2.490	1.156	2.879
30.00	0.703	2.905	1.012	2.940
35.00	0.743	3.320	0.901	2.992
40.00	0.777	3.735	0.810	3.025
45.00	0.806	4.150	0.734	3.048
50.00	0.829	4.565	0.675	3.080
55.00	0.846	4.980	0.630	3.139
60.00	0.858	5.395	0.598	3.227
65.00	0.867	5.810	0.575	3.339
70.00	0.874	6.225	0.557	3.466
75.00	0.879	6.640	0.544	3.609
80.00	0.881	7.055	0.536	3.783
85.00	0.882	7.470	0.534	3.989
90.00	0.882	7.885	0.534	4.213
95.00	0.883	8.300	0.532	4.417
100.00	0.886	8.715	0.524	4.571
105.00	0.890	9.130	0.511	4.670
110.00	0.895	9.545	0.500	4.771
120.00	0.895	9.960	0.500	4.978

Table 5-23 Estimated kVAR in IM 100 HP

Load (%)	PF	P(kW)	K	kVAR
20.00	0.291	16.250	3.289	53.445
25.00	0.358	20.313	2.606	52.944
28.00	0.398	22.750	2.305	52.438
30.00	0.424	24.375	2.136	52.065
35.00	0.486	28.438	1.796	51.083
40.00	0.544	32.500	1.544	50.168
45.00	0.595	36.563	1.352	49.414
50.00	0.639	40.625	1.203	48.890
55.00	0.676	44.688	1.089	48.674
60.00	0.710	48.750	0.992	48.379
65.00	0.731	52.813	0.933	49.271
70.00	0.751	56.875	0.881	50.083
75.00	0.766	60.938	0.840	51.188
80.00	0.778	65.000	0.808	52.490
85.00	0.788	69.063	0.781	53.923
90.00	0.797	73.125	0.757	55.358
95.00	0.806	77.188	0.735	56.726
100.00	0.814	81.250	0.714	58.001
105.00	0.822	85.313	0.694	59.216
110.00	0.828	89.375	0.676	60.432
120.00	0.838	97.500	0.651	63.513

5.9. Discussion

As mentioned earlier, induction motors are extensively used in commercial and industrial areas that consume the majority of generated electrical energy. Induction motors require both active and reactive current and power for rotation and useful work. The active power depends on the mechanical load and variation of the mechanical load creates a change in the active power. However, the active power at no-load cannot be zero because a small amount of active power is required in shaft rotation, which is called friction loss. The mechanical load can increase until reaching the rated power or a maximum of 20% over it. Increase of the mechanical load higher than the rated power not only creates more losses and reduces the motor efficiency, but also produces high heat, which results in damage to the motor.

However, reactive power is a significant quantity in inductive loads, and it is always used to provide a magnetic field. In induction motors, reactive power is required for magnetization reactance to create a magnetic field for rotation. It is also required in stator and rotor leakage reactance. The experimental study showed that the reactive power or current also changes when the mechanical load increases or decreases, because variation of the mechanical load creates a change in the magnetic field.

Since the power factor is a ratio between active and reactive power and will be changed by the load, it must be monitored because variation of the load generates a low power factor, which leads to a penalty charge for the user and energy losses in the grid systems. Utility companies are always concerned about a low power factor on the customer's side. A low power factor increases the current and creates a huge equipment cost for utility companies. For this reason, a charge has been considered for customers with a low power factor. The consumer must therefore take responsibility for improving the low power factor to the desired level through its own reactive power generation. In order to prevent a penalty charge and energy loss, the power factor must be maintained at unity. In the induction motor, holding the mechanical load on the rated power can make it possible to maintain the power factor as the same as the nominal power factor from the nameplate, which may be enough to meet the requirement. However, reactive losses in the induction motor winding and cable cause the power factor to become lower.

The best solution to maintain the desired power factor is to control the reactive power. Reactive power compensation by a capacitors bank is the best way to keep the power factor at unity at any loading point. However, initial prediction of the reactive power required to meet the desired power factor is necessary in all the considered induction motors. For instance, since a large amount of induction motors

with different sizes are used in industry, capacitors banks are required to improve the power factor at different loading conditions. To design the capacitors bank, initial prediction of the required reactive power for each induction motor from no-load to full-load and over-load conditions is required.

This prediction requires the initial power factor of each induction motor from no-load to full-load and over-load conditions, because the initial value of the power factor indicates how much reactive power is needed to compensate the power factor in unity. In theory, there are several procedures to obtain the required reactive power. For instance, the nominal power factor from the motor nameplate can indicate the required reactive power for correcting the power factor to a desired value or the no-load current from the manufacturer's data can be considered, which can be reactive current. However, the experimental study showed that considering the nominal power factor creates under- and over-load correction. Under-correction indicates a low power factor that will lead to a penalty charge. Over-correction generates more reactive power or current than the motor needs. In this situation, self-excitation takes place due to generating a higher reactive current than the magnetizing reactance needs.

Therefore, using this value is not suitable for finding the required reactive power at no-load and light load conditions. Since no-load current can be assumed as reactive current, it can be taken into account for obtaining the required reactive power or designing the size of capacitor. Nevertheless, when the motor load increases, the reactive current gradually increases such that the designed capacitor is not sufficient for full-load and over-load conditions. Therefore, using both values is suitable when the motor load is constant.

In the case of load variation, considering the input power and power factor synchronously is much more suitable to obtain the required reactive power for making a new power factor because in this approach involving the input power obtains the required reactive power at any loading point properly and prevents under- and over-correction at operating time. Therefore, in this method the power factor and input power at any loading point need to be determined. The experimental work found that, to measure these indices at any loading conditions, the motor load must be controlled at every single loading point during the measurement process. Otherwise, the device creates a numerical fluctuation, which makes it hard to read the measurement points. A power analyser is one of the significant measurement devices and is able to measure and store all components at every second with reasonable accuracy. However, to connect the power analyser, the induction motor needs to be shut down for a while and also it takes about an hour for the measurement process from no-load to full-load and over-load conditions.

This connection process not only takes time, but may also create a huge cost for the motor's user when the motor is out of service. Simulation work indicated that by using MATLAB/Simulink, the induction motor with a measurement device can be modelled in order to measure the voltage, current and power factor. However, in this approach, the induction motor parameters including the rotor and stator resistance, magnetization reactance and some other parameters are required to model the induction motor. As mentioned earlier, finding these parameters creates a difficulty for which locked and no-load tests and also some other techniques are needed.

Hence, the aforementioned reasons proved the importance of power factor monitoring from no-load to full/over-load conditions. It is observed that many devices can be used to measure and record the power factor at every loading

condition. These devices had limitations in the case of cable connection, where the power must be cut off, and also because their cost may mean that they are not economical to use in some cases.

In this research, several statistical methods, including Kriging and regression as numerical techniques and ANN and SVR as intelligent techniques, are introduced and analysed in terms of power factor estimation at any loading condition. In this project, to validate the proposed techniques several induction motors of sizes 250 W, 10 HP and 100 HP are considered as case studies. A power analyser is used to measure and record all the components of the three phases including voltage, current, active and reactive power, power factor and harmonics, from no-load to over-load conditions.

The connected power analyser stored all the components at 6-second intervals, providing 30 measurement points from no-load to over-load conditions. The input power measurement method is applied to obtain the motor load. MATLAB/Simulink is used to model the induction motors with the same specification of 100 HP in order to measure the power factor from no-load to full-load and over-load. In the simulation, the parameters of the 100 HP induction motor including resistance, reactance of the stator and rotor, and magnetizing reactance are added. The simulation results are compared with the results measured by the power analyser and it is shown that the simulation method produced an average error of about 3%. In addition, a method using measured current and the manufacturer's data from reviewed paper is applied in three different ranges of induction motors including 250 W, 10 HP and 100 HP. The measured current method was a numerical procedure that required two components [14].

The first was the nominal power factor from the data sheet or nameplate of the motor in order to calculate the nominal reactive current. The second was measurement of current from no-load to full-load condition. Then, using these components in numerical equations gives the power factor at any loading condition. In the induction motor, the motor current I is divided into two components, active current and reactive current. Active current is used for useful work and provides a linear correlation with the mechanical load from no-load to full-load. The reactive current is magnetization current and was used in the magnetization reactance. If the magnetization current or reactive current are assumed to be constant, the power factor can be estimated with this method.

The computation process in MATLAB programming is done in five steps. The first is measurement of the motor current and active power at any possible loading point from no-load to full-load and over-load condition. The second is to take all the values of measured power and current into the input power measurement equation to calculate the motor load. The third step is to consider the nominal power factor from the motor nameplate in order to compute the nominal reactive power. The fourth step is to take all the measured values of current from no-load to full-load and over-load conditions.

The fifth step, the measured current and computed reactive current are inserted into the numerical equation for computation. The results of this method indicated a small error in the 250 W induction motor, but huge errors in the larger 10 HP and 100 HP induction motors from no-load to full/over-load conditions, because in the large induction motors, the variation of reactive current is higher than in the small induction motors due to the large magnetic field.

Although this method provided satisfactory performance in the small 250 W and 2.2 kW induction motors because, in small induction motors, the reactive current is almost constant from no-load to full-load and over-load, it was not able to estimate the power factor in the large induction motors. In the large induction motors, the reactive current cannot be constant due to the large air gap which means that the reactive current changes from no-load to full-load and over-load. Kriging and regression methods are used to estimate the power factor and minimise the error. Kriging, which is an interpolation technique, was able to estimate the unknown values based on nearby observed values at surrounding locations and to weight the unknown points in order to minimise the error of a predicted value.

Kriging is more applicable in cases where the distance between each observed point and an unknown point is to be known. In the Kriging method, calculation of weights is important. To obtain the weights, Kriging uses a semivariogram. As previously explained, the key point of this method is to apply a suitable semivariogram model to provide high output accuracy. In this study, selecting the exponential model was more applicable since it was similar to the power factor curve. Therefore, an exponential function with a Lagrange matrix obtained all the weights between the observed power factor and a target power factor. The obtained weights times the observed power factor provided the power factor at the desired loading points.

The computation process in MATLAB programming is done in six steps. The first step needs to consider the computed load, which is obtained by the measured current method as the x -axis, and considers the power factor, which is computed by measurement of the current and input power at a few loading points from no-load to full-load condition as the y -axis. The second step computes the distance between each pair in the x -axis and makes it a 4×4 matrix.

The third step computes the distance between all x -axis points and a point that needs to be estimated. The fourth step selects an exponential function and inserts the semivariogram parameters from the computed distance in the x -axis. The fifth step adds the results obtained from the function and the results of the distance between all x -axis points and the point that needs to be estimated in the Lagrange matrix. The sixth step creates a loop function to iterate the algorithm in order to obtain the value at any desired loading point from no-load to full-load and over-load conditions.

Hence, the results of the Kriging method show that the estimated power factors in the 250 W, 10 HP and 100 HP induction motors are very close to the measured power factor from no-load to full-load conditions. However, the results at over-load conditions are far from the measured points. The reason is that Kriging is an interpolation technique and is not able to extrapolate the over-loading points. Although the Kriging method performed well in power factor estimation at unknown points from no-load to full-load conditions, the strategy of Kriging is geostatistical such that the computing distance between one unknown point and surrounding observed points is required. A large interval between two points creates a complexity with high errors. MSE and MAPE were used to indicate the quality of the estimator and measure the prediction accuracy of the Kriging method.

It is shown that Kriging can be a good estimator from no-load to full-load conditions and provided a satisfactory accuracy of 99% for the three different sizes of induction motor. However, it would not be a good estimator at over-load conditions due to producing high error at each point from full-load to over-load, where the errors indicated were between 6% and 7% in the proposed induction motors. In spite of the fact that this method mostly provided good performance from no-load to full-load conditions, in general, using this method is not reliable for modelling because only

the distance between each observed pair of points and also the interval between observed points and a point needs to be estimated to find a proper solution.

A small interval between these points causes the estimating point to become more accurate. In regression, a polynomial technique, which works based on the relationship between the independent variable x and the dependent variable y , provided a weight value between variables, which is known as a polynomial coefficient. The polynomial regression required a few observed values of x and y . In this case, some points of the motor load and the power factor are considered as x and y . The coefficients between the two values are predicted because the predicted coefficient multiplied by the independent values in the x -axis contributed to obtain the unknown values in the y -axis. The accuracy of the regression was dependent on the number of polynomial orders; by increasing the order, the coefficient increased. Increase of the coefficients or orders made the function more powerful, allowing it to reduce the errors and create a model with high fitness. Increase of the coefficients provided a desired model very close to the observed power factor curve.

In the regression, a polynomial function is applied in which the polynomial degrees had significant roles, such that each polynomial degree number created different models. *Polyval* and *Polyfit* in MATLAB programming are used to determine the polynomial coefficients and then create a model close to the observed model. The computation process follows four steps. The first step needs to consider the computed load, which is obtained by the measured current method as the x -axis, and to consider the power factor which is computed by measurement of the current and input power at a few loading points from no-load to full-load condition as the y -axis. The second step is to define the polynomial equation and consider a Vandermonde matrix to generalize the equation.

The third step uses the *polyval* technique to predict the polynomial coefficients. The fourth step uses the *polyfit* technique to place the obtained coefficients in the x -axis value that in the y -axis the points needs to be determined. With increase of the polynomial degrees by following these steps, the fitted model is obtained. The evidence confirmed that the 4th order polynomial regression produced the best fitting to the observed power factor curve.

Therefore, based on the existing model, the unknown power factor is estimated from no-load to full/over-load conditions. In this method, the errors between the estimated power factor and measured power factor from no-load to full-load are very small. However, there are huge gaps between the estimated and measured power factor from full-load to over-load. The results show that the 1st and 2nd orders in the three induction motors produced high errors. However, the 3rd and 4th orders obtained satisfactory results, very close to the measured power factor from no-load to full-load conditions.

Although the number of orders is proportional to the number of independent values in the x -axis and the last order provides high performance in terms of best fitting, in such cases the 4th order performed very well, with lower average error in estimating the unknown power factor of induction motors from no-load to full-load conditions. In spite of the fact that polynomial regression can provide a high performance from no-load to full-load condition, in these cases, polynomial regression with any degree is not able to extrapolate over-load points very well and produces a dramatic drop in the results from full-load to over-load conditions. The comparison results in this table indicated that the 4th order polynomial regression obtained results with errors less than 1% at most of the loading points in the 250 W, 10 HP and 100 HP induction motors.

However, it is shown that the estimated power factor at over-load conditions produced large errors from full-load to over-load, with the errors in the 250 W induction motor ranging from 2.466% to 11.138%. In the 10 HP induction motor, the minimum and maximum error observed were 0.530% at full-load and 5.847% at over-load respectively. In the 100 HP induction motor, the errors gradually increased from 2.145% to 9.515%, and the maximum load indicated the highest error. MSE and MAPE are used to show the performance of 1st, 2nd, 3rd and 4th orders. It is observed that the 4th order performed very well compared with the 1st, 2nd and 3rd orders, producing high accuracy in the three induction motors of about 99.60%.

The comparison between MCMD, Kriging and regression showed that the regression method in the 250 W induction motor produced errors of less than 4%, where the error in MCMD is 3% and in Kriging was 3.5%. However, MCMD creates high errors of more than 8% in the 10 HP and 100 HP induction motors, while the errors of both Kriging and regression in the 10 HP and 100 HP induction motors are 3% and 2%, 4% and 3% respectively. Therefore, it is observed that regression in the 10 HP and 100 HP induction motors reduced the errors and performed very well compared with the MCMD and Kriging methods.

Although both methods provided different techniques, where Kriging used an exponential function based on the distance between the measured points and prediction locations, and regression considered the correlation between the independent value and dependent value, which is modelled as an n^{th} degree polynomial, both the Kriging and regression methods estimated the power factor with extreme errors at over-load. The reason is that Kriging is an interpolation technique and is not able to extrapolate points from the considered points.

To optimize these issues, the study found intelligent techniques including ANN and SVR to estimate the power factor not only between the known observation, but also to at over-load conditions with acceptable performance. The artificial neural network, which is an intelligent technique, was able to generalize and create a desired model. The ANN contained neurons in which every neuron was connected to at least one other neuron. Each connected neuron was evaluated by a weight coefficient. The training process determined the weights. MLF, which is trained with a back propagation algorithm, was a significant element of the neural network. In MLF, some measured values are required for the network (input layer) as a training sample in order to find the weights. To update weights, the error between the predicted and actual output values is back propagated via the network. The back propagation algorithm is used to minimise the error and predict the coefficient. Selecting the appropriate number of neurons in the hidden layer led to a great performance.

In this process, three kinds of samples were needed as inputs, including training, validation and testing data. In these cases, 9 input data are selected for training, of which 5 points are for training, 2 points for testing and 2 points for validation. The training values are presented to the network and the network is adjusted according to its error. The validation is used to measure network generalization and stop training when the generalization has improved. Testing provides an independent measure of network performance during and after training. In addition, selecting the most suitable number of hidden layers and the least squares algorithm are considered in order to fit the inputs and targets, where 2 neurons in the hidden layer and Levenberg–Marquardt as the training algorithm with 8–14 epochs provided a significant generalization with a small average squared error between the trained and

target values. The computation process involves six steps. The first step needs to consider the computed load, which is obtained by the measured current method, as the x -axis and considers the power factor, which is computed by measurement of the current and input power in a few loading point from no-load to full-load condition, as the y -axis. The second step is to make x and y into a column and define it in the neural network toolbox in MATLAB programming. Then, from those values, it considers 60% as training, 40% as testing and 40% as validation. The third step is to select the number of hidden layers based on the number of input data. The fourth step is to select an appropriate least squares method to train the network. The fifth step is to add the points in the x -axis column for the y -axis the value needs to be estimated. The sixth step is to run the algorithm several times in order to identify the best model.

Consequently, the estimated results illustrated that NNBP provided a great fitting from no-load to over-load. In spite of the fact that NNBP produced results very close to the measured points with small error, it has to be applied several times to initialize the network to find the best solution. Obtaining the best result in this way creates the difficulty that the program needs to be closed and opened again to enable the several running times that are required to find the best model. This is a major disadvantage of the ANN method. MSE and MAPE are applied to show the accuracy of this method, where MSE is used to measure the performance of the ANN and MAPE shows a measure of the prediction accuracy of the proposed method. The MSE in the considered induction motors presented values of 2.09E-05, 4.17E-05 and 4.18E-05, and also the MAPE indicated was 0.5195%, 0.6135% and 0.599% respectively from no-load to over-load conditions.

In the support vector regression, the load and power factor of the proposed induction motors at some points are determined as input data. The SVR based on these values constructed a hyperplane in high-dimensional space between the defined upper and lower bounds and created a model very close to the observed model. The SVR method constructs a hyperplane in order to minimise the generalization error between the defined upper and lower bounds. The coefficients of the SVR equation are obtained by minimising the regularized risk equation. In the risk function, C and ϵ must be assumed, where C is the regularization constant that measures the trade-off between empirical risk and the flatness of the model. ϵ defines the upper and lower bounds. A kernel function, which is the most widely used in SVR, is considered to solve the minimization. In this function, σ is selected manually, where the value of σ is tested within each 5 intervals in order to find the optimum value to achieve the best model.

Proper design of σ in the kernel function has a positive effect on the model, and the value of 25 is considered in the 250 W, 10 HP and 100 HP induction motors. As the original model was smooth, the ϵ considered had the small value of 0.00015. The selected capacity was 30 in the 250 W, 10 HP and 100 HP induction motors as well. From these predicted models, the unknown values of the power factor of the considered induction motors from no-load to full/over-load conditions can be estimated properly. In the SVR method, the computation involves seven steps. The first step is to select the input data defined on x and y in a column. The second step is to design a hyperplane with high-dimensional space by selecting proper SVR parameters. The third step is to define a loss function with the considered constraints for minimization. The fourth step is to define a kernel function and predict a σ value based on assumptions.

The fifth step is to obtain the support vector coefficient with a quadratic program. The sixth step is to compute bias from the obtained support vector coefficients and other parameters. The seventh step is to insert the desired x points (load points) to find the desired y points (desired power factor values).

As a result, SVR in the three induction motors produced great results with overall errors less than 2% from no-load to full-load conditions. In spite of the fact that adjusting the SVR parameters is tricky, the SVR is able to estimate the power factor at unseen points and produce constant results with high performance from no-load to full-load and over-load conditions. Hence, the SVR method is not only faster, but also more powerful and reliable through the modelling techniques. MSE and MAPE demonstrated the accuracy of the SVR, with MSE values of 5.18E-06, 3.16E-06 and 3.08E-06 in the considered induction motors, and MAPE values of 0.2535%, 0.179% and 0.214% respectively.

Even though the ANN and SVR methods provided similar estimated results at some load points, SVR indicated significantly better performance in time and accuracy, and once the parameters of SVR were adjusted, it produced fixed output results. In spite of the fact that two neurons in one hidden layer provide good generalization, several running times are required to identify the best fitting. However, SVR is not only faster, but also required just one run to produce results close to the measured power factor from no-load to full- and over-load conditions.

Figure 5-37 presents a comparison of the error results between the considered methods. It is confirmed that numerical techniques including Kriging and regression produced high errors of more than 3% in the three induction motors from no-load to over-load conditions. However, the intelligent techniques of ANN and SVR minimised the errors in the three cases, at less than 1%.

In addition, it can be seen from Figure 5-38 that MCMD created high errors particularly in medium and large induction motors. MATLAB/Simulink produced an average error of about 3%. However, SVR reduced the errors to less than 0.5% at any loading point.

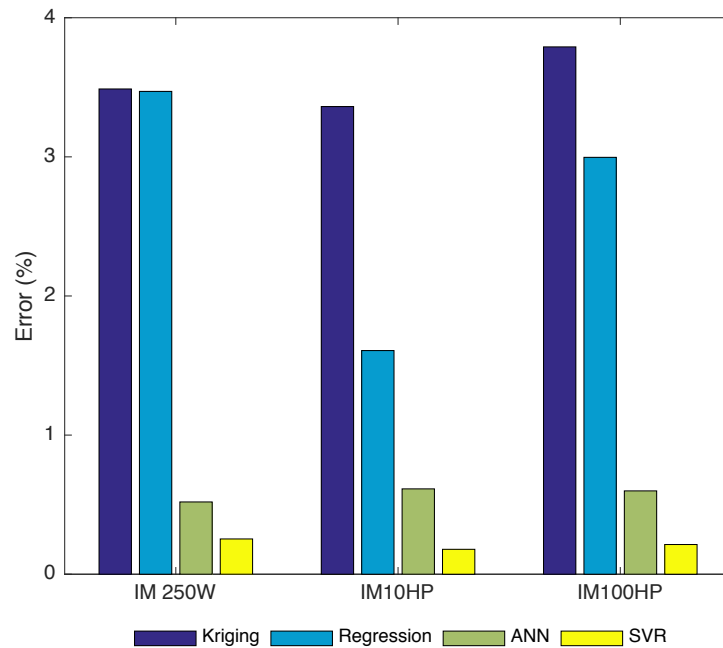


Figure 5-37: Comparison of results of recent methods with SVR

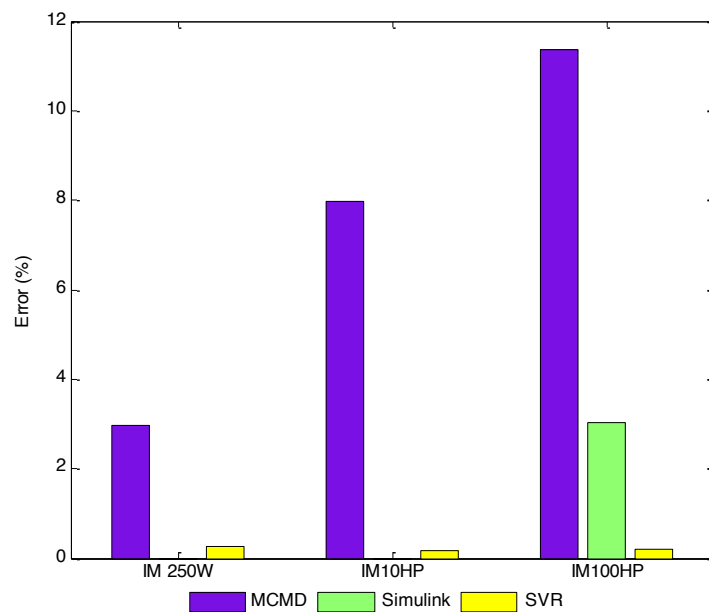


Figure 5-38: Comparison of results of MATLAB/Simulink and MCMD with SVR

Consequently, the obtained results proved that the SVR method can be a beneficial technique in electrical systems for the following reasons.

- Reduces the time and provides high performance in predicting the power factor at every single loading point
- Eliminates the permanent device and performs very well in offline and online monitoring
- Is able to store more data as well as data logger devices
- Is capable of monitoring the power factor versus motor load from no-load to full-load conditions
- Determines the power factor even at uncertain loading points from full-load to over-load conditions
- Is able to find the optimum value of the required reactive power for power factor correction at different load conditions.

5.10. Summary

In this chapter, the results of the measured power factor of the considered 250 W, 10 HP and 100 HP induction motors are presented. Also, the results of MATLAB/Simulink are shown and compared with the power factor measured by a power analyser. The results of the proposed methods, including the measured current method, Kriging, regression, a neural network and support vector regression, in the considered induction motors are presented separately. It is observed that the neural network and support vector regression methods estimated the power factor of the considered induction motors from no-load to full-load and over-load conditions with high performance compared with conventional techniques, and that the support vector regression demonstrated greater speed and robustness than the neural network.

Chapter 6: Conclusions and Future Work

6.1. Conclusions

This chapter summarises the main contributions that have been made in this research. The motivation of this research is presented in the thesis and is outlined in the first chapter. There is a tendency to believe that a remarkable amount of enhancement needs to be implemented in electrical systems in order to meet energy-saving requirements. Since the majority of loads are inductive, the power factor must be monitored and maintained toward unity with regard to energy losses. For that reason, more state-of-the-art estimation techniques such as the support vector regression method are planned to be deployed within various induction motors to predict the power factor at any loading point and to be able to obtain the amount of required reactive power for achieving a unity power factor at loads with a low power factor. Ultimately, such mathematical techniques could potentially affect the electrical system at the steady state condition. In addition, although measurement devices can help to monitor the power factor, in many cases they create difficulties due either to the need to disconnect the power to connect the device, or to access limits in the network.

In spite of the fact that the impedance of individual induction motors can be used to obtain the power factor, first the equivalent circuit parameters are required in order to obtain the impedance. Chapter 2 presents a comprehensive review of past research surrounding the issue of power factor determination and the latest proposed solutions for estimating the power factor at any loading point using intelligent techniques. This completed evaluation represents the first contribution of the thesis, which reveals that many of the methods proposed in past research have looked into the scalability, difficulty and mostly the requirements for implementation of these proposed techniques in different case studies. In this thesis, chapter 3 covers and reviews the evaluation of induction motor characteristics against load and provides a complete description of the power factor versus load, which could be valuable for understanding power factor behaviour and means of improvement.

Several empirical techniques for computing the motor load and power factor by measurement of voltage and current waveforms are presented. MATLAB/Simulink is used as a simulation tool for modelling the induction motor and to determine the power factor from no-load to full-load and over-load conditions. The equivalent circuit parameters of the induction motor are needed for this simulation. In addition, three different sizes of induction motors, 250 W, 10 HP and 100 HP, are considered for online power factor measurement from no-load to full-load and over-load conditions to validate the proposed method. These completed measurements represent the second contribution. In the measurement process, a power analyser with a recorder and load controller are connected to the induction motor for measurement.

Methods of power factor correction in a single induction motor or even group induction motors are presented in full. As the third original contribution of this research, the recent and latest proposed estimation techniques, including a method using the measured current and manufacturer's data, Kriging, regression, an artificial neural network and support vector regression, are implemented in different induction motors for power factor estimation. The overall structure and process of the proposed techniques are illustrated in chapter 4. Chapter 5 presents the results and discusses the methods implemented in the considered induction motors.

The results of the measured current method indicated a better performance in the 250 W induction motor compared with the 10 HP and 100 HP induction motors because the operated reactive current from no-load to full-load approximately corresponded to the reactive current computed from the nominal power factor, which is used in the mathematics, and was almost constant. This method was weak in medium and large induction motors where the reactive current is not constant from no-load to full-load and over-load conditions. Kriging and regression methods are implemented in the considered induction motors to resolve the

measured current method; Kriging used a semivariogram technique and regression used a polynomial technique to predict the power factor from no-load to full-load and over-load conditions. The results showed that both methods created an overshoot problem at the over-load condition. Kriging and regression methods are only able to interpolate the points between observed points. To resolve this issue, intelligent techniques including an artificial neural network and support vector regression are used, both of which are able to extrapolate unseen points.

In this case, the artificial neural network used 5 points for training, 2 points for testing and 2 points for validation with 2 hidden neurons. The results indicated that the neural network predicted the power factor of the induction motors from no-load to full-load and over-load conditions very well. However, the algorithm has to be run many times to achieve satisfactory results. This is a significant disadvantage of the neural network method that in many cases creates a difficulty. Furthermore, the support vector regression method, which is one of the most recently developed evolutionary algorithms, indicated the high performance in different conditions.

The support vector regression method also was applied in the considered induction motors. The results showed that this method predicted the power factor at any loading point from no-load to full-load and also full-load to over-load better than others. The parameters of support vector regression have significant roles in the accuracy of estimation. Proper design of the parameters produced satisfactory results that were very close to the measured points. The comparison between the recent methods and the proposed method showed that support vector regression is faster and also provided a greater performance with high accuracy at any desired loading point. Consequently, it can be asserted that support vector regression is a significant method to obtain accurate values of the power factor at any loading conditions.

Then, the obtained values determine the proper size of capacitors and thus help to correct the power factor to the desired values without under- or over-correction.

6.2. Future Research

The work presented in this thesis has fulfilled all of the research aims that were initially defined. However, there are plenty of areas to extend this work in order to enhance the ideas and methods that have been developed. Further investigation into the optimization techniques can be undertaken in order to find the parameters of support vector regression in various case studies. As demonstrated in chapter 4, a wide range of estimation techniques are used for determining the induction motor power factor against loading. These include Kriging, regression, artificial neural networks and support vector regression. It would be appropriate to conduct a comprehensive study and investigate a hybrid algorithm to estimate the power factor curve of induction motors by adding power rating.

A hybrid algorithm can extend and enhance the performance of the method, in order to design a proper model that is able to predict the power factor of induction motor with different rated power. Also, in the future work various induction motors needs to be tested to validate the hybrid algorithm. As discussed in chapter 2, many researchers have stated that, although the power factor is the cosine angle between the voltage and current waveforms, the presence of total harmonic distortion of the voltage and current in a non-linear load affects the power factor and must therefore be taken into account. Further research is required to analyse the total harmonic distortion of the voltage and current and seek a proper solution to determine the harmonics, and then obtain the true power factor against load. Further investigation is required with regard to a self-excitation and power factor correction against load at the right time.

References

- [1] L. Saribulut, "Electrical Power and Energy Systems," *Electrical Power and Energy Systems*, vol. 62, no. 5, pp. 66-71, 2014.
- [2] A. Feher, "Definitions and Measurement of Power Factor," *8th International Symposium of Hungarian Research on Computational Intelligence and Informatics*, Hungary, 2001.
- [3] F. Marafao, "Power Factor Analysis Under Nonsinusoidal Systems and Unbalanced Systems," *Conference on Harmonics and Quality of Power*, vol, no, pp.1-8, Oct 2003.
- [4] C. Sankaran, *Power Quality*, CRC Press, 2002, p. 202
- [5] M. Abdel Aziz, "Power Factor and your Electrical Utility Bill in Egypt," *Transactions on Power Delivery* , vol. 18, no. 4, pp. 1567 - 1568, 10 Oct 2003.
- [6] L. Cividino, "Power Factor, Harmonic Distortion; Causes, Effects and Considerations," *14th International Telecommunications Energy Conference*, vol, no, pp. 1-7, Oct 1992.
- [7] E. F. Fuchs, *Power Quality in Power Systems and Electrical Machines*, Academic Press, 2008, p. 664.
- [8] A. Zobaa, "Comparing Power Factor and Displacement Factor Corrections Based on IEEE Std. 18-2002," *11th International Conference on Harmonics and Quality of Power*, vol, no, pp. 1-5 Sep 2004.
- [9] J. Bednarczyk, "Induction Motor Theory," PDH, 2012, p. 52
- [10] P. Bimbhra, *Electrical Machinery*, Khanna, 1997, p. 420.
- [11] S. J. Chapman, *Electric Machinery Fundamentals*, Mc Graw Hill, 2012, p. 680.
- [12] J. Siar, "Power Factor of Motors and Generators," ABB Company, 2014, p. 68.
- [13] S. Khanchi, "Power Factor Improvement of Induction Motor by Using Capacitors," *International Journal of Engineering Trends and Technology (IJETT)*, vol. 4, no. 7, pp. 2967-2971, 10 July 2013.
- [14] A. Ukil, R. Bloch and A. Andenna, "Estimation of Induction Motor Operating Power Factor From Measured Current and Manufacturer Data," *IEEE Transactions on Energy Conversion*, vol. 26, no. 2, pp. 699-706, June 2011.
- [15] C. P. Kumar, "Power Factor Measurement and Correction Techniques," *Electric Power Systems Research* , vol. 32, no. 4, pp. 141-143, 10 Oct 1994.

-
- [16] N. Erving, "Power Factor Improvement," ABB Company in US, 2015, p. 42.
- [17] S. Bhattacharyya, "Case Study on Power Factor Improvement," *International Journal of Engineering Science and Technology*, vol. 3, no. 1, pp. 8372-8378, 2011.
- [18] C. Artech, "Power Factor Capacitors Low Voltage," IPQ, 2010, p. 110.
- [19] D. Zuart, Power Factor-Wiring and Service, BChydro, 2010.
- [20] C. A. Dasilva, "Power Factor Calculation by the Finite Element Method," *Transactions on Magnetics*, vol. 46, no. 8, pp. 3002-3005, Aug. 2008.
- [21] K. Zhou, "Online Measuring Power Factor in AC Resistance Spot Welding," *IEEE Transactions on Industrial Electronics*, vol. 66, no. 1, pp. 575-582, 10 January 2014.
- [22] M. Khodapanah, A. F. Zobaa and M. Abbod, "Monitoring of Power Factor for Induction Machine Using Estimation Technique," *50th International Universities Power Engineering Conference, (UPEC)*, vol, no, pp. 1-5, Sep 2015.
- [23] M. Khodapanah, A. Zobaa and M. Abbod, "Estimating Power Factor of Induction Motors at any Loading Conditions using Support Vector Regression," *Journal of Electrical engineering*, pp. 1-8, Submitted Oct 2017.
- [24] R. Guntaka, "Regression and Kriging Analysis for Grid Power Factor Estimation," *Journal of Electrical Systems and Information Technology*, pp. 223-233, 2014.
- [25] R. Gunaka, Regression and Kriging Analysis for Grid Power Factor Estimation, Lamer university, 2013, p. 98.
- [26] M. Khodapanah, A. Zobaa and M. Abbod, "Estimating Power Factor of Induction Motors Using Regression Technique," *International Conference on Harmonics and Quality of Power (ICHQP)*, vol, no, pp. 1-5 Oct 2016.
- [27] Z. J. Paracha, "Estimation of Power Factor by the Analysis of Power Quality Data for Voltage Unbalance Zahir," *Third International Conference on Electrical Engineering*, vol, no, pp. 1-6, Sep 2009.
- [28] P. Huynh, "Parameter Estimation for Single-Phase Induction Motors Using Test Measurement Data," *North American Power Symposium (NAPS)*, vol, no, pp. 1-6, 18-20 Sep 2016.
- [29] J. Pedra, "Parameter Estimation of Squirrel-Cage Induction Motors Without Torque Measurements," *IEE Proceedings-Electric Power Applications*, vol. 153, no. 2, pp. 85-89, 20 March 2006.
- [30] J. Guimarães, "Parameter Determination of Asynchronous Machines From Manufacturer Data Sheet," *Transactions on Energy Conversion*, vol. 29, no. 3, pp. 689-697, 2 Sep 2014.
-

-
- [31] K. Lee, "Estimation of Induction Motor Equivalent Circuit Parameters from Nameplate Data," *North American Power Symposium (NAPS)*, vol. no, pp. 1-6, Oct 2012.
- [32] T. Phumiphak, "Estimation of Induction Motor Parameters Based on Field Test Coupled with Genetic Algorithm," *International Conference on Power System*, vol. 2, pp. 1199-1203, Sep 2002.
- [33] M. Wlas, "Neural-Network-Based Parameter Estimations of Induction Motors," *IEEE Transaction on Industrial Electronics*, vol. 55, no. 4, pp. 1783-1794, 10 April 2008.
- [34] A. Dehghani-Pilehvarani, "Induction Motor Parameter Estimation Based on the Nonlinear State Space Model," *19th Iranian Conference on Electrical Engineering (ICEE)*, vol. no, pp. 1-6, Sep 2011.
- [35] M. Abdelaziz, "Estimation of Induction Motor Single-Cage Model Parameters from Manufacturer Data," *Power and Energy Society General Meeting (PES)*, Vancouver, BC, Canada, vol. no, pp. 1-6, Sep. 2013.
- [36] J. L. Zamora, "Online Estimation of the Stator Parameters in Induction Motor Using Only Voltage and Current Measurements," *IEEE Transaction on Industry Applications*, vol. 36, no. 3, 3 May 2016.
- [37] K. Sundareswaran, "Induction motor Parameter Estimation Using Hybrid Genetic Algorithm," *Third international Conference on Industrial and Information Systems*, vol. no, pp. 1-6, Sep 2008.
- [38] D. C. Huynh, "Parameter Estimation of an Induction Machine Using a Chaos Particle Swarm Optimization Algorithm," *5th IET International Conference on Power Electronics, Machines and Drives (PEMD)*, vol. no, pp. 1-6, Oct 2010.
- [39] D. Huynh, "Parameter Estimation of an Induction Machine Using Advanced Particle Swarm Optimisation Algorithms," *Electric Power Applications*, vol. 4, no. 9, pp. 748-760, 10 Nov 2010.
- [40] D. C. Huynh, "Parameter Estimation of an Induction Machine using a Dynamic Particle Swarm Optimization Algorithm," *International Symposium on Industrial Electronics (ISIE)*, vol. no, pp. 1-6, Oct 2010.
- [41] J. Pedra, "On the Determination of Induction Motor Parameters From Manufacturer Data for Electromagnetic Transient Programs," *IEEE Transaction on power systems*, vol. 23, no. 4, pp. 1709-1718, Nov 2008.
- [42] M. H. Haque, "Determination of NEMA Design Induction Motor Parameters From Manufacturer Data," *IEEE Transaction on Energy Conversion*, vol. 23, no. 4, pp. 997-1004, December 2008.
- [43] A. Accetta, "Parameter Identification of Induction Motor Model by Means of State
-

-
- Space-Vector Model Output Error Minimization,”*International Conference on Electrical Machines (ICEM)*, vol, no, pp. 1-7, Oct 2014.
- [44] M. Stocks, “Estimation of Induction Machine Parameters at Start-up Using Current Envelope,”*37th IAS Annual Meeting Conference Record of the Industry Applications*, vol, no, pp. 1163-1170, 13-18 Oct. 2002.
- [45] J. Marcondes, “Parameter Determination of Asynchronous Machines from Manufacturer Data Sheet,” *IEEE Transaction on Energy Conversion*, vol. 29, no. 3, pp. 689-697, Sep 2014.
- [46] J. M. C. Guimarães, “Determination of Three-Phase Induction Motors Model Parameters from Catalog Information,” *PES General Meeting Conference & Exposition*, National Harbor, MD, USA, vol, no, pp. 1-6, Oct 2014.
- [47] J. Susanto and S. Islam, “Estimation of Induction Motor Parameters Using Hybrid Algorithms for Power System Dynamic Studies,” *IEEE Power Engineering Conf*, vol, no, pp. 1-6, Oct 2013.
- [48] F. Alonge, “Parameter Identification of Linear Induction Motor Model in Extended Range of Operation by Means of Input-Output Data,” *IEEE Transactions on Industry Applications*, vol. 50, no. 2, pp. 959-972, March/April 2014.
- [49] J. M. Gutiérrez-Villalobos, “Hybrid Artificial Neural Network for Induction Motor Parameter Estimation” *6th European Embedded Design in Education and Research Conference (EDERC)*, Italy, vol, no, pp. 1-7, Sep 2014.
- [50] H. Li, “A Hybrid Method for Online Rotor Parameters Estimation,”*Fourth International Conference on Intelligent Control and Information Processing (ICICIP)*, vol, no, pp. 1-6, Sep 2013.
- [51] S. Villazana, “SVM-based and Classical MRAS for On-line Rotor Resistance Estimation: A Comparative Study,”*International Symposium on Intelligent Signal Processing*, vol, no, pp. 1-6, Oct 2007.
- [52] S. A. Villazana, “Rotor Resistance Estimator Using Support Vector Machines and Model Reference Adaptive System,”*International Symposium on Industrial Electronics*, vol, no, pp. 1-6, March 2006.
- [53] S. Villazana, “A Novel Method to Estimate the Rotor Resistance of the Induction Motor Using Support Vector Machines,” *IEEE Industrial Electronics conference* , vol, no, pp. 1-6, Sep 2006.
- [54] G. Liu, “Robust Sliding-Mode Control for Induction Motor Drive with RBF Neural Network Based Rotor Speed Estimation,”*International Conference on Electrical Machines and Systems*, vol, no, pp. 1-5, Sep 2008.
-

-
- [55] A. Goedel, "Neural Approach for Speed Estimation in Induction Motors," *Seventh International Conference on Intelligent Systems Design and Applications*, vol, no, pp. 1-6, Oct 2007.
- [56] A. Goedel, "Intelligent System Based Speed Estimation of Induction Motors for Industrial Sensorless Schemes," *International Conference on Control Applications*, vol, no, pp. 1-6, Nov 2007.
- [57] L. Yi, "Application of Fuzzy Neural Network in the Speed Control System of Induction Motor," *International Conference on Computer Science and Automation Engineering (CSAE)*, vol, no, pp. 1-6, Oct 2011.
- [58] B. Han, "A Novel Speed Identification Method of Induction Motor Based ANFIS," *Chinese Automation Congress*, vol, no, pp. 1-6, Oct 2013.
- [59] M. Noghdari, "General Regression Neural Network Based Fuzzy Approach for Sensorless Speed Control of Induction Motor Drives," *39th International Universities Power Engineering Conference (UPEC)*, vol, no, pp. 1-5, Sep 2004.
- [60] Y. Xiaoting, "Speed Estimation of Induction Motor based on Neural Network," *2nd International Conference on Intelligent Control and Information Processing (ICICIP)*, vol, no, pp. 1-6, May 2011.
- [61] B. Karanayil, "Induction Motor Parameter Determination Technique Using Artificial Neural Networks," *IEEE International Conference on Electrical Machines and Systems (ICEMS)*, vol, no, pp. 1-6, Oct 2008.
- [62] W. Lacerda Silva, "A Method for Measuring Torque of Squirrel-Cage Induction Motors Without any Mechanical Sensor," *IEEE transactions on instrumentation and measurement*, vol. 64, pp. 1223-1231, May 2015.
- [63] E. Babu, "Shaft Torque Estimation Method for Inservice Underloaded Induction Motors," in *International Conference on Power Electronics*, vol,no,pp.1-4, Oct, 2016.
- [64] J. Holmquist, "Practical Approach for Determining Motor Efficiency in the Field Using Calculated and Measured Values," *Transactions on Industry Applications*, vol. 40, no. 1, pp. 242 - 248, 5 Jan 2014.
- [65] A. Gharakhani Siraki, "Full Load Efficiency Estimation of Refurbished Induction Machines From No-Load Testing," *Transactions on Energy Conversion*, vol. 28, no. 2, 7 June 2013.
- [66] M. S. Aspalli, "Estimation of Induction Motor Field Efficiency for Energy Audit and Management Using Genetic Algorithm," *3rd International Conference on Sensing Technology*, vol, no, pp. 1-8. Nov. 2008.
- [67] R. B. Godoy, "Voltage Estimation in Electrical Distribution Systems," *9th International*
-

-
- Conference on Electrical Power Quality and Utilisation, EPQU*, vol, no, pp. 1-6, Oct 2009.
- [68] M. Mohd Hussain, "Voltage Estimation Using ICA on Distribution System," *IEEE 7th International Power Engineering and Optimization Conference (PEOCO)*, vol, no, pp. 1-6, Aug 2013.
- [69] I. Vujošević, "One Method for the Estimation of Voltage Drop in Distribution Systems," *Power Engineering Society Summer Meeting*, vol, no, pp. 1-6, Sep 2002.
- [70] B. Wang, "Voltage Sag State Estimation for Power Distribution Systems," *IEEE Transactions on Power Systems*, vol. 20, no. 2, pp. 806-812, 2 May 2005.
- [71] P. Raghavendra, "Voltage Estimation in Smart Distribution Networks with Multiple DG Systems," *Annual India Conference (INDICON)*, vol, no, pp. 1-5, April 2015.
- [72] E. Espinosa-Juarez, "A Method for Voltage Sag State Estimation in Power Systems," *Transactions on Power Delivery*, vol. 22, no. 4, pp. 2517-2526, 4 Oct 2007.
- [73] D. Timothy Chessmore, "Voltage-Profile Estimation and Control of a Distribution Feeder," *Transactions on Industry Applications*, vol. 45, no. 4, 19 July 2009.
- [74] L. Jorge, "Voltage Sag State Estimation in Power Systems by Applying Genetic Algorithms," *IET Generation, Transmission & Distribution*, vol. 5, no. 1, pp. 223-230, 4 August 2010.
- [75] B. Hayes, "State Estimation Techniques for Electric Power Distribution Systems," *European Modelling Symposium (EMS)*, vol, no, pp. 1-5, Sep 2014.
- [76] R. Kamali, "Online Voltage Estimation for Distribution Networks in Presence of Distributed Generation," *Indian Journal of Science and Technology*, vol. 9, no. 18, pp. 1-5, 8 May 2016.
- [77] A. Ghosh, "A New Approach to Load Balancing and Power Factor Correction in Power Distribution System," *IEEE Transactions on Power Delivery*, vol. 15, no. 1, pp. 417-422, Oct 2000.
- [78] I. Daut, "Improvement of Induction Machine Performance Using Power Factor Correction," *International Conference on Electrical, Control and Computer Engineering (INECCE)*, Pahang, Malaysia, vol, no, pp. 1-6, Sep. 2011.
- [79] A. Sarkar, "A novel Instantaneous Power Factor Measurement Method Based on Wavelet Transform," *Power India Conference*, vol, no, pp. 1-6, Oct 2006.
- [80] J. Lalotra, "Examination of the Change in the Power Factor Due to Loading Effect," *International research journal of advanced engineering and science*, vol. 1, no. 1, pp. 25-28, 2016.
-

-
- [81] F. M. Fernandez, "Influence of Power Factor Compensating Capacitors on Estimation of Harmonic Distortion," *9th International Conference on Electrical Power Quality and Utilisation (EPQU)*, vol, no, pp. 1-6, Oct 2007.
- [82] M. Aziz, "Comparing Capacitive and LC Compensators for Power Factor Correction," *10th International Conference on Harmonics and Quality of Power*, vol, no, pp. 42-4, 56-9 Oct 2002 .
- [83] A. Zobaa, "Power Factor Optimization Based on Manufacturers Standards of the Capacitors for Nonlinear Loads," *Large Engineering Systems Conference on Power Engineering*, vol, no, pp.138-142, May 2003.
- [84] A. Zobaa, "Cost-Effective Applications of Power Factor Correction for Nonlinear Loads," *Transactions on Power Delivery* , vol. 20, no. 1, pp. 359 - 365, 14 Feb 2005.
- [85] A. F. Zobaa, "The Most Economical Power Factor Correction According to Tariff Structures in Egypt," *IEEE Transaction on Power Delivery* , vol. 20, no. 2, pp. 912-918, 2005.
- [86] A. T. Baitade, "Harmonic Reduction, Power Factor Improvement and Speed Detection for 3-Phase Induction Motor Drive System Baitade," in *Conference on Advances in Signal Processing (CASP)*, vol, no, pp. 1-6, Oct 2016.
- [87] W. C. Bloomquist, "Application of capacitors for power-factor improvement of induction motors," *Electrical Engineering*, vol. 64, no. 5, pp. 274 - 278, 7 May 1945.
- [88] J. Gyeum Kim, "A study on the Optimum Selection of the Power Factor Compensation Condenser According to the Improved Efficiency of Induction Motor," *The Transaction of the Korean Institute of Electrical Engineers*, vol. 65, no. 7, pp. 1311-1315, 2016.
- [89] A. Hassanpour Isfahani, "Design Optimization of Linear Induction Motor for Improved Efficiency and Power Factor," *International Electric Machines & Drives Conference (IEMDC)*, Turkey, vol, no, pp. 1-5, Aug 2007.
- [90] S. Gharat, "Automatic Power Factor Correction Using Microcontroller," *International Journal of Engineering Technology Science and Research*, vol. 4, no. 4, pp. 182-184, 2017.
- [91] S. Rana, "Automatic Power Factor Improvement by Using Microcotroller," *Global Journal of Researches in Engineering Electrical and Electronics Engineering*, vol. 13, no. 6, pp. 1-7, 2013.
- [92] G. Balakrishna, "Power Factor Compensation Using PIC," *International Journal of Advanced Research in Electrical, Electronics and Instrumentation Engineering*, vol. 5, no. 4, pp. 3178-3183, 2016.
-

-
- [93] R. Jain, "PLC Based Power Factor Correction of 3-Phase Induction Motor," *1th International Conference on Power Electronics, Intelligent Control and Energy Systems (ICPEICES)*, vol, no, pp. 1-6, Oct 2016.
- [94] L. Guo, Y. Cheng, L. Zhang and H. Huang, "Research on Power-Factor Regulating Tariff Standard," in *IEEE Electricity Distribution Conf*, vol, no, pp. 1-5, Oct 2008.
- [95] P. Orsag, "Impact of Mains Power Quality on Operation Characteristics of Induction Motor," *14th International Conference on Environment and Electrical Engineering (EEEIC)*, vol, no, pp. 1-6, Oct 2014.
- [96] A. Al-Ali, "A PLC Based Power Factor Controller for a 3-Phase Induction Motor," *Industry Applications Conference*, Rome, Italy, vol, no, pp. 1-7, Oct. 2000.
- [97] A. Jimoh, "A Study of Improving the Power Factor of a Three-Phase Induction Motor Using a Static Switched Capacitor," *12th International Power Electronics and Motion Control Conference*, vol, no, pp. 1088-1093, Aug 2006.
- [98] S. Sagiroglu, "Power Factor Correction Technique Based on Artificial Neural Networks," *Energy Conversion and Management*, vol. 47, no. 3, p. 3204–3215, 24 March 2006.
- [99] Motor Challenge, "Determining Electric Motor Load and Efficiency," *Energy US*, 1997, p. 45.
- [100] Energy Services, "Improving Load and PowerFactor to Reduce Demand," *Electrical Energy Management Guidelines Series*, 2012, p. 84.
- [101] R. Kumar, "RFID Based Smart Grid with Power Factor Maintenance in Load Side," *International Journal of Innovative Research in communication engineering*, vol. 2, no. 1, pp. 1-8, 2014.
- [102] Feedback Instrument, *Power Frame System Utilities Manual 60-070-UM*, Sussex: FI LTD, Crowborough, 2011, p. 90
- [103] E. Maor, *The Pythagorean Theorem*, Princeton university press, 2007, p. 22.
- [104] D. Philip, *Interpolation and approximation*, Dover Publications, 1975, p. 75.
- [105] "Desktop Arcgis," ARCMAP, 04 May 2016. [Online]. Available: <http://desktop.arcgis.com>.
- [106] "Kriging Interpolation – The Prediction is Strong in this One," GIS Geography, 2012. [Online]. Available: <http://gisgeography.com>
- [107] W. Huizan, "Improved Kriging Interpolation Based on Support Vector Mashine and its Application in Oceanic Massing Data Recovery," *International conference on computer*
-

-
- science and software engineering*, vol, no, pp. 1-4, Sep 2008.
- [108] N. Wiener, *Extrapolation, Interpolation and Smoothing of Stationary Time Series with Engineering Applications*, Cambridge, Mass, 1964, p.95.
- [109] M. Harvey, *Fitting Models to Biological Data Using Linear and Nonlinear Regression a Practical Guide to Curve Fitting*, Oxford University Press, 2004, p.110.
- [110] G. Seber, *Nonlinear regression*, wiley, 1989. p.120.
- [111] W. Cleveland, "Locally Weighted Regression: An Approach to Regression Analysis by Local Fitting," *Journal of American Statistical Association*, vol. 83, no. 403, pp. 596-610, 1998.
- [112] S. Li, "Comparative Analysis of Regression and Artificial Neural Network Models for Wind Turbine Power Curve Estimation," *Journal of Solar Energy Engineering*, vol. 123, no. 2, pp. 327-332, 10 Nov 2001.
- [113] Tool box-MATLAB, "Goodness of Fit in Statistical Techniques," MATLAB, 2014, p.130.
- [114] MATLAB, *Statistics Toolbox, Math Work*, 2015, p.190.
- [115] B. Al-hnaity, "Predicting FTSE 100 Close Price Using Hybrid Model," *SAI Intelligent Systems Conference*, vol, no, pp. 1-5, Sep 2015.
- [116] S. Haykin, *Neural Networks and Learning Machines*, McMaster University, 2008, p.100.
- [117] K. P. Murphy, *Machine Learning*, Massachusetts, 2012, p.140.
- [118] K. L. Du, *Neural Networks and Statistical Learning*, Research gate, 2013, p.290.
- [119] M. Hudson Beale, *Neural Network Toolbox*, Math Works, 2017, p.120.
- [120] N. Cristianini, *An Introduction to Support Vector Machines*, Cambridge University Press, 1968, p.170.
- [121] A. Smola, "A Tutorial on Support Vector Regression," *Statistics and Computing*, vol. 14, no. 4, pp. 199-222, 2004.
- [122] "Support Vector Machine," Math Work, 2017. [Online]. Available: <https://uk.mathworks.com>.
-